

EPSTEIN, REUBEN

UOFR

*Laser Plasma
Interaction*

*Ionospheric
Modification*

*Inertial
Confinement Fusion*

*Related Science &
Applications*

26TH ANNUAL ANOMALOUS ABSORPTION CONFERENCE

**August 26-30, 1996
Fairbanks, Alaska**

Presented by: University of Alaska, Fairbanks / University of California, Los Angeles

Twenty-Sixth Annual Anomalous Absorption Conference

*The Wedgewood Resort Hotel
Fairbanks, Alaska
August 26 – 30, 1996*

Program Committee: *Prof. Alfred Wong, UCLA, Chairman
Dr. Donald DuBois, LANL
Prof. Joseph Kan, UAF
Dr. William Kruer, LLNL
Dr. Warren Mori, UCLA*

Secretarial Staff: *Annie Love, UCLA
Cyndi Hersey, UCLA/HIPAS
Physics Administrative
Support Group, UCLA*

Program Coordinator: *Tom Thompson, Tigtek, Inc.*

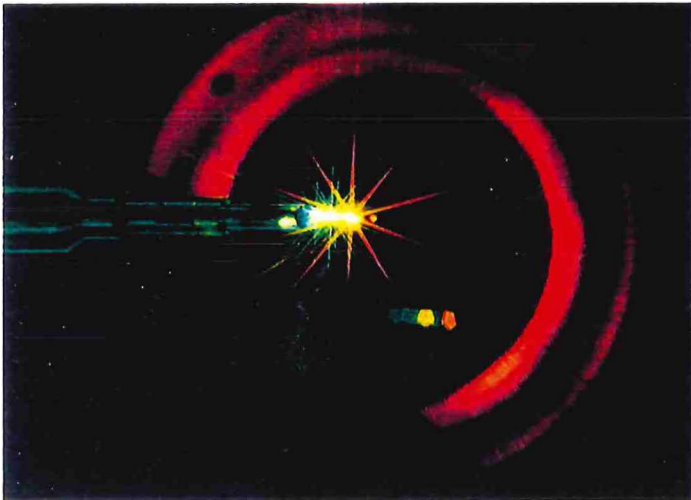
26th Anomalous Absorption Conference
The Wedgewood Resort, Fairbanks, Alaska
August 26-30, 1996

**A Joint Meeting on
Laser Plasma Interaction
Ionospheric Modification
Inertial Confinement Fusion
Related Science & Applications
in Astrophysics & Plasma physics**

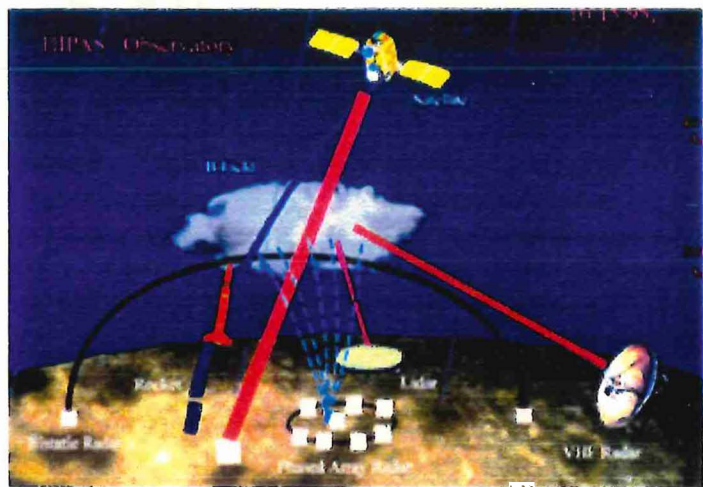
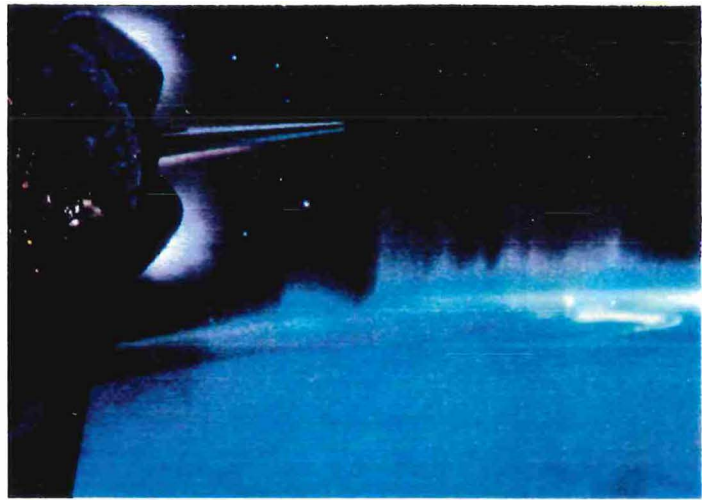
Conference Web Page: <http://www.physics.ucla.edu>
Abstract Submission, one page, by June 14th, 1996
Electronic (email-ftp) to: aa26conf@physics.ucla.edu

Tel: 310 825-9531
Fax: 310 206-2173

Laser



Aurora from the Shuttle



Laser Facility (SHIVA)

HIPAS Observatory

Committee

Dr. Donald DuBois, LANL
Prof. Joseph Kan, UAF
Dr. William Kruer, LLNL
Dr. Warren Mori, UCLA
Prof. Alfred Wong, UCLA - Chairman

Sponsors

University of Alaska Fairbanks; and
UCLA Center for Advanced Science & Technology
Knudsen Hall m.s. 154705
Box 951547
Los Angeles, CA 90095-1547

Table of Contents

Monday AM Oral Presentations (8:30 – 12:30)

First Author	Org.	Time	Title	Page
Wong, Alfred	ucla	08:30	Doing Large-Scale Plasma Physics Experiments in the Auroral Region	3
Rodriguez, Paul	nrl	09:15	Plasma Wave Interactions in the Ionospheric Focused Heating Experiment	4
Mjølhus, E.	tromso	09:30	Theory of Stimulated Electromagnetic Emissions Generated in Ionospheric Radio Heating Experiments	5
Cheung, Peter	ldstr	09:45	Can the Plasma Turbulence Excited by the Two-Plasmon Decay Instability be Observed During Heating at Arecibo?	6
Wuerker, R.F.	ucla	10:00	The HIPAS Arctic Lidar	7
Rowland, H.L.	nrl	10:15	Observations and Simulations of VLF Harmonic Generation With the HIPAS Heater Array	8
<i>coffee break</i>		<i>10:30</i>		
Lynn, A.	ucla	10:45	HIPAS Imaging Riometer Ionospheric Studies	9
Zwi, H.	ucla	11:00	Meridian Scan of Electrojet Using ELF/VLF Modulation	10
Collins, R. L.	uaf	11:15	Analysis of Lidar Systems for Profiling Auroral Molecular Species	11
Rankin, R.	alberta	11:30	Ponderomotive Saturation of Magnetospheric Field Line Resonances	12
Suter, L.J.	llnl	11:45	Efficient Production of 2-10 keV X-rays by Laser Heated "Underdense Radiators"	13
Cauble, R.	llnl	12:00	High Resolution Interferometry of Localized Small Signal Gain in Yttrium X-ray Lasers	14
Bar-Shalom, A.	artep	12:15	A Non LTE Collisional Radiative Model Based on Super Configurations	15

Monday Evening Invited Talk (7:30 PM)

Clayton, C. E.	ucla	7:30	Laser-Plasma Accelerator Experiments	17
----------------	------	------	--------------------------------------	----

Monday Evening Poster Session (8:30 – 10:30 PM)

First Author	Org.	Post.	Title	Page
Larroche, O.	cea	M-01	MULTIF: a Multifluid Code for Interpenetrating Plasma Simulations	19
Kotelnikov, A. D.	dart	M-02	Computing Imploding Shock Propagation Through Inhomogeneous Materials	20
Koenig, M.	ecolep	M-03	Colour Temperature Measurement in Laser Shocks	21
Pollaine, Steve	llnl	M-04	Modal Analysis of Directly Driven ICF Targets	22
Swenson, F.J.	lanl	M-05	Numerical Simulations of Perturbation Growth in ICF Ignition Capsules	23
Weber, S.V.	llnl	M-06	Simulations of Laser Imprint on Nova, Vulcan, and NIF	24
Schmitt, A.J.	nrl	M-07	Megajoule Scale Direct-Drive Target Designs Using KrF Lasers	25
Remington, Bruce	llnl	M-08	Laser-Driven Hydrodynamics experiments at NOVA	26
Schnittman, J. D.	llnl	M-09	Tetrahedral Hohlräume on the NIF	28
Goldman, S. R.	lanl	M-10	Joints and Gaps in ICF Targets	29
Pollak, Greg D.	lanl	M-11	Mix, Temperature, and Density Capsule Conditions in a 1-ns Square Pulse Convergence Study	30
Oertel, John A.	lanl	M-12	Recent Indirect and Direct Drive Implosion Images taken with a Gated KB Microscope at the Omega Laser Facility	31
Kruer, William L.	llnl	M-13	Strongly-Driven Laser Plasmas with Self-Consistent Electron Distributions	32
Guzdar, N. Parvez	umd	M-14	Multi-Beam Pump Driven Raman Instability	33
Chaturvedi, P. K.	umd	M-15	Self-Focusing Instabilities in the Presence of Quasi-Random Density Fluctuations in Plasmas	34
Hinkel, D. E.	llnl	M-16	Filamentation and Beam Deflection in Flowing Plasmas: Latest Results	35
Bezzerrides, B.	lanl	M-17	Three-Dimensional Modeling of Laser Propagation in the Presence of a Random Phase Plate	36
Mourenas, D.	cea	M-18	Spacial and Temporal Laser Smoothing Effects	37

Casanova, M.	cea	M-19	Piranah: A Post-Processor to Model Laser-Plasma Interactions	38
Wharton, Kenneth	llnl	M-20	Measurement of Near-wp Light as Evidence of the Electromagnetic Decay Instability	39
Eliseev, V.	alberta	M-21	Spreading of Intense Laser Beams in Underdense Plasmas	40
Myatt, J.F.	alberta	M-22	Nonlocal Electron Transport Inferred from Thomson Scattering by Thermal Fluctuations	41
Moody, J. D.	llnl	M-23	Effects of Laser-Plasma Interactions on Light Transmitted Through Nova Gasbag Plasmas	42
Walling, R. S.	llnl	M-24	X-Ray Emission from Plasmas Produced by Ultra-Short Pulse Lasers	43
Takahashi, K.	osaka	M-25	19.6nm XUV Laser Probing of Laser-Produced Plasma	44
Decker, Chris D.	llnl	M-26	Calculation of a Compact Ni-Like Tungsten Soft X-ray Laser	45
Malka, V.	ecolep	M-27	Stimulated Raman Backscattering Instability in Short Pulse Laser Interaction with Helium Gas	46
Gaeris, A. C.	uofr	M-28	Brillouin Scattering of Picosecond Laser Pulses in Preformed, Short-Scale-Length Plasmas	47
Mori, W. B.	ucla	M-29	The Physics of the Nonlinear Optics of Plasmas at Relativistic Intensities	48
Tzeng, K-C.	ucla	M-30	Generation of Higher-Order Gaussian Modes from the Coupling between RFS and Relativistic Self-Focusing	49
Najmudin, Z.	icuk	M-31	Observation of Raman Forward Scattering and Electron Acceleration in the Relativistic Regime	50
Chiou, Tzeng Chih	usc	M-32	Half-Harmonic Forward Raman Scatter	51
Bingham, R.	ral	M-33	Anomalous Absorption of Neutrinos in Dense Supernova Plasmas	52

Tuesday AM Oral Presentations (8:30 – 12:30)

First Author	Org.	Time	Title	Page
Bradley, D. K.	uofr	08:30	Initial Mix Experiments on the 60-Beam Omega Laser System	54

Pawley, Carl J.	nrl	08:45	Measurement of Raleigh-Taylor Growth of Regular and Random Perturbations Driven with Uniform Pressure from the Nike Laser	55
Azechi, Hiroshi	osaka	09:00	Direct-Drive Hydrodynamic Instability Experiments at GEKKO XII	56
Boehly, T. R.	uofr	09:15	Laser Imprinting Studies Using Multiple-UV-Beam Irradiation of Planar Targets	58
Kalantar, D. H.	llnl	09:30	Measurements of Laser Imprint in a Thin Foil Using an X-ray Laser for XUV Radiography	59
Budil, K. S.	llnl	09:45	Multimode Classical Rayleigh-Taylor Experiments at Nova	60
Delettrez, J. A.	uofr	10:00	Modeling of Mix Due to the Rayleigh-Taylor Instability in Burnthrough Experiments using the One-Dimensional Hydrodynamic Code LILAC	61
Smitherman, D. P.	lanl	10:15	NOVA Feed-out/Feed-in Experiments	62
<i>coffee break</i>		10:30		
Betti, Riccardo	uofr	10:45	Dynamic Stability and Linear Feedthrough in ICF Implosions	63
Mason, Rodney J.	lanl	11:00	Simulations of Foam-Buffered Laser-Target Interactions	64
Town, R. P. J.	uofr	11:15	Fokker-Planck Simulations of Foam-Buffered Targets	65
Rothenberg, E. J.	llnl	11:30	Effects of Beam Smoothing on the Hydrodynamics of Direct Drive Inertial Confinement Fusion	66
Gauthier, J. C.	ecolep	11:45	Time and Space-Resolved Optical Probing of Femtosecond Laser-Driven Shock Waves in Aluminum	67
Epstein, Reuben	uofr	12:00	Time-Averaging of Irradiation Nonuniformity in Laser-Driven Plasmas due to Target Ablation	68
Cremer, Shlomo	uofr	12:15	Diagnosing High rR Implosions using Elastically Scattered DT Neutrons	69

Tuesday Evening Invited Talk (7:30 PM)

Montgomery, D.	lanl	7:30	Laser-Plasma Interaction Experiments in Gas-Filled Targets	71
----------------	------	------	--	----

Tuesday Evening Poster Session (8:30 – 10:30)

First Author	Org.	Post.	Title	Page
Klapisch, Marcel	artep	T-01	Improvements to Busquet's Non LTE algorithm in NRL's Hydro Code	73
Honrubia, J. J.	ifn	T-02	Preheating Effects in Laser Driven Shock Waves	74
Wilson, D. C.	lanl	T-03	Foam Buffered Direct Drive Implosion Experiments at 527 nm	75
Gardner, John H.	nrl	T-04	The Effect of Dopants on Direct Drive ICF Target Design	77
McLean, E. A.	nrl	T-05	Studies of the Temporally and Spatially Resolved Front and Rear Side Light Emission from Laser Irradiated Targets	78
Wan, A. S.	llnl	T-06	Electron Density Measurement of a Colliding Plasma Using Soft X-ray Laser Interferometry	79
Marinak, M. M.	llnl	T-07	Three-Dimensional Simulations of National Ignition Facility Capsule Implosions	80
Ho, Darwin	llnl	T-08	Laser Cooling for Heavy Ion Fusion	81
Amendt, Peter	llnl	T-09	Shocked Witness Foam-Ball Drive Diagnostic at Target Center	82
Orzechowski, T.J.	llnl	T-10	Energetics of Small, High Temperature Laser-Driven Hohlräume	83
Powers, Linda V.	llnl	T-11	Radiation Temperature Scaling in Hohlräume for Nova and NIF	84
Hanssen, Alfred	tromso	T-12	Mesoscale modeling of Laser Plasma Instabilities in Macroscopic Sized Systems	85
Newman, D. L.	ucb	T-13	Eigenmode Structure of Convective and Absolute Parametric Instabilities Near the Critical Density in Inhomogeneous Ionospheric and Laboratory Plasmas	86
Montgomery, D.	llnl	T-14	Persistent Anti-Correlation of Stimulated Raman Scattering and Stimulated Brillouin Scattering in Gasbag Plasmas	87
Turano, E. J.	uofr	T-15	Spatiotemporal Evolution of Stimulated Raman Scattering	88
Bezzerrides, B.	lanl	T-16	Deflection of An Unsmoothed Laser Beam by a Transverse Flowing Plasma	89
Hinkel, D. E.	llnl	T-17	Laser Light Smoothing and Filamentation in Plasmas with Transverse and Axial Flows	90

Hüller, S.	ecolep	T-18	Interaction of Two Neighboring Hot Spots taking into account the effects of plasma dynamics	91
Langdon, A. B.	llnl	T-19	Spot and Speckle Motion in SSD Illumination	92
Maximov, A. V.	alberta	T-20	Saturation of Stimulated Brillouin Scattering by Hydrodynamic and Kinetic Nonlinearities	93
Rose, Harvey A.	lanl	T-21	Saturation of Stimulated Brillouin Scattering by Self Consistent Flow Profile Modification in Laser Hot Spots	94
Rambo, Peter W.	llnl	T-22	Hybrid PIC Simulations of Stimulated Brillouin Scattering Including Ion-Ion Collisions	95
Langer, Steven H.	llnl	T-23	Yield and Emission Line Ratios from ICF Target Implosions with Multi-Mode Rayleigh-Taylor Perturbations	96
Mostovych, A.	nrl	T-24	Reflective Probing of the Electrical Conductivity of Hot Aluminum in the Solid, Liquid and Plasma Phases	97
Shepard, Ronnie	llnl	T-25	Spectroscopy of Thin Foils Heated with Ultra Short Laser Pulses	98
Wharton, Kenneth	llnl	T-26	Investigation of the Conversion of Laser Energy to Relativistic Electrons at Intensities of 1020 W/cm ²	99
Malka, G.	cea	T-27	Observation of Relativistic Electrons Produced in the Interaction of a 400-fs Laser Pulse with a Solid Target	100
Wilks, Scott C.	llnl	T-28	Absorption Mechanisms for Ultra-Intense Laser-Plasma and Solid Target Interactions	101
Lefebvre, Erik	cea	T-29	Electron/Ion Heating in the Interaction of an Ultra-Intense Laser Pulse with an Overdense Plasma	102
Hatchett, S. P.	llnl	T-30	Designs for Hole-Boring and Integrated Fast Ignitor Experiments	103
Fedosejevs, R.	mpiq	T-31	Femtosecond Optical Probe Measurements of the Propagation of Terawatt Laser Pulses in Underdense Gas Targets	104
De Wispelare, E.	cnrs	T-32	Interaction of a Chirped Picosecond Laser Pulse with He Gas: Time-Resolved Ionization-Induced Refraction and Compton Back-Scattering	105
Malka, V.	ecolep	T-33	Second Harmonic Generation in the Interaction of a Short-Pulse Laser with Underdense Plasma	106

Tzeng, K-C.	ucla	T-34	Suppression of Cavitation by the Occurrence of RFS	107
-------------	------	------	--	-----

Wednesday AM Oral Presentations (8:30 – 12:30)

First Author	Org.	Time	Title	Page
Wilks, Scott C.	llnl	08:30	Foil-Terminated Free Wave Acceleration	109
Startsev, E.A.	uofr	08:45	Electron Acceleration By a Laser Pulse in a Plasma	110
McKinstrie, C. J.	uofr	09:00	Multiple-Scale Derivation of the Relativistic Ponderomotive Force	111
Chiou, Tzeng C.	usc	09:15	Stabilities of Intense Laser Propagating in Underdense Plasma Channels	112
Siders, C.W.	lanl	09:30	An Experimental Demonstration of the Laser Wakefield "Photon Accelerator": Longitudinal Interferometric Diagnostics for Plasma Based Accelerators	113
Marques, J.R.	ecolep	09:45	Laser Wakefield: First Temporal and Spacial Measurement of the Electron Density Oscillation	115
Cobble, J. A.	lanl	10:00	Exploded Foil Transmission Experiments with an Ultra-Intense Laser	116
Meyer, Jochen	ubc	10:15	Development of an Ultrafast, High Energy Pulse CO2 Laser	117
<i>coffee break</i>		<i>10:30</i>		
Fernandez, J.C.	lanl	10:45	Dependence of Stimulated Raman Scattering on Ion Acoustic Damping	118
Wood, W. M.	lanl	11:00	Study of SRS and SBS from NOVA Targets Using the Axial Imager	119
Kirkwood, R.K.	llnl	11:15	Saturation of SRS By the Stimulation of Ion Waves in Ignition Relevant Plasmas	120
Russell, David	ldstr	11:30	Saturation of SRS By Excitation of Langmuir Turbulence	121
DuBois, D.F.	lanl	11:45	Saturation of SRS in Regimes Where Secondary Langmuir Decay is Inaccessible	122
Afeyan, Bedros	llnl	12:00	Electron Plasma and Ion Acoustic Waves in Flat Top Electron Velocity Distributions	123
Simon, Albert	uofr	12:15	Raman Scattering in Gas-Filled Hohlräume and Gasbags	124

***Wednesday Evening Banquet at Alaskaland
(6:30 PM Show; 7:30 PM Dinner)***

Thursday AM Oral Presentations (8:30 – 12:30)

Speaker	Org.	Time	Title	Page
Murphy, T.J.	lanl	08:30	Indirect-Drive Proof-of-Principle Experiments on Omega	126
Wallace, J. M.	lanl	08:45	Design and Modeling of Hohlraum Experiments at Omega	128
Delamater, N. D.	lanl	09:00	Observations of Beam Deflection in Laser Heated Gas-Filled Thin-Wall Hohlraum Experiments at NOVA	129
Magelsen, G.R.	lanl	09:15	Early Time Laser Beam Motion Suggested by Time Dependent Symmetry Measurements in Methane-Filled Hohlräume	130
Lindman, Erick L.	lanl	09:30	Modeling the Effects of Laser-Plasma Interactions on Drive Symmetry in Gas-Filled Hohlräume at Nova	131
Kauffman, R. L.	llnl	09:45	Effects of Beam Conditioning on Wall Emission from Gas-Filled Hohlräume	132
Pollaine, Steve	llnl	10:00	Selection of Beam Angles for the National Ignition Facility (NIF)	133
Craxton, R. S.	uofr	10:15	Tetrahedral Hohlräume--A Way to Achieve Time-Independent Uniformity on the NIF?	134
<i>coffee break</i>		<i>10:30</i>		
Shepard, T.D.	llnl	10:45	Compression of a High-Z Foil by Hydrodynamic Pressure of Radiatively Heated Matter	135
Alon, Uri	nrcn	11:00	Scaling Laws for Rayleigh-Taylor and Richtmyer-Meshkov Instability Based on Bubble and Vortex Competition Models	136
Shvarts, Dov	nrcn	11:15	Scaling of the Rayleigh-Taylor Nonlinear Evolution in Ablatively Driven ICF	137
Vu, Hoanh X.	lanl	11:30	Hybrid Guiding Center/Paraxial Model for Laser Propagation in Prescribed Density Profiles	138

Kishony, Roy	nrcn	11:45	ICF Ignition Criteria and Critical Profiles using Self-Similar Solutions to the Burn Wave Propagation Problem	139
Beck, James B.	lanl	12:00	Computational Design of the Radiatively Driven Cylindrical Implosion Experiments	140

Thursday Evening Invited Talk (7:30 PM)

Sulzer, M. P.	arcibo	7:30	Experiments on EM Wave Interactions with the Ionosphere	142
---------------	--------	------	---	-----

Thursday Evening Poster Session (8:30 – 10:30)

First Author	Org.	Post.	Title	Page
Gold, D. M.	llnl	Th-01	Chirped Pulse Reflectometry for High-Precision Measurements of Shock Velocity	144
Estabrook, K. G.	llnl	Th-02	An Improved Pinhole Spatial Filter	145
Kopp, R. A.	lanl	Th-03	On the Effects of Fine-Scale Structure in Foam-Buffering Calculations	146
Goncharov, V. N.	uofr	Th-04	Ablative Rayleigh-Taylor Instability: Applications of the Linear Theory to Target Designs Relevant to Inertial Confinement Fusion	147
Shepard, T. D.	llnl	Th-05	Simulation of Indirectly Driven Implosions Using a Gas-Filled Hohlräum Heated by KPP-Smoothed Laser Beams	148
Varnum, W. S.	lanl	Th-06	A Non-Cryogenic Double-Shell Ignition Target	149
Tabak, Max	llnl	Th-07	A Distributed Radiator Heavy Ion Target Design	150
Cowley, Steve	ucla	Th-08	Studies of Pulse Compression and Beat Wave Excitation in Ionospheric Heating	151
Wong, A. Y.	ucla	Th-09	Generation of Large Density Perturbations by Frequency Matching at the Peak of the Ionospheric Density Profile	152
Riazuelo, Gilles	cea	Th-10	2D/3D Simulations of Filamentation with Space/Time beam smoothing in ICF context	153
Still, Bert	llnl	Th-11	Laser Filamentation Simulations with Nonlinear Hydrodynamics	154

Schmitt, A. J.	nrl	Th-12	Changes in Filamentation Behavior Due to the Presence of Hydrodynamic Axial Coupling and Flow	155
Mourenas, D.	cea	Th-13	Enhanced Scattering in Magnetized Laser-Produced Plasma	156
Berger, R. L.	llnl	Th-14	Multi-Dimensional Evolution of Stimulated Scattering and Filamentation	157
Afeyan, Bedros	llnl	Th-15	SOFTSTEP Simulations of Stimulated Raman Scattering in Inhomogeneous Plasmas Driven by Structured Laser Beams	158
Matte, J. P.	inrs	Th-16	Heat Flux Inhibition by Electron Nonlocality and Ion Acoustic Turbulence in Laser-Produced Plasmas	159
Tikhonchuk, V. T.	pnlpi	Th-17	Stimulated Brillouin Scattering from a Smoothed Laser Beam in an Inhomogeneous Plasma	160
Pennington, D. M.	llnl	Th-18	Petawatt Laser System	161
Giacone, R. E.	lanl	Th-19	Numerical Simulations of Stimulated Brillouin Scattering in Two and Three Spatial Dimensions	162
Lasinski, B. F.	llnl	Th-20	Stimulated Brillouin Scatter in Pic-Fluid Simulations	163
Malka, V	ecolep	Th-21	Laser Interaction with Helium Gas Jet in the Nanosecond Pulse Regime	164
Fontes, C. J.	lanl	Th-22	A Detailed Configuration, Non-Lte Model for Gold	165
Columbant, Denis	nrl	Th-23	NLTE Calculations of X-Ray Flux from Burnthrough Au Foils	166
Estabrook, K. G.	llnl	Th-24	Electron Temperature and Density Measurements in Large Scale-length Gasbag Plasmas by K-Shell Spectroscopy	167
Rousseaux, C.	cea	Th-25	High Intensity Interaction of a Sub-Picosecond Laser-Pulse with a Preformed Critical Plasma	168
Guethlein, Gary	llnl	Th-26	Expansion Velocity Measurements of Solid Density Plasmas Produced by Intense Ultrashort Laser Pulses	169
Guerin, S.	ecolep	Th-27	Interaction of an Ultra-Intense Electromagnetic Wave with an Overdense Plasma	170
Gauthier, J. C.	ecolep	Th-28	Space and Time Resolved Measurements of Ultra Short Pulse Laser-Produced Plasma Density Gradients	171

Mason, Rodney J.	lanl	Th-29	Magnetic Fields in Short-Pulse Laser-Matter Interactions	172
Liu, C. S.	umd	Th-30	UV Coherent Emissions and Parametric Instabilities in Laser Irradiated Semiconductors	173

Friday AM Oral Presentations (8:30 – 12:00)

Speaker	Org.	Time	Title	Page
Rose, Harvey A.	lanl	08:30	Whole Beam Flow Exclusion	174
Glenzer, Siegfried	llnl	08:45	Thomson Scattering from Two Species Laser-Produced Plasmas	176
Short, R. W.	uofr	09:00	Filamentation of Laser Light in Inhomogeneous Plasmas: Effects of Refraction and Plasma Flow	177
MacGowan, B. J.	llnl	09:15	The Influence of Smoothing by Spectral Dispersion on Laser Scattering and Beam Propagation in Large-Scale-Length Plasmas Relevant to National Ignition Facility Hohlräume	178
Moody, J. D.	llnl	09:30	Transmitted Light Characteristics in Nova Gasbag Plasmas	179
Seka, W.	uofr	09:45	Plasma Diagnostics on Omega	180
Vu, Hoanh X.	lanl	10:00	Large-Scale Three-Dimensional Particle-In-Cell Simulations of Laser Beam Deflection and Stimulated Brillouin Scattering	181
Labauve, C.	ecolep	10:15	Modeling of a Stimulated Brillouin Scattering	182
<i>coffee break</i>		<i>10:30</i>		
Williams, E. A.	llnl	10:45	Ion Wave Parametric Instabilities	183
Hüller, S.	ecolep	11:00	Laser Hot Spot Interaction Taking into Account the Effects of Plasma Dynamics	184
Smalyuk, V. A.	uofr	11:15	Power Exchange Between Crossed Laser Beams and the Associated Frequency Cascade	185
Malka, Gerard	cea	11:30	Observation of Relativistic Electrons Produced in the Interaction of a 400-fs Laser Pulse with a Solid Target	186
Eliseev, V	alberta	11:45	Spreading of Intense Laser Beams in Underdense Plasmas	187
Index				188

26th Anomalous Absorption Conference

Monday, August 26 – Friday, August 30, 1996

Reception & registration on Sunday evening, August 25, at the Wedgewood.

Time	Event	Monday	Tuesday	Wednesday	Thursday	Friday
7:30-8:30	Breakfast	Wedgewood	Wedgewood	Wedgewood	Wedgewood	Wedgewood
8:30-12:30	ORAL	IM/SAP	Hydro	SP/LP	Hohl/Hydro	LP
12:30-6:30	lunch/tour	self-tour	HIPAS tour	self-tour	self-tour	END
6:30 PM	Dinner	Wedgewood	Wedgewood	Show*	Wedgewood	
7:30-8:30	Invited Talk	Clayton	Montgomery	Banquet*	Sulzer	
8:30-10:30	POSTER	Session 1	Session 2		Session 3	

Meals: The committee decided to provide breakfast and dinner, rather than breakfast and lunch to permit a quicker getaway for the afternoon "self-touring" and to ensure a prompt beginning for the evening sessions.

MONDAY:

Introductory Lecture: Al Wong
 IM: Ionospheric Modification
 SAP: Spectroscopy & Atomic Physics
 Invited Speaker: Chris Clayton

Session Chair: Don DuBois
Session Chair: Chris Decker
Session Chair: W. B. Mori

TUESDAY:

Hydro: Hydrodynamics
 Invited Speaker: David Montgomery

Session Chair: Erick Lindman
Session Chair: Bedros Afeyan

WEDNESDAY:

SP: Short Pulse Laser
 LP: Long Pulse Laser

Session Chair: Chris Clayton
Session Chair: Colin McKinstrie

THURSDAY:

Hohl: Hohlräum Physics
 Hydro: Hydrodynamics
 Invited Speaker: Mike Sulzer

Session Chair: Larry Suter
Session Chair: Doug Wilson
Session Chair: Al Wong

FRIDAY:

LP: Long Pulse Laser

Session Chair: Denise Hinkel

*ALASKALAND:

A local tourist attraction; includes the Alaska Salmon Bake/Palace Saloon. This is where the Wednesday evening banquet will be held.

For more information, contact: Tom Thompson at (310) 825-9531
 Fax: (310) 206-2173 / email: thompson@physics.ucla.edu

Monday

ORAL PRESENTATIONS
8:30 AM – 12:30 PM

Introductory Lecture: Al Wong

Ionospheric Modification
Don DuBois, Session Chair

Spectroscopy & Atomic Physics
Chris Decker, Session Chair

Doing Large-Scale Plasma Physics Experiments in the Auroral Region

A.Y. Wong

HIPAS Observatory, Dept of Physics, UCLA

Auroral region with its free energy sources is extremely dynamic and challenging for research. Electron, ion beams and cross-field currents are frequently observed during auroral precipitations with often dramatic optical displays. Active excitation of plasma waves are used to both probe the auroral environment and utilize its free energy sources.

This introductory talk will present physics of the auroral region, the methodology of using electromagnetic waves at resonant plasma frequencies to interact actively with auroral free energies using high power ground-based transmitting facilities.

A comprehensive array of diagnostics will be described to probe the heated region which can be of the order of 100 km. This includes lidars, radars, RF holographic imaging, satellites, rockets with proper coordination to simultaneously observe this dynamic phenomenon.

Experiments on large-scale density perturbations, the excitation of globally propagating electromagnetic waves, the tracking of auroral currents and collapsing cavitons driven by electron beams or electromagnetic waves will be described. Search for large-scale solutions to certain environmental problems will also be discussed. The excitation of ion cyclotron waves can bring about the selective acceleration of polluting ions out of the atmosphere. Energetic electron and ion beams have been observed to reduce the level of ozone when they penetrate down to the mesosphere and stratosphere. The scattering of these energetic particles by excited plasma waves can ameliorate such processes.

Plasma Wave Interactions in the Ionospheric Focused Heating Experiment*

P. Rodriguez, C.L. Siefring, and P.A. Bernhardt

Plasma Physics Division, Naval Research Laboratory, Washington, DC

The Ionospheric Focused Heating (IFH) rocket experiment created an ionospheric hole above the Arecibo HF radiowave heater by the release of an electron-attachment chemical at an altitude of about 280 km. The hole served as a focusing lens for high power HF pump waves at 5.1 MHz launched from the ground-based transmitter, producing various radiowave effects measured by the rocket diagnostic instruments. In this report we present new evidence for the occurrence of plasma wave interactions driven by the HF pump at various altitudes above and below the level where the local electron plasma frequency is equal to the pump. The plasma wave interactions were observed at the critical density, the quarter critical density, and at pre-release altitudes where standing waves at the pump wavelength are detected. Wave scattering effects were detected in the upper side gradient of the ionospheric hole. The data suggest that the frequency and wavenumber matching requirements for coupled waves are met in various regions. In addition, waveform measurements show frequency shifts associated with the upgoing (transmitted) and the downgoing (reflected) HF waves. The frequency shifts arise from the Doppler effect and variation in the wave vector. The characteristic signature in the dynamic spectrum provides an accurate method to locate the interaction region altitude.

* Work supported by ONR and NASA.

Theory of Stimulated Electromagnetic Emissions Generated in Ionospheric Radio Heating Experiments

E. Mjølhus and E. Helmersen
University of Troms, Troms, Norway

Ionospheric radio heating experiments have over a long time generated significant contributions to our insights into the interaction of a plasma and electromagnetic radiation. Up to now, the use of VHF/UHF radars in Arecibo and Troms to study the nonlinear saturation of HF-driven Langmuir turbulence, has received much attention [1], [2]. An even more significant process in these experiments is the formation of magnetic-field-aligned small-scale electron density striations [3] and the accompanying anomalous absorption [5]. Since the early 1980s, the sidebands of the reflected HF wave have been detected, and shown to contain interesting and highly reproducible structure [4]. This is known under the term Stimulated Electromagnetic Emissions (SEE).

Recent experiments [5] strongly indicate that the SEE are associated with striations. Much recent theoretical effort has considered the striations as “waves” and considered “wave-wave interactions” of various kinds. In contrast, some of the theoretical developments to explain the formation of the striations themselves, e.g. [3], emphasize electrostatic wave activity within each individual density depression, noticing that upper hybrid oscillations can be generated and trapped in them.

The theoretical effort to be reported here, pursues this picture, including a preexisting density depletion (formed by slow processes) as well as a contribution formed by the more rapidly varying ponderomotive pressure. A one-dimensional (slab) model is solved numerically, and a source for SEE [6] is computed and frequency-analysed. We have found that nontrivial SEE is associated with certain new parametric instabilities of the trapped upper hybrid oscillations. One instability is of a decay type, where the daughter oscillation is a free standing upper hybrid oscillation (or cavity resonance) in the density depletion, and the frequency downshift is slightly larger than the lower hybrid frequency. This process is consistent with the downshifted maximum (DM) observed in the experiments. Another instability occurs when the applied frequency is nearly at the mean of two frequencies of cavity resonances, so that the Stokes component of the downshifted resonance and the anti-Stokes component of the upshifted resonance are similar. This instability often leads to broad SEE spectra and is proposed to explain the observed Broad Continuum (BC).

1. Sulzer M.P., Fejer J.A., *J. Geophys. Res.*, 99A, 15035, 1994.
2. Kohl, H., Rietveld M.T., *J. Geophys. Res.*, 101A, 5391, 1996.
3. Gurevich A.V., Lukyanov A.V., Zybin K.P., *Phys. Lett.*, A206, 247, 1995.
4. Thidé B., Kopka H., Stubbe, P., *Phys. Rev. Lett.*, 49, 1561, 1982.
5. Stubbe P., Stocker A.J., Honary F., Robinson T.R., Jones T.B., *J. Geophys. Res.*, 99, 6233, 1994.
6. Mjølhus E., Hanssen A., DuBois D.F., *J. Geophys. Res.*, 100A, 17527, 1995.

Can the Plasma Turbulence Excited by the Two-Plasmon Decay Instability Be Observed During HF Heating at Arecibo?*

Peter Cheung^a, Don DuBois^b, David Russell

Lodestar Research Corp. 2400 Central Ave. Boulder CO 80301

We study the Two-Plasmon Decay (TPD) instability and the turbulence it engenders at one quarter of reflection density in the hf-driven ionosphere over Arecibo using a reduced (generalized Zakharov) model that couples (magnetized) Langmuir wave and ion acoustic wave fluctuations to the TPD driving current.^[1] Recent advances in Incoherent-Scatter Radar (ISR) diagnostics and the upgrade of the heater transmission lines promise to make Arecibo a good place to study TPD, however, the 430 MHz radar cannot *directly* detect the linearly most unstable TPD Langmuir waves. We explore the possibility that secondary Langmuir waves, produced by such turbulence effects as cascade and caviton collapse, may be detected by the ISR, depending on altitude and the extent to which the threshold for TPD is exceeded. We characterize these enhanced fluctuations by their energy- and power-spectra. The precedent of seeing nonlinearly produced fluctuations instead of those predicted by linear instability theory was established^[2] in earlier work which predicted^[3] cavitation and free mode signatures in the turbulence excited near reflection density at frequencies and altitudes where no observable linearly unstable modes exist. Other possible diagnostics such as SEE emissions and alternative radar probes will be discussed.

1. D.F. DuBois, D. Russell, and H.A. Rose, Phys. Rev. Lett. **74**, 3983(1995).
2. M.P. Sulzer, and J.A. Fejer, J. Geophys. Res. **99**, 15035, (1994).
3. D.F. DuBois, D. Russell, and H.A. Rose, Phys. Rev. Lett. **60**, 581(1988).

* Supported by NSF Grant #ATM-9503147.

^a Also at UCLA.

^b Also at Los Alamos National Laboratory.

The HIPAS Arctic Lidar⁺

R. F. Wuerker, A. Y. Wong, and H. Zwi

*UCLA, Plasma Physics Laboratory, Los Angeles, CA 90095-1547 and
HIPAS Observatory, Fairbanks, AK 99712*

A new lidar system is being assembled at the HIPAS Observatory (65°N-147°W), around a 2.7 m diameter, 4.5 m focal length (fl) Liquid Mirror Telescope (LMT),¹ within an insulated tower with "float glass" skylight, for winter (-40°C) auroral observations. The LMT consists of an air bearing (Professional Instr. Minn.) and a foam-Kevlar container (Euclid Research, Vancouver, Canada). Air is delivered underground from a remote compressor to minimize vibrations. The container was pre-configured and then given a final spin coat of polyurathane resin at HIPAS. The reflecting surface is 2 mm of mercury (150 kg). The rotational speed is 10 rpm, $fl = g/2\omega^2$; where, g is local gravity, ω is the angular rotation of the dish, and 2 is due to the law of reflection. The dish is Mylar belt (0.1 x 3 mm)-pulley driven from a 60 Hz synchronous motor, via a 150 W audio amplifier, and ($\pm 5/10^6$) oscillator (SRS DS335). An eight leg quadrupod holds detectors at the focal plane, as well as a pair of 3 mW HeNe lasers. The two HeNe beams are initially retro aligned (absolutely vertical) off the non rotating mercury in the container. When the mirror rotates, the beams locate the focus of the parabolic reflector. The detector aperture is centered on this point; a Uniblitz VSR6 shutter (6 mm aperture), a pair of 5 cm dia. glass condensing lenses on either side of 5 cm dia. narrow band filter, and the photomultiplier (PMT, Hamamatsu R636-10 with Ga-As-Cs cathode). The glass lenses focus the shutter aperture onto the PMT cathode. The mercury vapor level in the tower is safe after a few weeks, due to oxidation. The mirror has been run continuously for 3 months. The lidar's laser is housed in an adjacent room, and presently consists of an excimer pumped dye laser (7 mJ/pulse at 10 Hz) tuned to the Na D₂ (589 nm) resonance line, by observing fluorescence in a Na lamp. Since the detector aperture is aligned to the vertical, the dye laser beam is also aligned absolutely vertical, by retro reflecting the beam off an oil surface in a cup with a flat glass bottom. Laser light resonantly scattered from 100 km is collected by the LMT and detected with a multichannel scalar analyzer (MS/A, SRS SR430). Each trace is the result of typically 1000 shots (100 sec). We have seen (on 3/18/96), sporadic Na layers 30 km above the "normal" Na layer at 90 km altitude. It is proposed that Na is released from ionospheric compounds by solar protons penetrating to 120 km altitudes.¹ Our lidar will soon include a tunable "Doubled flashlamp pumped Ti-sapphire laser" (700-950 nm oscillator with SBS amplifier, product MPB Technology, Dorval, Canada, 10 Hz, >125 mJ/pulse at 391.4 nm), which will be used for ranging off of arctic Ca⁺ (391.4 nm), Fe (375 nm), Mg (383.8 nm), and N₂⁺ (391.4 nm bandhead) layers.

1. F. Sigernes, et al., J. Atmos. Terrs. Phys., **58**, 1281-1291, 1996.

⁺ Under ONR N00014-91-C-0191.

Observations and Simulations of VLF Harmonic Generation With the HIPAS Heater Array

H.L. Rowland and M.J. Keskinen

*Beam Physics Branch, Plasma Physics Division, Naval Research Laboratory,
Washington, DC 20375-5346*

J.S. Villasenor* and A.Y. Wong

*Department of Physics, University of California, Los Angeles,
Los Angeles, CA 90024-1328*

We report experimental results from the High-Power Auroral Stimulation (HIPAS) facility showing that the lower D-region can be heated so as to produce either a single narrow-band ELF/VLF radiation signal or a very broad signal containing many odd harmonics. The measurements are compared to a new 2-1/2 D simulation code that models the lower D-region and the earth-ionospheric waveguide. The simulation spectra show good agreement with the observations. Rapidly switching the HF power off and on leads to perturbing currents in the D-region that vary in time in a square wave type pattern. This generates an ELF/VLF wave with high, odd harmonics observed up to $n=13$ ($f = nf_0$, where f_0 is the modulating frequency). A more smoothly changing power variation generates a narrow band signal at f_0 . Simulations show how the D-region affects the spectral shape. From these results we find that the heating should occur at a low altitude in the D-region (approximately 75 km). Using the simulation results we determine that the D-region current needed to produce the observed broad-band magnetic field spectrum has a square wave time variation.

* Present address, MIT.

HIPAS Imaging Riometer Ionospheric Studies

A. Lynn, J. Pau, J. Villasenor, H.R. Zwi, E. Nichols, A.Y. Wong

Department of Physics and HIPAS Observatory, University of California at Los Angeles

An imaging riometer was installed at Gilmore Creek, Fairbanks, Alaska (35 km from HIPAS) for measuring the background absorption of the auroral regions. The antenna consists of an eight element dipole array and a phasing matrix (Butler matrix) produces 8 pencil beams. With the aid of a personal computer, we can record all the 8 channels data on a sequential basis at a rate of ~2 Hz.

Results obtained in February 1994 have maximum effect at channel 6 and 7 during the O-mode polarization heating. This is consistent with the direction of HIPAS heated region and the beam width pattern of HIPAS. Recent results also show consistency with the SELDADS riometer data.

22

Meridian Scan of Electrojet Using ELF/VLF Modulation

H.R. Zwi, A.Y. Wong, J. Pau

Department of Physics and HIPAS Observatory, University of California at Los Angeles

D. Sentman

Geophysical Institute, University of Alaska, Fairbanks

A series of experiments were carried out using the HIPAS heater ($f_0 = 2.85$ MHz, $P_{\text{rad}} = 800$ kW) in 1994. The results of those experiments show the optimum conditions for ELF/VLF generations are having the aurora north of the heating region and the electrojet directly overhead. A series of follow-up experiments have been carried out in March 1996. The experimental goal is to correlate systematically the spatial ELF/VLF signal strength with the aurora arc and the electrojet by using the ELF/VLF setup at Gilmore Creek, AK.

With the ability to beam the heater array in different directions and transmitting in AM, DM, and/or DF mode, the HIPAS heater array was continuously scanned in five positions along the magnetic N-S direction at AM 1.11 kHz, AM 2.5 kHz, DF 24 Hz, or DF 29 Hz modulation. The experimental results show that both ELF and VLF receivers have different signal strengths at different heating directions.

Analysis of Lidar Systems for Profiling Auroral Molecular Species

Richard L. Collins, Dirk Lummerzheim, and Roger W. Smith
Geophysical Institute, University of Alaska-Fairbanks

The potential of lasers to probe thermospheric molecular species has been recognized since the 1960s. Interest in radio ionospheric modification experiments has prompted further analysis of the problem. Recently, a detailed analysis of auroral lidar systems based on laser technology that is currently available and considered scattering from a 10-km thick layer of aurorally produced scatterers has been reported. In this paper we extend this analysis to consider profiling the auroral species under realistic conditions; we survey the spectroscopy of molecular nitrogen to determine the optimum frequencies for the lidar, we couple photometric observations of the aurora with an ionospheric chemistry model to determine the expected profiles of aurorally-excited species. Thus, we determine the actual requirements for the optimum lidar system under actual auroral conditions.

We first review upper atmosphere resonance lidar techniques. We then determine representative molecular profiles found in typical aurora based on photometric observations. Finally we determine the requirements for an actual auroral lidar system and discuss them in terms of available technologies.

Ponderomotive Saturation of Magnetospheric Field Line Resonances

R. Rankin, P. Frycz and J.C. Samson

Department of Physics, University of Alberta, Edmonton, Canada

V.T. Tikhonchuck

P.N. Lebedev Physics Institute, Moscow, Russia

Compressional Alfvén waves in the terrestrial magnetospheric cavity constitute a discrete spectrum of global modes which can resonate with specific components of the continuum spectrum of standing shear Alfvén wave field line resonances (FLRs). The compressional modes are excited by solar wind impulsive perturbations and the experimental evidence suggests that their resonance absorption results in FLR intensifications and is responsible for the optical emissions from discrete auroral arc structures.

We investigate the effect of the ponderomotive force of standing shear Alfvén waves on the nonlinear saturation of FLRs. In the low β magnetospheric plasmas the FLR saturation occurs due to a nonlinear phase slip between the compressional mode driver and the shear wave field. Ponderomotive force also leads to density depletions at the ionospheric ends of the resonator, nonlinear narrowing of FLR up to meridional scales comparable to the electron inertia scale length. At these scales the parametric decay instability of the shear Alfvén wave takes place which is responsible for the FLR structuring comparable to scales comparable to those embedded within temporally modulated discrete auroral arcs. Observational features relating to these effects will be discussed.

Efficient Production of 2-10 keV X-rays by Laser Heated "Underdense Radiators"

L.J. Suter, R.L. Kauffman, M.S. Maxon,

Lawrence Livermore National Laboratory, University of California, Livermore, CA 94551

J.F. Davis

Alme Associates, Alexandria, VA

The next generation of high power lasers offers the prospect of creating multi-kilovolt x-rays with >10% efficiency. Such efficiencies are achieved with "underdense radiators", a non-traditional source of laser generated x-rays. Applications of these sources with the proposed National Ignition Facility (NIF) include volume preheating of experiments; bright, multi-keV backlighting; pumps for fluorescent imaging of capsule dopants and doppler velocimetry; uniform irradiation of large test objects.

Work performed under the auspices of the U.S. Department of Energy by the Lawrence Livermore National Laboratory under Contract W-7405-ENG-48.

High Resolution Interferometry of Localized Small Signal Gain in Yttrium X-ray Lasers

R. Cauble, L. B. DaSilva, P. Celliers, C. Decker, R.A. London, J.C. Moreno,
J.E. Trebes, A.S. Wan and F. Weber

Lawrence Livermore National Laboratory Livermore, California USA

Predicted average gains of collisionally-pumped, neon-like x-ray lasers have always been 1.5–2 times the observed value. One possible source of uncertainty has been the atomic kinetics codes used to predict the small signal gain that is amplified. Another mystery has been the observed persistent lack of spatial coherence from x-ray laser targets. We have simultaneously measured small signal gain and electron density of a 2-mm-long yttrium x-ray laser plasma employed as an amplifier for a separately-produced yttrium x-ray laser. The plasma was viewed end-on with $\sim 2 \mu\text{m}$ resolution. Measured small signal gains were found to be between 10 and 15 cm^{-1} , in agreement with predictions. This indicates that signal loss due to refraction is greater than calculated. More importantly, images showed that high gain was produced irregularly in spots with dimensions of $\sim 10 \mu\text{m}$. We suspect that this localization is caused by intensity variations in the optical drive laser, but it is uncertain whether the small regions are due to a developed plasma instability. The fact that much of the laser gain is produced in small regions explains why coherence is much less than expected.

* Work performed under the auspices of the U. S. Department of Energy by Lawrence Livermore National Laboratory under contract number W-7405-ENG-48.

~~A Non LTE Collisional Radiative Model Based on
Super Configurations~~

Avraham Bar-Shalom(a) and Marcel Klapisch(b)
ARTEP, Inc. Columbia, MD 21045.

Busquet's model RADIOM[1], has been successfully implemented in the NRL hydro codes^[2,3]. It is very efficient, and apparently takes into account most of the non LTE effects, but it is difficult to find experimental data to test its accuracy or the validity of its many approximations. In order to benchmark RADIOM, we developed a full radiative collisional radiative model based on the concept of superconfigurations^[4,5] and using one-electron cross sections extracted from HULLAC.^[6,7]

We will describe an overlook of the model, the formulas for the rates, and show first results on a variety of atoms from Al to Au in the optically thin case. Comparisons with RADIOM show satisfactory agreement in many cases.

1. M. Busquet, Phys. Fluids B. 5, 4191 (1993).
2. J. H. Gardner, M. J. Herbst, F. C. Young, J. A. Stamper, S. P. Obenschain, C K. Manka, K. J. Kearney, J. Grun, D. Dustin and P. G. Burkhalter, Phys. Fluids B. 29, 1305 (1986).
3. M. Klapisch, D. Colombant, J. P. Dahlburg, J. H. Gardner, A. J. Schmitt and D. A. Garren, Bull. Am. Phys. Soc., 40, 1806 (1995).
4. A. Bar-Shalom, J. Oreg, W. H. Goldstein, D. Shvarts and A. Zigler, Phys. Rev. A, 40, 3183 (1989).
5. A. Bar-Shalom, J. Oreg, J. F. Seely, U. Feldman, C. M. Brown, B. A. Hammel, R.W. Lee and C. A. Back, Phys. Rev. E, 52, 6686 (1995).
6. A. Bar-Shalom, M. Klapisch and J. Oreg, Phys. Rev. A, 38, 1773 (1988).
7. The HULLAC code for Atomic Physics was developed by M. Klapisch, A. Bar-Shalom and others in the 80's and 90's as a collisional radiative model generator and solver for one ion stage. It was recently rewritten to handle an arbitrary number of ion stages, and goes now by the name MICCRON.

* Supported by U.S. Department of Energy

^a Permanent address: NRCN, Be'er Sheva, Israel

^b Mailing address: Naval Research Laboratory, Code 6730, Washington, DC 20375

Monday

INVITED TALK
7:30 – 8:30 PM

Chris Clayton
W.B. Mori, Session Chair

Laser-Plasma Accelerator Experiments

C.E. Clayton

Department of Electrical Engineering, University of California at Los Angeles

The use of a coherent longitudinal electron plasma wave (EPW) traveling at near the speed of light to accelerate particles was proposed by Tajima and Dawson¹ in 1979. In this seminal paper, three distinct methods of driving the “relativistic” electron plasma wave were proposed and are referred to in today’s literature as; the Laser Wakefield Accelerator (LWFA), the Plasma Beat Wave Accelerator (PBWA), and the so-called Self-Modulated Laser Wakefield Accelerator (SMLWFA). All these schemes make use of the longitudinal ponderomotive force associated with an intensity-modulated light wave to push on the background plasma electrons and set them oscillating at the plasma frequency ω_p . In this talk, I will review most of the experimental efforts and highlight some of the milestones achieved in the pursuit of a feasible ultra-high gradient (i.e., compact) particle accelerator.

It is perhaps counterintuitive that the ultimate energy gain ΔW_{\max} achievable by the accelerating particle goes inversely with the plasma density n_e for a given EPW amplitude ϵ and laser frequency ω_0 . The reason for this is that the driving ponderomotive force, and thus the phase velocity v_ϕ of the trailing EPW, moves at the group velocity of light v_{gr} and is therefore closer to light-speed at lower densities. One can show that the maximum Lorentz factor $\gamma_{\max} \sim 2W_{\max}$, where W_{\max} is expressed in MeV units, is given approximately by $2\epsilon\gamma_\phi^2 \sim 2\epsilon\omega_0^2/w_p^2$. This is the “dephasing limit” where the accelerating particle has rolled down the entire potential well in the wave frame. Of course, there are other experimental constraints on ΔW_{\max} . For example, the limited depth of focus of an unguided laser beam.

Of the three schemes, the PBWA is the most experimentally mature with many groups around the world showing results though limited not by dephasing but by the Rayleigh range of the laser. For example, the demonstration of 30 MeV electrons at UCLA from a 2 MeV injection source over about 1 cm.² But in the last few years, the LWFA scheme has made progress due to the ever-decreasing laser pulse widths in the TW range with each group bringing interesting diagnostics on-line. Finally, the SMLWFA concept, which requires high power *and* a laser pulse width many plasma periods long (i.e., high density) has been demonstrated in several labs with the 25 TW Vulcan laser at RAL giving the best results to date; that is, dephasing limited energy gains approaching 100 MeV from self-trapped electrons.³

1. T. Tajima and J.M. Dawson, Phys. Rev. Lett. 43, 267 (1979).
2. M. Everett et al., Nature 368, 527 (1994).
3. A. Modena et al., Nature 377, 606 (1995).

* This work is supported by the US DOE contract no. DE-FG03-92ER40727.

Monday

**POSTER SESSIONS
8:30 – 10:30 PM**

MULTIF: A Multifluid Code for Interpenetrating Plasma Simulations

O. Larroche

CEA Limeil-Valenton, 94195 Villeneuve Saint Georges Cedex, France

For the interpretation of plasma collision experiments, there is a need for a standard, versatile, easy to use multifluid simulation tool, which is far less costly in terms of CPU time than Fokker-Planck simulations, to be used in much the same way as the classical one-fluid hydrodynamics codes available in all laboratories involved with laser-matter interaction. A new one-dimensional multifluid code (called "MULTIF") has been written to this end.

MULTIF uses a 1-D description of hydrodynamics in plane, cylindrical or spherical geometry, with all computations performed on a single eulerian mesh. An eulerian mesh was chosen because we aimed at simplicity of the code structure and programming, and a possible extension to 2-D would be easier. We worked out a new hydrodynamics scheme aiming at good properties in both plasma expansion problems with high density contrasts and shock wave fronts. The code solves the hydrodynamics equations governing density, bulk velocity, parallel and transverse temperatures for an arbitrary number of interpenetrating ion species, along with the heat equation for electrons. We made the assumption of quasineutrality, which is valid in plasma collision problems except in the very early interpenetration phase, involving very tenuous fluids. Additional terms were included to account for radiative losses and laser absorption in a simplified way. Ionization states of the various ion species are either held fixed or calculated in the frame of a Local Thermodynamic Equilibrium taking into account all species present at a given point in space.

Lateral expansion is taken into account in the frame of a so-called "one and a half dimensional" (" $1^{1/2}$ -D" for short) model. This is a phenomenological modeling of transverse expansion assuming self-similar transverse profiles of all quantities. Although this model obviously cannot yield as much information as a genuine 2-D code, comparisons with experimental results performed so far indicate that the $1^{1/2}$ -D simulations are already quite satisfactory.

Although laser absorption can be treated in a simple way, the code can use instead initial conditions calculated by classical hydrodynamics simulations with the code FILM^[1]; hydrodynamical quantities computed by MULTIF and properly sampled in time are then passed over to atomic physics post-processors such as FLY^[2] or TRANSPEC^[3].

Typical results for plasma collision experiments involving exploded foils as well as massive targets will be shown.

1. J.-C. Gauthier, J.-P. Geindre, N. Grandjouan, and J. Virmont, *J. Phys. D: Appl. Phys.* 16, 321 (1983) and references therein.
2. R. W. Lee, B. L. Whitten and R. E. Strout, *J. Quant. Spectrosc. Radiat. Transfer* 32, 91 (1985).
3. O. Peyrusse, *Phys. Fluids B4*, 2007 (1992).

Computing Imploding Shock Propagation Through Inhomogeneous Materials*

Alexei D. Kotelnikov and David C. Montgomery

Department of Physics and Astronomy, Dartmouth College, Hanover, NH 03755

In imploding ICF targets, it may be that shocks will be propagated through materials with strong density inhomogeneities embedded in them: for example, a foam supported by higher-density fibers. In order to calculate the effects of such inhomogeneities on shocks, we have developed a numerical two-phase fluid code, so far limited to two spatial dimensions. The code generalizes a kinetic theory method developed by Prendergast and Xu^[1] and Xu et al^[2]. The key theoretical ingredient is the generalization of the Bhatnagar-Gross-Krook^[3] method to more than one mass species. The method is implemented through finite-volume discretization; moments of the distribution functions are calculated on the basis of Chapman Enskog procedures, and are corrected with Van Leer limiters. Expressions for thermal conductivity and viscosity emerge naturally and shocks are preserved as discontinuities. Operator splitting methods are applied to enable convection and thermal equilibration steps separately. Mach numbers from 2 to 60 have been considered in a variety of planar and circular geometries. We have treated the passage of shocks through inhomogeneities of higher and lower density than background. Two-dimensional implosions and explosions can be treated. Unstable behavior associated with differing mass densities (e.g., Rayleigh-Taylor and/or Richtmyer-Meshkov) appears to be calculable into the nonlinear regime, although the range of required computational resources remains to be fully explored.

1. K. Prendergast and K. Xu, *Journal of Computational Physics*, 109, 53 (1993).
2. K. Xu and K. Prendergast, *Journal of Computational Physics*, 114, 17 (1994). K. Xu, L. Martinelli, and A. Jameson, *Journal of Computational Physics*, 120, 48 (1995).
3. A. Bhatnagar, E. Gross, and M. Krook, *Phys. Rev.* 94, 511 (1954).

* This work was supported in part by U.S.N.R.L. under Grants Nos. N000014951-G001 and N000014-96-1-G005.

Colour Temperature Measurement In Laser Shocks

M. Koenig, J. Krishnan, A. Benuzzi, J.M. Boudenne

*Laboratoire pour l'Utilisation des Laser Intenses (CNRS), Ecole Polytechnique, 91128
Palaiseau, France*

Th. Löwer

Max Planck Institut für Quantenoptik, Garching, Munich, Germany

T.A. Hall, M. Mahdih

University of Essex, Dept. of Physics, Wivenhoe Park, 504 3SQ Colchester, UK

D. Batani, S. Bossi, D. Beretta

University of Milan, Dept. of Physics, via Celoria 16, 20133 Milan, Italy

A method for the determination of the colour temperature in shock waves produced with lasers is presented. The experiments have been performed at the LULI laboratory of the Ecole Polytechnique. Aluminium foil targets were irradiated using the LULI laser at $0.53 \mu\text{m}$ with an average intensity $I_L < 10^{14} \text{ W/cm}^2$. High quality flat shocks were produced with Phase Zone Plates (PZP) on the beams. Using a biprism and two coloured filters, we recorded the target rear side emissivity at “two visible wavelengths” onto the same streak camera photocathode. The spectral sensitivities of the two “channels” (taking into account the filters and the streak camera spectral responses) had a maximum around 400 nm (blue) and 600 nm (orange). The ratio of the two emissions allowed us to determine the colour temperature. The shock velocity was also measured and it was used to deduce the real shock temperature. We show some experimental results and a comparison with a simple model based on self-similar plasma expansion and a power law for opacities.

Modal Analysis of Directly Driven ICF Targets

Steve Pollaine and David Eimerl

Lawrence Livermore National Laboratory

Inertial Confinement Fusion has two main approaches: indirect drive and direct drive. In both cases, a capsule must be compressed by a factor of 30 to 40, so that the drive asymmetry can be no more than about 1%. Indirect drive achieves this uniformity by first converting the laser light to x-rays inside a cavity, with the transport of x-rays from the cavity wall to the capsule smoothing out the high-order modes. Direct drive requires very smooth, carefully placed laser beams. High-order modes initiate hydrodynamic instabilities, which cause the capsule shell to break up as it implodes. Low-order modes cause the capsule to implode asymmetrically, preventing the capsule from compressing as needed.

This poster derives and presents analytic formulas that predict the asymmetry in direct drive targets from low-order modes due to beam geometry, variations in beam power, and beam pointing errors. These formulas are then applied to proposed direct-drive targets for the National Ignition Facility (NIF), a proposed 1.8 MJ laser with 192 beamlets organized into 48 sets of beams, and the Omega Upgrade, a 30 KJ laser at the Laboratory for Laser Energetics (LLE) at U. Rochester.

Numerical Simulations of Perturbation Growth in ICF Ignition Capsules

F.J. Swenson and N.M. Hoffman

Lawrence Livermore National Laboratory, Livermore, CA 94551

Numerical simulations of perturbation growth are used to evaluate the impact of inherent surface roughnesses on capsule performance and thereby lead to fabrication requirements for ICF ignition targets. While these hydro instability calculations are straightforward in concept, it is quite difficult to obtain definitive results because of (1) numerical difficulties associated with distorted meshes and (2) sensitivities to mesh refinement. Although there are additional problems as well, it is these two difficulties that we address in the present work.

Modeling is done in 2-D using the computer code LASNEX. We model two ignition targets: the NIF point design and France's Limeil 1000. Both targets consist of a bromine-doped plastic shell encapsulating a shell of DT ice which in turn contains DT gas. The calculations incorporate the surface roughness present on the outside of the plastic ablator shell and the roughness present on the inside of the DT ice. These are multimode calculations in that 24 modes are imposed on each surface. The model capsules are driven with an isotropically uniform radiation field.

Because these calculations follow the evolution of perturbation growth far into the nonlinear regime, severe distortions eventually develop in the mesh. Initial calculations of the Limeil 1000 showed some surprising and erratic behavior which has now been traced to an interaction between mesh hour-glassing and the perturbations. We found that during the evolution, perturbation growth eventually seeds hour-glassing in the mesh. This hour-glassing spreads just outside the ablation surface and, through some unidentified means, unrealistically enhances the growth of the perturbations. Results of calculations with and without this instability will be presented. We have also found that the NIF capsule results are sensitive to the zoning employed in the calculations. Lastly, we will present our current best estimates of the limits that need to be placed on the RMS roughness of both surfaces.

Simulations of Laser Imprint on Nova, Vulcan, and NIF

S. V. Weber, S. G. Glendinning, D. H. Kalantar, B. A. Remington, J. E. Rothenberg
Lawrence Livermore National Laboratory, Livermore, CA 94551

M.H. Key and E. Wolfram
Rutherford Appleton Laboratory

C.P. Verdon and J.P. Knauer
Laboratory for Laser Energetics, University of Rochester

In direct drive ICF, nonuniformities in laser illumination seed ripples at the ablation front in a process called imprint. These nonuniformities grow during the capsule implosion and can penetrate the capsule shell, impede ignition, or degrade burn. We have simulated imprint for several recent experiments performed on the Nova laser at LLNL and on the Vulcan laser at Rutherford Lab. One set of Nova experiments measure imprint for planar CH₂ foils probed with a thermal (U) x-ray backlighter at ~1.5 keV. These foils were illuminated with 0.53 or 0.35 μm light using random phase plates, with or without SSD smoothing. Another Nova experiment employs a Y XUV laser to probe imprint of 0.35 μm light on 3 μm thick Si foils. The Vulcan experiments measure imprint of 0.53 μm light on 2 mm thick Al foils probed with a Ge XUV laser, for variety of beam smoothing conditions. Most of these experiment use laser intensities similar to the early part of an ignition capsule pulse shape, $I \cong 10^{13}$ W/cm². We will present comparisons of these imprint measurements with simulations. We have also simulated imprint upon National Ignition Facility (NIF) direct drive ignition capsules. We will show simulated imprint amplitudes and resulting shell modulation though the course of the implosion. SSD with 0.5 THz bandwidth is predicted to give an imprint modulation amplitude comparable to an intrinsic surface finish of ~40 nm rms. Imprinted modulation is treated as an equivalent surface finish for the purpose of addressing the modulation growth through the implosion and stagnation of the capsule shell. This growth has been examined both by the Haan model, where linear growth factors as a function of spherical harmonic mode number are obtained from an analytic dispersion relation, and by direct numerical simulation using two-dimensional multimode LASNEX calculations. This analysis may be used to set beam smoothing requirements for the laser.

* Work performed under the auspices of the U. S. Department of Energy by the Lawrence Livermore National Laboratory under Contract W-7405-ENG-48.

Megajoule Scale Direct-Drive Target Designs Using KrF Lasers*

Andrew J. Schmitt, Denis Colombant

Plasma Physics Division, Naval Research Laboratory, Washington, DC 20375

John H. Gardner

Laboratory for Computational Physics and Fluid Dynamics, Naval Research Laboratory, Washington, DC 20375

Direct-drive ICF has the potential of high gain using minimal laser pulse energy because of the relatively high coupling of laser energy to the target. However, the potential high gain is limited by the ablative Rayleigh-Taylor (RT) hydrodynamic instability: Higher gain requires lower fuel isentrope, which implies higher RT growth rates. Ablative RT growth rates for the lowest adiabat pellets, combined with the seed amplitudes one expects from fabrication and laser imprinting, predict failure of the fuel shell integrity even before shell deceleration occurs.

Final RT perturbations can be reduced both by minimizing the initial perturbation and by reducing the instability growth rates. The initial perturbation can be minimized in part with optically smoothed laser drive which reduces the laser imprinting. Reduction of RT growth rates is accomplished by increasing the ablation velocity and/or increasing the ablation density scalelength, both of which require increasing the ablator isentrope. If the fuel isentrope is also raised, however, the target gain drops.

We are developing large scale direct-drive targets using our 1D hydrocode^[1] as the initial design tool. Stability constraints are a posteriori calculated by a conventional multimode Takabe-Haan type quasi-linear growth model^[2] and further evaluated with 2D spherical hydrocode simulations^[3]. The resulting designs explore tradeoffs between gain and hydrodynamic stability. Pure DT and multilayer plastic-foam/DT designs are considered and compared.

1. A.J. Schmitt, D. Colombant, and J.H. Gardner, document in preparation; A.J. Schmitt, D. Colombant, J.P. Dahlburg, and J.H. Gardner, *Bull. Am. Phys. Soc.* 39, 1683 (1994).
2. H. Takabe, K. Mima, L. Montierth, and R.L. Morse, *Phys. Fluids* 28, 3676 (1985); S.W. Haan, *Phys. Rev. A* 39, 5812 (1989).
3. J.H. Gardner et al., this conference.

*Supported by U.S. Department of Energy

Laser-Driven Hydrodynamics Experiments at Nova

B.A. Remington, S.G. Glendinning, D.H. Kalantar, K.S. Budil, M.M. Marinak,
S.V. Weber, J. Colvin, D. Griswold
LLNL, Livermore, CA 94550

J.P. Knauer
LLE, Rochester, NY

M. Key, RAL
UK

W.W. Hsing
LANL, Los Alamos, NM

D. Galmiche
CEA Centre d'Etudes de Limeil-Valenton, France

A. Rubenchik
Univ. of Calif.-Davis

J. Kane, W.D. Arnett
Univ. of Arizona, Tucson, AZ

W.M. Wood-Vasey
Harvey Mudd College, Claremont, CA

Hydrodynamic instabilities play a critical role in inertial confinement fusion capsule performance, both in direct and in indirect drive. In our indirect-drive work at the Nova laser, we have examined the effects on Rayleigh-Taylor (RT) growth of 2D versus 3D single-mode perturbation shape,^[1] and perturbation location at the ablation front versus at an embedded interface.^[2] In our current experiments, we are investigating multimode coupling effects at an imbedded interface,^[3] the differences in single-mode RT growth in planar versus convergent geometry using face-on radiography of hemispherical implosions, and the RT dispersion curve of an unstable embedded interface in the solid state versus liquid state.^[4] In the solid-state experiment, our initial efforts are focused on characterizing the state of samples of Si and Cu as they get compressed, while remaining in the solid state.

In our direct-drive work, we have measured the RT dispersion curve in the linear regime over perturbation wavelengths of 20-70 nm, using a 1D SSD smoothed, $\lambda_{\text{laser}} = 0.528 \mu\text{m}$ (green) single Nova beam at $I = 1 \times 10^{14} \text{ W/cm}^2$. We are also examining the critical issue of laser imprinting, using both thin foils of Si with an XUV backlighter^[6] and drive laser at $\lambda_{\text{laser}} = 0.351 \mu\text{m}$ (blue), $I = 3 \times 10^{12} \text{ W/cm}^2$, and thick foils of CH_2 with an U backlighter⁶ and drive laser at $\lambda_{\text{laser}} = 0.528 \mu\text{m}$, $I = 1 \times 10^{14} \text{ W/cm}^2$. Our latest experiments compare imprint from blue versus green laser light under similar gross hydrodynamics. The

drive laser was smoothed only with a static random phase plate, the intensity was held fixed at $I = 1 \times 10^{13} \text{ W/cm}^2$, and the lasers were subapertured (f/11 for green, f/15.6 for blue) to have the same speckle power spectrum. Data and simulations both indicate that the imprint from the blue laser is considerably larger than that from the green laser,^[7] consistent with the simple picture of smoothing via a thermal standoff layer.

Under the new university use of Nova program, we have initiated an experiment on the Nova laser in collaboration with the University of Arizona to investigate specific issues regarding hydrodynamic instabilities in supernovae.^[8] The goal is to investigate the evolution of the Richtmyer-Meshkov and RT instabilities in the deep nonlinear regime in a scaled setting similar to that occurring at the He-H interface of a Type II supernova.

1. M.M. Marinak et al., Phys. Rev. Lett. 75, 3677 (1995); K.S. Budil et al., in preparation for submittal to Phys. Plasmas (1996).
2. K.S. Budil et al., Phys. Rev. Lett. 76, 4536 (1996).
3. K.S. Budil et al., Rev. Sci. Instrum., in press (1996).
4. E.M. Campbell, N.C. Holmes, S.B. Libby, B.A. Remington, and E. Teller, in preparation for submittal to Laser and Part. Beams (1996).
5. D.H. Kalantar, Phys. Rev. Lett. 76, 3574 (1996); Rev. Sci. Instrum., in press (1996).
6. S.G. Glendinning et al., Phys. Rev. E, in press (1996).
7. S.G. Glendinning, in preparation for submittal to Phys. Rev. Lett. (1996).
8. J. Kane et al., ICF Quarterly Report (1996), and in preparation for submittal to the Astrophysical Journal (1996); E.M. Campbell, Bull. Am. Phys. Soc. 41, 933 (1996).

*Work performed under the auspices of the U.S. Department of Energy by the Lawrence Livermore National Laboratory under contract number W-7405-ENG-48.

Tetrahedral Hohlräume on the Nif

J.D. Schnittman^a and S.M. Pollaine

Lawrence Livermore National Laboratory, Livermore, California 94550

^aAlso University of Rochester, Laboratory for Laser Energetics, Rochester, NY 14623

Spherical hohlraums with four laser entrance holes (LEH's) arranged in a tetrahedral geometry promise an alternative approach to designing indirect drive targets for the National Ignition Facility (NIF). With the current target chamber design, a tetrahedral hohlraum could be illuminated by 44 of the 48 NIF laser beams with radiation temperatures of 300 eV and high radiation uniformity throughout the laser pulse. The symmetry on the capsule has been evaluated in terms of spherical-harmonic modes, including in particular the higher modes which are more likely to lead to Rayleigh-Taylor instability.

The principal issues to be considered in designing a tetrahedral hohlraum include clearances between the laser beams and the LEH's and the fuel capsule. By varying the locations of the LEH's on the sphere with respect to the target chamber, the trade-off between the minimum and maximum clearance angles has been analyzed. The effect of laser refraction caused by ablating plasma within the hohlraum has also been investigated. A robustness study has been carried out to look at the effects on uniformity of inexact beam pointing and variations in laser beam energies (up to 8%). Using realistic numbers, sufficient radiation uniformity should still be achieved. A detailed NIF design for tetrahedral hohlraums is proposed with good uniformity for the duration of the laser pulse.

* This work was partially supported by the U.S. Department of Energy Office of Inertial Confinement Fusion under Cooperative Agreement No. DE-FC03-92SF19460, the University of Rochester, and the New York State Energy Research and Development Authority. The support of the DOE does not constitute an endorsement by DOE of the views expressed in this article.

Joints and Gaps in ICF Targets

S.R. Goldman, I.D. Wallace and D.C. Wilson

Los Alamos National Laboratory

Spherical copper doped beryllium capsules with an inside layer of DT ice are being considered as alternative targets for the NIF. In comparison to targets with plastic shells, the spherical shell must be formed by bonding two hemispheres. This necessitates a material discontinuity along the juncture of the hemispheres. Gaps could exist in the bond as long as DT from the interior of the spherical shell does not have an open path to the outside. Mismatches in the inner or outer shell surfaces are also possible across the interface.

The essential problem is to determine the effect of various types of joints and gaps on the NF target, and, in coordination with target fabrication efforts, to design junctures to minimize drive inhomogeneities. In a general sense, joint dynamics, which can be sensitive to radiative preheat, includes the effect of joints with density and opacity which separately can be either greater or less than the corresponding quantities for copper doped beryllium. We have compared simulations in Cartesian geometry for a joint within the NIF capsule, subject to the anticipated NS radiation drive, with simulations of aluminum or CH joints with NOVA drive. Typically, development of structure and drive non-uniformity in the capsule results from the interaction between the predominant drive, assumed parallel to the joint, and additional hydrodynamic motion perpendicular to the joint which extends outward into the surrounding copper doped beryllium.

The simulations have suggested experiments on NOVA to assess the effect and control of inhomogeneities due to joints. We will present our experimental results, as well as the theoretical basis.

Mix, Temperature, and Density Capsule Conditions in a 1-Ns Square Pulse Convergence Study

Greg D. Pollak and David B. Harris

Los Alamos National Laboratory, Los Alamos, NM 87545

A set of indirect drive capsule implosion experiments have been performed using a 1-ns square pulse. A variety of capsules were fielded, all with basically the same fabrication, but with different gas fills, ranging from 2 atmospheres to 50 atmospheres (DD). Neutron diagnostics included yield, ion-temperature, and fuel Rho-R. X-Ray diagnostics included K-shell streaked spectroscopy of Ar and Cl dopants, gated x-ray imaging, and absolutely calibrated time-integrated pinhole camera images. We compare these experimental data against various 1 and 2D calculations with and without mix.

Recent Indirect and Direct Drive Implosion Images taken with a Gated KB Microscope at the Omega Laser Facility

John A. Oertel, Tom Archuleta, and Frederic J. Marshall *

Los Alamos National Laboratory, POB 1663, Los Alamos, NM 87545

**University of Rochester, 250 E. River Rd., Rochester, NY 14623*

Development and testing of a dual microchannel plate (MCP) module to be used in the national Inertial Confinement Fusion (ICF) program has recently been completed. The first indirect drive target campaign and earlier direct drive implosions at the Omega upgrade laser have provided images of compressed cores to test this new diagnostic. The MCP module is a major component in the new Gated Monochromatic X-ray Imager (GMXI). This diagnostic, which has monochromatic capabilities, was designed around a 4 channel Kirkpatrick-Baez microscope and diffraction crystals. See figure 1. The MCP module has two separate MCP active regions with centers spaced 53 mm apart. Each active region contains a 25 mm MCP proximity focused to a P-11 phosphor coated fiberoptic faceplate. The two $L/D = 40$, MCPs have a 10.2 mm wide, 8 ohm stripline constructed of 5000 Å Copper over-coated with 1000 Å Gold. A 4 kV, 150 ps electrical pulse provides an optical gatewidth of < 80 ps and spatial resolution has been measured at better than 20 lp/mm. Specific details of the instrumentation will be discussed as well as data from the direct and indirect drive implosion experiments.

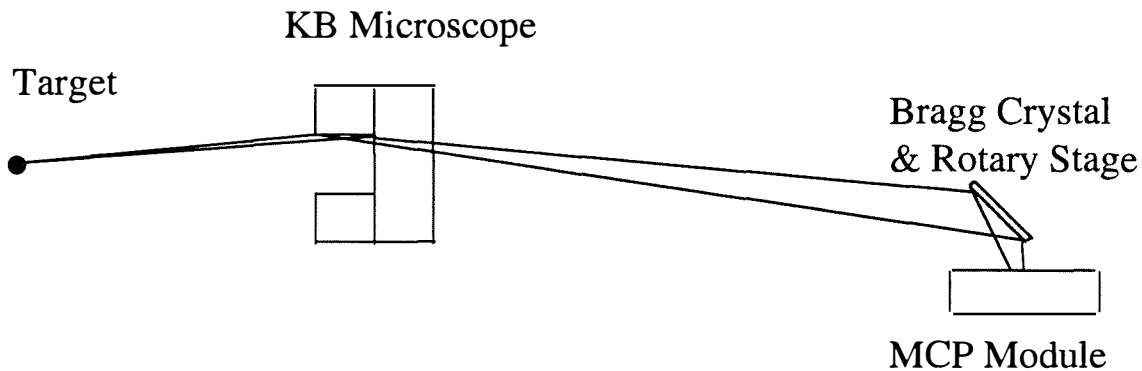


Figure 1. Schematic of the gated monochromatic imaging system.

* This work was performed under the auspices of the U. S. DOE by LANL under Contract No. W-7405-Eng-36.

Strongly-Driven Laser Plasmas with Self-Consistent Electron Distributions

William L. Kruer, Bedros B. Afeyan, Scott C. Wilks
Lawrence Livermore National Laboratory

Al Chou
University of California, Los Angeles

In high temperature hohlraums and many other applications,¹ the laser heated electrons have a zeroth-order distribution function which is quite different^{2,3} from Maxwellian. The numerous consequences include changes in the Landau damping and instability thresholds, reductions in the inverse bremsstrahlung coefficient, as well as changes in the heat transport, density profiles and atomic physics. In addition, unexpected absorption processes can be introduced. These absorption mechanisms are discussed and illustrated in PIC simulations.

1. For example, see talks by T. Orzechowski and R. Kirkwood (Anomalous Absorption Conference 1996).
2. A. B. Langdon, *Phys. Rev. Lett* **44**, 575 (1980); R. Jones and K. Lee, *Phys Fluids* **25**, 2307 (1982).
3. For general distributions, see J.P. Matte et al., *Plasma Phys. Conf. Fusion* **30**, 1665 (1988).

* Work performed under the auspices of the U.S. Department of Energy by the Lawrence Livermore National Laboratory under Contract W-7405-ENG-48.

Multi-Beam Pump Driven Raman Instability

N. Guzdar

Institute for Plasma Research, University of Maryland, College Park, MD

H. Lehmberg

Plasma Physics Division, Naval Research Laboratory, Washington, D.C.

The NIKE KrF laser facility at NRL consists of a 2D array of multiple beams which focus onto a planar target. The finite angle between the beams and the specific geometry gives rise to SRS with one plasma wave and multiple back-scattered waves or a single back-scattered wave with multiple plasma waves. We have developed a 2D code for SRS which has a realistic geometry for the multi-mode pump wave. The code computes the threshold for the onset of SRS averaged over many realizations. The symmetry of the beam geometry with respect to the axis, normal to the planar target, is very important in determining the threshold for SRS. The spectral characteristics of the scattered waves as well the plasma waves for intensities beyond the threshold value is also obtained. We have made a systematic study of the threshold as a function of the number of beams as well as the angle between the beams. The code has been developed to study SRS in homogeneous as well as inhomogeneous plasmas.

Self-Focusing Instabilities in the Presence of Quasi-Random Density Fluctuations in Plasmas

P. K. Chaturvedi, P. N. Guzdar and K. Papadopoulos
University of Maryland, 1 College Park, MD

L. Ossakow

Plasma Physics Division, Naval Research Laboratory, Washington, D.C.

We have studied the thermal self-focusing instability (SFI) in the presence of quasi-random density irregularities in under-dense plasma. The role of the amplitude of the irregularity and its correlation length on SFI has been examined. We find that a modest level of density fluctuations (1%-5%) leads to excitation of a broad band spectrum of SFI. Typically modes with wave-numbers five to ten times larger than the marginally stable mode (for the homogeneous plasma) can be excited because of the background fluctuations. The spectrum of the side band falls off as k^{-2} . The present model predicts that the long wavelength and the short wavelength modes (coupled through the pre-existing density irregularity) grow at the same rate. The study of SFI is being extended to the critical surface in an inhomogeneous plasma.

Filamentation and Beam Deflection in Flowing Plasmas: Latest Results

D. E. Hinkel, E.A. Williams, R.L. Berger, and A.B. Langdon
Lawrence Livermore National Laboratory, Livermore, CA 94550

It has been recently shown^{1,2} that transverse plasma flow deflects the laser beam in the direction of the flow. Analytic estimates of a single Gaussian hotspot predict that when the flow is subsonic ($M < 1$, where M is the Mach number flow), beam deflection scales as $M/(2-M^2)^2$. F3D simulations support this scaling. Transverse plasma flow also enhances filamentation. Subsonic flow estimates for a single-Gaussian-hotspot are that the spatial gain rate of the beam width scales as $1/(1-M^2/2)$, i.e., filamentation is greater by 50% in plasma with $M=1$ than in plasma with $M=0$. F3D simulations show a similar trend. We have also performed a series of simulations quantifying the effects of SSD³ (smoothing by spectral dispersion) with and without multiple color cycles, and different flow profiles on both an $f/4$ and an $f/8$ RPP beam. Critically dispersed SSD with $\sim 3 \text{ \AA}$ of bandwidth (before frequency conversion) is sufficient to suppress beam deflection and filamentation with flow for Scale 1 hohlraum parameters near peak power, i.e., $n/n_c = 0.1$, $T_e = 3 \text{ keV}$, $I = 3 \times 10^{15} \text{ W/cm}^2$. Multiple color cycles have little benefit on beam deflection or filamentation beyond that obtained with one color cycle at a fixed bandwidth. The orientation of the SSD dispersion direction with respect to the transverse flow direction has a small effect of beam deflection suppression. On time scales short compared to an FM cycle, SSD itself leads to "beam deflection," an effect that time averages to zero over the period of an FM cycle.

1. H.A. Rose, Phys. Plasmas **3**, 1709 (1996).
2. D.E. Hinkel, E.A. Williams and C.H. Still submitted to Phys. Rev. Lett., 01/96.
3. S. Skupsky et al., J. Appl. Phys. **66**, 3456 (1989).

* Work performed under the auspices of the U.S. Department of Energy by the Lawrence Livermore National Laboratory under Contract No. W-7405-ENG-48.

Three-Dimensional Modeling of Laser Propagation in the Presence of a Random Phase Plate

B. Bezzerides, H.X. Vu, C.A. Thompson, and J.M. Wallace

Applied Theoretical and Computational Physics Division, Los Alamos National Laboratory, Los Alamos, NM 87545

The Random Phase Plate (RPP) has recently come under consideration as a means of smoothing spatial irradiance profiles for Inertial Confinement Fusion (ICF) applications. Although the RPP removes long-wavelength inhomogeneities, short-wavelength structures (hotspots) are introduced. The hotspots can induce filamentation and self-focusing in laser-produced plasmas typical of ICF, thereby affecting laser propagation and potentially causing additional parametric processes. It is therefore important that one understands the spatial and statistical properties of the laser beam in the presence of a RPP. A method is presented in which an analytic formulation and a numerical algorithm are combined to give a computationally efficient scheme for obtaining spatially-resolved laser intensities over an extended three-dimensional volume in the presence of a RPP. This method has been implemented on a CRAY-T3D, and has been used to compute three-dimensional laser intensity profiles from which laser intensity and hotspot distributions can be obtained. These results will be presented together with a description of the numerical scheme.

Spatial and Temporal Laser Smoothing Effects

D. Mourenas¹, S. Hüller¹, M. Casanova¹, Ph. Mounaix², D. Pesme³

¹*CEL-V/CEA, 94195 Villeneuve St. Georges Cedex, France*

²*CPHT, Ecole Polytechnique, Palaiseau, France* ³*LULI, Ecole Polytechnique, Palaiseau, France*

Results from a 2D numerical model treating the interaction between a smoothed laser beam and an underdense plasma are presented. The model includes both filamentation and stimulated Brillouin scattering (SBS) without resorting to paraxial approximation. Significant levels of Brillouin reflectivity are obtained for parameters comparable to NIF or LMJ projects. The Brillouin scattering displays a great temporal and angular variability in case of ISI beam smoothing.

Piranah: A Post-Processor to Model Laser-Plasma Interactions

M. Casanova, L. Divol

C.E.A., Centre d'Etudes de Limeil-Valenton
94195 Villeneuve, St. Georges, Cedex FRANCE

In order to estimate roughly the effects of parametric instabilities in laser-plasma interactions, we have developed a post-processor for the Limeil simulation codes FCI1 and FCI2. Such a post-processor may be used to plan and analyze experiments, to obtain estimates for target design, or to study combined effects. The model is based on standard gain calculations in the convective regime^[1-5]. The validity of this model is assessed by computing absolute thresholds in the corona^[6]. The instabilities considered are stimulated Raman and Brillouin scattering in the hydrodynamic and kinetic regimes. Application of the model to recent experiments will be discussed.

1. L. M. Gorbunov, A. N. Polyanichev, *Sov. J. Plasma Phys.* 5, 316 (1979).
2. G. R. Mitchel, T. W. Johnston, H. Pepin, *Phys. Fluids* 26, 2292 (1983).
3. W. Seka, E. A. Williams, R. S. Craxton, L. M. Goldman, R. W. Short, K. Tanaka, *Phys. Fluids* 27, 2181 (1984).
4. R. L. Berger, E. A. Williams, A. Simon, *Phys. Fluids B* 1, 414 (1989); B. J. MacGowan *et al.*, *Phys. Plasmas* 3, 2029 (1996).
5. B. Bezzerides, H. X. Vu, J. M. Wallace, *Phys. Plasmas* 3, 1073 (1996).
6. D. Pesme, in *La fusion thermonucleaire inertielle par laser*, edited by R. Dautray and J. P. Watteau (Collection du Commissariat a l'Energie Atomique, Eyrolles, 1993), Vol. 1, pp. 363-386.

Measurement of Near-wp Light as Evidence of the Electromagnetic Decay Instability

K. Wharton, R. Kirkwood, B. Afeyan, C. Back, R. Berger, M. Blain, K. Estabrook,
S. Glenzer, W. Kruer, B. MacGowan, J. Moody

Lawrence Livermore National Laboratory, Livermore, CA 94550

We report on experiments which measure electromagnetic emission near the plasma frequency from laser produced plasmas at the Nova laser facility. The measurement is motivated by earlier studies¹ which indicate that the SRS generated electron plasma wave is stimulating a secondary decay involving an ion wave and a third wave. The Electromagnetic Decay Instability (EDI) is a secondary decay process in which the electron plasma wave decays into both an ion wave and a light wave near wp. Because this instability inhibits the growth of SRS it may affect the fraction of scattered light in a wide variety of laser-plasma experiments. Experiments to measure both SRS and EDI spectra in both thin foils and gas-filled targets will be discussed.

1. R. K. Kirkwood et. al., submitted to Phys. Rev. Lett. and also at this conference.

* Work performed under the auspices of the U.S. Department of Energy by the Lawrence Livermore National Laboratory under contract number W-7405-ENG-48.

Spreading of Intense Laser Beams in Underdense Plasmas

V. Eliseev*, I. Ourdev, W. Rozmus and V.T. Tikhonchuk*
Department of Physics, University of Alberta, Edmonton, Canada

C.E. Capjack
Department of Electrical Engineering, University of Alberta, Edmonton, Canada

P.E. Young
Lawrence Livermore National Laboratory, Livermore, CA, USA

We present results of multidimensional numerical studies employing our nonparaxial wave interaction code^[1]. For parameters of the experiment^[2], we have confirmed the important role of filamentation and self-focusing as explained in the previous interpretation of the measurements^[3]. However, we also found that the stimulated Brillouin scattering affects in an essential way most of the processes occurring during the beam propagation in a plasma. The initial dynamical evolution of backscattered light reflectivity is affected by self-focusing and displays characteristic time oscillations. The forward and side Brillouin scattering instabilities are the main contributors to transmitted light spreading. Initially the filamentation instability provides enhancement of ion acoustic fluctuations which scatter the light and provide the seed for the forward SBS. At later times, the scattering instability is a dominant factor. The angular spread of the laser beam is defined by the side SBS gain and the width of the pump in the front of the target. After accounting for the additional increase in the pump width due to nonlinear evolution of self-focusing we have obtained good agreement between linear side SBS growth estimates and results of full simulations. Experimentally observed spectra of transmitted light is red-shifted in agreement with a SBS scenario.

1. V. Eliseev, W. Rozmus, V. T. Tikhonchuk, and C. E. Capjack, *Phys. Plasmas*, 2, 1712 (1995); 3, 2215 (1996).
2. P. E. Young, et al., *Phys. Plasmas* 2, 7 (1995); *Phys. Rev. Lett.* 75, 1082 (1996).
3. S. Wilks, P. E. Young, J. Hammer, M. Tabak, and W. L. Kruer, *Phys. Rev. Lett.* 73, 2994 (1994).

* On leave from Russian Academy of Sciences, Moscow, Russia.

Nonlocal Electron Transport Inferred from Thomson Scattering by Thermal Fluctuations

J.F. Myatt, V. Yu. Bychenkov*, W. Rozmus, and V.T. Tikhonchuk*

Department of Physics, University of Alberta, Edmonton, Canada

This work is concerned with the theoretical description of low frequency thermal fluctuations in plasmas. In particular, we focus our attention on the ion acoustic resonance in the Thomson scattering cross section. The latter is defined by the dynamical form factor, $S(k, \omega)$ — the Fourier transformed electron density fluctuation correlation function. Our theory of $S(k, \omega)$ encompasses a complete description of ion acoustic dispersion and damping over the full range of particle collisionality^[1]. The nonlocal electron heat conductivity associated with these waves has also been included. These results have been achieved by two methods. First, in the phenomenological approach we start from the fully nonlocal formulation of the electron hydrodynamics^[2]. We assume that this closed, linearized system of fluid equations describes the evolution of hydrodynamical fluctuations, including the fluctuations of electron density, δn^e . Solving for δn^e we can construct $S(k, \omega)$ using the appropriate initial conditions defined by the equilibrium correlation function. In the second approach we solve the rigorous kinetic equation for the phase space density fluctuation correlation function by the method of Ref. 2. Both approaches lead to the same expression for $S(k, \omega)$, which is examined in the vicinity of the ion acoustic resonance in the weakly collisional regime. As an example, we have identified a region of plasma parameters ($Z \sim 30$, $T_e \sim 100\text{eV}$, $n_e \sim 10^{21}/\text{cm}^3$) where by scattering from ion acoustic waves at different wave numbers (e.g. $0.01 < k\lambda_{ei} < 0.1$) one can observe distinct characteristics of the ion acoustic resonance that can be attributed to nonlocal electron thermal conductivity.

1. V. Yu. Bychenkov, J. Myatt, W. Rozmus and V. T. Tikhonchuk. Phys. Rev. E. 52 6759 (1995); *ibid* 50, 5134 (1994); Phys. Plasmas 1, 2419 (1994).
2. V. Yu. Bychenkov, W. Rozmus, V. T. Tikhonchuk, and A. V. Brantov, Phys. Rev. Lett. 75, 4405 (1995).

* On leave from Russian Academy of Sciences, Moscow, Russia.

Effects of Laser-Plasma Interactions on Light Transmitted Through Nova Gasbag Plasmas

J.D. Moody, B.J. MacGowan, R.K. Kirkwood, C.A. Back, S.H. Glenzer, D.E. Munro,
and R.L. Berger

Lawrence Livermore National Laboratory, Livermore, CA, 94550

Measurements of the angular spreading and spectra of the light transmitted through Nova gasbag plasmas show features which may suggest the presence of filamentation. A single probe beam at 351 nm having intensity ranging from $0.8 \times 10^{15} \text{W/cm}^2$ to $6 \times 10^{15} \text{W/cm}^2$, and probe f/number either 4.3 or 8, impinges on a Nova gasbag target with plasma having $T_e = 3$ to 4 keV and $n_e/n_{cr} = 0.07$ to 0.15. We find that the angular divergence increases with increasing intensity and that the narrowband spectra near 351 nm broadens with increasing intensity. Changing the plasma density also leads to changes in the angular spreading and narrowband spectra. We compare the measurements with calculations of refraction and filamentation using the hydrodynamic code Lasnex and the three dimensional filamentation code F3D.

* Work performed under the auspices of the U. S. Department of Energy by the Lawrence Livermore National Laboratory under contract number W-7405-ENG-48.

X-Ray Emission from Plasmas Produced by Ultra-Short Pulse Lasers

R.S. Walling, R.L. Shepherd, R.M. More, A.L. Osterheld, R.W. Lee, R.E. Stewart
Lawrence Livermore National Laboratory, Livermore, CA 94551

Several applications drive a strong interest in creating X-ray emission of short temporal duration. Plasmas heated rapidly by 100-fs lasers may provide one possible method. Now experiments with picosecond time resolution are providing time-resolved spectra that may help us understand the time history of the X-ray emission from plasmas produced by these lasers.

We use the LASNEX hydrodynamics code for simulations of the energy absorption, conduction, and target compression and expansion. For K-shell spectra, we use a more sophisticated NLTE model for the aluminum emission and postprocess the hydrodynamics calculation.

We apply these techniques to spectra from recent experiments on the LLNL Ultra-Short-Pulse (USP) Laser Experimental Facility.

* Work performed under the auspices of the U.S. Dept. of Energy by the Lawrence Livermore National Laboratory under Contract No. W-7405-Eng-48.

19.6 nm XUV Laser Probing of Laser-Produced Plasma

K. Takahashi, R. Kodama, K.A. Tanaka, H. Hashimoto, H. Daido, Y. Kato and K. Mima
Institute of Laser Engineering, Osaka University, 2-6 Yamada-oka Suita, Osaka 565, Japan

H. Takenaka

NTT Interdisciplinary Research Laboratories

L.B. DaSilva, A. Wan and T.W. Barbee

Lawrence Livermore National Laboratory

Recent progress in the development of collisionally pumped XUV lasers is opening up the possibility of using these systems for a variety of applications. With its short wavelength (20 nm), high peak brightness, short controllable pulse and sufficient coherence, the XUV laser is ideally suited as probing high density and large plasmas relevant to inertial confinement fusion (ICF). The Ne-like Ge XUV laser (19.6 nm) has been made progress in the development at ILE. Its stable operation with small beam divergence ($<1-3$ mrad), short pulse duration (80 ps) and high brightness is now possible. We have used the 19.6 nm Ne-like Ge X-ray laser for probing laser-produced plasmas. Grid imaging optics with x-ray laser was examined to obtain the diffraction information in a plasma, which provided the density profile. X-ray backlighting was also demonstrated to image the modulation from laser imprint on a foil target.

The experiments were carried out using the GEKKO XII laser system at Osaka University. Plasma expansion was measured with a grid-imaging configuration using the x-ray laser probe system. The x-ray laser light side-light a CH pre-plasma created with $0.35 \mu\text{m}$ laser lights at 1 nsec before x-ray laser probing. The x-ray laser beam was relayed to a x-ray CCD camera with Mo/Si multilayered flat mirror. $120 \mu\text{m}$ thickness CH targets were irradiated to produce the pre-plasma with two beams at an intensity of 10^{14} W/cm^2 and a spot diameter of $300 \mu\text{m}$. $200 \mu\text{m}$ pitch mesh was set on the imaging point and the detector was set at 95 cm behind the focusing position.

We have also demonstrated transmission radiography of laser produced plasmas by using the 19.6 nm XUV laser for study of the hydrodynamic imprinting of laser pattern. We will show details at the poster session.

Calculations of a Compact Ni-like Tungsten Soft X-ray Laser

Chris D. Decker and Richard A. London

Lawrence Livermore National Laboratory, Livermore, CA 94550

We propose a scheme for a compact nickel-like tungsten soft x-ray laser operating on the $4d - 4p, J = 0-1$ transition at 43.1 \AA . High gains are achieved by operating at high electron densities ($n_e > 10^{22} \text{ cm}^{-3}$) for short times ($t < \text{psec}$). In this regime the gain during non-equilibrium ionization can greatly exceed that of the steady state. The duration of this transient gain is on the order of the ionization time which makes picosecond-pulsed high-intensity ($I > 10^{16} \text{ W/cm}^2$) optical pumps ideal. Target designs including solid tungsten targets and high Z-foams are considered. Techniques to maximize the spatial extent of the gain and techniques of minimizing refraction of the x-rays are discussed.

*Work performed under the auspices of the U.S. Department of Energy by the Lawrence Livermore National Laboratory under Contract W-7405-ENG-48.

Stimulated Raman Backscattering Instability In Short Pulse Laser Interaction With Helium Gas

V. Malka, E. DeWispelaere, J.R. Marquès, R. Bonadio, F. Amiranoff

**Laboratoire pour l'Utilisation des Lasers Intenses, Ecole Polytechnique, 91128 Palaiseau Cedex, FRANCE*

Ph. Mounaix

Centre de Physique Théorique, Ecole Polytechnique, 91128 Palaiseau, FRANCE

G. Grillon, E. Nibbering

**Laboratoire d'Optique Appliquée, Ecole Nationale Supérieure des Techniques Avancées, 91120 Palaiseau, FRANCE*

Experimental and theoretical results on the stimulated Raman backscattering (SRS) reflectivity of a 0.8 μm short laser pulse (120 fs) interaction with an optically-ionized helium gas are presented. The reflectivity is measured as a function of the gas pressure from 1 to 100 Torr. A mono dimensional (1D) theoretical model, including the refraction induced during the ionization process, describes the dependence of the SRS reflectivity with the gas pressure and explains its maximum at around 35 Torr. In the very low pressure case (<15 Torr), the radial ponderomotive force expels the electrons out of the propagation region before the laser pulse reaches its peak intensity and significantly reduces the observed reflectivity. A 1-D hydrodynamic calculation, included in the model, describes this density depletion and a good agreement is obtained between theory and experiments in the whole range of pressures.

* Laboratoires associés au Centre National de la Recherche Scientifique.

Brillouin Scattering of Picosecond Laser Pulses in Preformed, Short-Scale-Length Plasmas

A.C. Gaeris, Y. Fisher, J.A. Delettrez, and D.D. Meyerhofer
Laboratory For Laser Energetics, University of Rochester

Brillouin scattering (BS) has been studied in short-scale-length plasmas. The backscattered and specularly reflected light resulting from the interaction of high-power picosecond pulses with preformed silicon plasmas has been measured.

A first laser pulse forms a short-scale-length plasma without significant BS—while a second delayed pulse ($0 \leq \Delta\tau \leq 1600$ ps) interacts with an expanded, drifting underdense region of the plasma ($0 \leq L_n \leq 600 \lambda_L$). The pulses are generated by the T³ laser operating at $\lambda_L = 1054$ nm, with intensities up to 10^{16} W/cm² and prepulse to main pulse ratios of 0.1 to 10.

The backscattered light spectra, threshold intensities, and enhanced reflectivities at both P- and S-polarization have been determined for different plasma density scale lengths. The results are compared to Liu, Rosenbluth, and White's^[1,2] WKB treatment of stimulated Brillouin scattering in inhomogeneous drifting plasmas.

1. C. S. Liu, M. N. Rosenbluth, and R. B. White, *Phys. Fluids* 17, 1211 (1974).
2. C. S. Liu and P. K. Kaw, in *Advances in Plasma Physics*, edited by P. K. Kaw, W. L. Kruer, C. S. Liu, and K. Nishikawa, *Parametric Instabilities in Plasma, Part I*, (Wiley, New York, 1976), Vol. 6.

* This work was supported by the U.S. Department of Energy Office of Inertial Confinement Fusion under Cooperative Agreement No. DE-FC03-92SF19460, the University of Rochester, and the New York State Energy Research and Development Authority. The support of DOE does not constitute an endorsement by DOE of the views expressed in this article.

The Physics of the Nonlinear Optics of Plasmas at Relativistic Intensities

W.B. Mori

*Departments of Electrical Engineering, and Physics and Astronomy
University of California of Los Angeles, Los Angeles, CA 90095*

The nonlinear optics of plasmas at relativistic intensities is analyzed using only the physically intuitive processes of longitudinal bunching of laser energy, transverse focusing of laser energy, and photon acceleration, together with the assumption of conservation of photons, i.e. the classical action. All that is required are the well known formula for the phase and group velocity of light in plasma, and the effects of the ponderomotive force on the dielectric function. This formalism is useful when the dielectric function of the plasma is almost constant in the frame of the light wave. This is the case for Raman forward scattering (RFS), envelope self-modulation (SM), relativistic self-focusing (SF), and relativistic self-phase modulation (SPM). In the past, the growth rates for RFS and SPM have been derived in terms of wave-wave interactions. Here we rederive all of the aforementioned processes in terms of longitudinal bunching, transverse focusing and photon acceleration. As a result the physical mechanisms behind each are made clear and the relationship between RFS and envelope SM is made explicitly clear. This allows a single differential equation to be obtained which couples RFS, SM and SF, so that the relative importance between each process can now be predicted for given experimental conditions. In addition new instabilities are recognized.

* Work supported by LLNL contract no. 4-444-25-DA-26955 and DOE grant no. DE-FG03-92ER40727.

Generation of Higher-Order Gaussian Modes from the Coupling Between RFS and Relativistic Self-Focusing

K.-C. Tzeng and W.B. Mori

*Departments of Electrical Engineering, and Physics and Astronomy
University of California of Los Angeles, Los Angeles, CA 90095*

In conventional analyses of relativistic self-focusing and envelope self-modulation of Gaussian laser pulses it is assumed that the pulse remains a Gaussian. We find in PIC simulations that the pulse evolution is much more complicated than this and the laser intensity contours show distinct shapes. Therefore, envelope self-modulation cannot be accurately described as a simple spot size modulation. We show that if instead the laser pulse is first deconvolved into pump, Stokes and anti-Stokes waves with each having its own spot size, focal position and mode number, then most contours observed in the simulations can be reproduced. If the mode number corresponds to an odd or even Hermite mode, it determines whether laser hosing or sausageing occurs. Such an analysis sheds light on how relativistic self-focusing affects the evolution of Raman forward scattering.

* Work supported by LLNL contract no. 4-444-25-DA-26955 and DOE grant no. DE-FG03-92ER40727.

Observation of Raman Forward Scattering and Electron Acceleration in the Relativistic Regime

Z. Najmudin, A. Modena and A.E. Dangor
Imperial College, London, U.K.

C.E. Clayton, K.A. Marsh, P. Muggli and C. Joshi
UCLA, Los Angeles, USA

V. Malka
Ecole Polytechnique, Palaiseau, FR

C.N. Danson, D. Neely and F.N. Walsh
Rutherford Appleton Lab., Oxon, U.K.

Raman Forward Scattering (RFS) is observed in the interaction of a high intensity ($>10^{18}$ W/cm²) short pulse (<1 ps) laser with an underdense plasma ($n_e \sim 10^{19}$ cm⁻³). Electrons are trapped and accelerated to more than 80 MeV by the high amplitude plasma wave produced by RFS, indicating electric fields in excess of 100 GV/m. The laser spectrum is strongly modulated by the interaction, showing sidebands at the plasma frequency. Furthermore, as the quiver velocity of the electrons, in the high electric field of the laser beam, becomes relativistic, various effects are observed which can be attributed to the variation of electron mass with laser intensity. Signature of self-channeling is also observed which indicates that the laser propagates for 10 times the Rayleigh length in the plasma.

Half-Harmonic Forward Raman Scatter ($\omega_0 \pm \omega_{p/2}$)

T.C. Chiou, T. Katsouleas

*Department of Electrical Engineering-Electrophysics
University of Southern California, Los Angeles, CA 90089-0484*

W.B. Mori

University of California, Los Angeles, CA 90024

Recent experiments involving high intensity laser pulses ($I < 10^{18} \text{W/cm}^2$) have shown a Stoke component in the forward output spectrum at a frequency $\omega = \omega_0 - \omega_{p/2}$ where ω_0 is the laser frequency and $\omega_{p/2}$ is the plasma frequency. Interestingly, prior to our work, no clear evidence of this instability has been seen in Particle-In-Cell (PIC) simulations. The origin of this half-shift component is non-linearities in the wave equation due to the relativistic mass increase of quivering electrons. Previous analytic work by G. Shvets et al. predicted explosive growth rates for this instability. However, we find two effects neglected by this earlier work alter the instability considerably. These are the higher harmonic terms and the effect of regular Raman Forward Scattering (RFS).

Since regular RFS is always present even without relativistic effects, in our work we try to include the regular RFS and relativistic effects simultaneously. Our calculation shows that in fact the coupling of this half-shift component is through the higher harmonics of the laser. Specifically, the terms involving $2\omega_0 \pm \omega_p$ and $2\omega_0 \pm \omega_{p/2}$ dominate the coupling. Thus in PIC simulations the half-shift component may not appear unless the resolution is fine enough to resolve higher harmonics of the laser. After improving the resolution in our simulations, we observed this half-shift phenomenon for the first time. Our simulation results also show that this instability is even more robust than the regular RFS. That is, even when we seed a large noise source for the regular RFS, the half-shift term appears much earlier than the regular RFS. However, the amplitude of the half-shift seems to saturate and after the regular RFS has developed, the half-shift seems to be suppressed and the regular RFS becomes dominant.

Anomalous Absorption of Neutrinos in Dense Supernova Plasmas

R. Bingham,* J.M. Dawson† and S. Dalhed‡

The interaction of neutrinos with matter is an important topic in high energy astrophysics. How supernova explode is still an unsolved problem and depends critically on the transport of neutrinos within the star. During the implosion phase or collapse electron capture occurs, i.e. a proton and an electron coalesce to yield a neutron and a neutrino. The super-dense core is optically thick to the neutrinos and a thermal distribution results with a temperature of a few MeV. Due to the rapid density fall-off as one leaves the core, the stellar material becomes rapidly transparent to neutrinos. The core radiates neutrinos more or less like a black body at its temperature with a neutrino intensity of 3×10^{29} W/cm² at a distance of 300 km. The neutrinos carry away energy and entropy allowing the collapse process to accelerate. It is widely recognized that more than 1% of the total neutrino energy must be absorbed by electrons in the layers surrounding the super-dense core of the star for a supernova to explode. Previous studies have concentrated on collisional energy losses between neutrinos and electrons and nucleons. However, the loss rate is not sufficient to produce the required heating. We propose an entirely new neutrino interaction mechanism based on the coupling between the neutrinos and collective plasma oscillations in the dense plasma surrounding the core, namely stimulated neutrino-plasma scattering. The stimulated scattering process described has an analogy with laser coupling to plasma oscillation. Using the fluid or kinetic description for the plasma we obtain a set of coupled equations describing stimulated neutrino scattering in dense plasmas. We formulate the interaction in terms of the ponderomotive force which allows us to treat the problem of neutrino filamentation or self-focussing. Using the kinetic description we can treat high temperature plasmas, where the electron plasma waves are strongly Landau damped and the scattering process goes over to the equivalent of stimulated Compton Scattering.

For the particular problem of supernova neutrino plasma coupling we show that the anomalous absorption of neutrinos by plasma waves is orders of magnitude greater than collisional absorption, thus demonstrating the significance of collective effects between neutrinos and electrons during the explosive phase of supernova.

* Rutherford Appleton Laboratory, Chilton, Didcot, Oxon, OX11 0QX

† University of California, Los Angeles, Physics Department, Los Angeles, CA 90024-1547

‡ LLNL, Lawrence Livermore National Laboratory, Livermore

Tuesday

ORAL PRESENTATIONS

8:30 AM – 12:30 PM

Hydrodynamics

Erick Lindman, Session Chair

O-TUESDAY

Initial Mix Experiments on the 60-Beam Omega Laser System

D.K. Bradley, J.A. Delettrez, and P.A. Jaanimagi
Laboratory For Laser Energetics, University of Rochester

We present the results of experiments to study acceleration phase hydrodynamic instability growth in spherical targets imploded by the 30-kJ OMEGA laser system.¹ In these initial experiments, we are using the so-called burnthrough technique, where time-resolved x-ray spectroscopy is used to detect the onset of characteristic line emission from a signature layer buried under several microns of plastic. Previous works has shown that the emission time is highly sensitive to instability growth and is a strong indicator of incident drive nonuniformity. We have previously done an extensive study of the effects of drive-uniformity enhancements (through the use of SSD) and target parameter changes using the old 24-beam OMEGA system.² We now present our initial results for the upgraded 60-beam system, which will be used as our baseline measurements for subsequent uniformity and pulse-shape changes. The burnthrough times will be compared with 1-D simulations that include a mix model.

1. J. Delettrez, D. K. Bradley, P. A. Jaanimagi, and C. P. Verdon, Phys. Rev. A 41, 5583 (1990).
2. D. K. Bradley, J. A. Delettrez, and C. P. Verdon, Phys. Rev. Lett. 68, 2774 (1992); J. Delettrez, D. K. Bradley, and C. P. Verdon, Phys. Plasmas 1, 2342 (1994).

* This work was supported by the U.S. Department of Energy Office of Inertial Confinement Fusion under Cooperative Agreement No. DE-FC03-92SF19460, the University of Rochester, and the New York State Energy Research and Development Authority. The support of DOE does not constitute an endorsement by DOE of the views expressed in this article.

Measurement of Rayleigh-Taylor Growth of Regular and Random Perturbations Driven with Uniform Pressure from the Nike Laser

C.J. Pawley, S.P. Obenschain, V. Serlin, C.A. Sullivan, S.E. Bodner, D. Colombant,
J.P. Dahlburg, K. Gerber, R.H. Lehmborg, E.A. McLean, M.S. Pronko,
A.J. Schmitt, J.D. Sethian, J.A. Stamper

Code 6730, Plasma Physics Division, Naval Research Laboratory, Washington, D.C. , 20375

T. Lehecka, Y. Aglitskiy, A.V. Deniz, Y. Chan, J. Hargrove
Science Applications International Corp., Mclean, VA., 22102

J. Seely, C. Brown, U. Feldman
Code 7608, Space Science Division, Naval Research Laboratory, Washington, D.C. , 20375

J.H. Gardner
*Code 6440 Laboratory for Computational Physics, Naval Research Laboratory,
Washington, D.C. , 20375*

G. Holland, M. Laming
SFA Inc., Landover, MD. , 20785

M. Klapisch
Artep Inc., Columbia, MD. , 21045

The Nike KrF laser system provides a very uniform flat topped focal profile which allows precise measurements of Rayleigh-Taylor amplified perturbations under fusion-like conditions. We will be presenting recent measurements of mass perturbation growth using a backlighter and an X-Ray framing camera. The primary imaging method used 20 μm and 10 μm pinhole arrays. Images can be taken at four different times in one shot with 200-300 ps resolution. We also used a unique spherically curved quartz crystal at the Bragg angle for silicon He-like line radiation. This crystal imager only gave one image but was far more efficient than a pinhole and had a larger field of view. We have driven plastic targets with varying thickness from 20 to 60 μm . Some targets have impressed 60 and 30 μm wavelengths with peak to valley amplitudes as small as .25 μm as well as targets with .2 μm RMS randomly rough surface. The limits of the gray scale resolution and the spatial resolution of the camera determine the detectable perturbations of the plastic target to 5% mass variation and 10 μm diameter. The measured amplitudes of the perturbations will be compared with code results and expected growth factors for various wavelengths. Laser parameters for these shots are an approximately 750 μm FWHM flat-top profile with 900 to 1600 Joules on target in a 4 ns pulse with varying prepulse conditions. Side-on X-ray streaked imaging provide target acceleration data. Optical shock-breakout measurements and rear optical pyrometry measure the shock breakout uniformity and rear surface temperature.

* Work supported by the U. S. Department of Energy

lab

Direct-Drive Hydrodynamic Instability Experiments at GEKKO XII

H. Azechi, M. Nakai, K. Shigemori, N. Miyanaga, M. Honda, H. Shiraga, R. Kodama,
O. Maekawa, R. Isizaki, H. Takabe, K. Nishihara, and K. Mima

Institute of Laser Engineering, Osaka University, Yamada-oka, Suita, Osaka 565, JAPAN

When ablation pressure is first applied on an inertial-confinement-fusion target, a rippled shock wave is launched in accordance with a target surface perturbation, which is due either to the initial target manufacturing or to the imprint of the non-uniform laser irradiation. It has been shown^[1] that the rippled shock propagation amplifies the areal-density and momentum perturbations of the target. Such perturbation growth before the shock breakout will determine the initial condition of the subsequent R-T instability.

In this report, we will present accumulated database on the rippled shock propagation with varying initial perturbation. We will also present the first single-mode experiments on the initial imprint, where un-modulated targets were irradiated with the sinusoidally modulated laser light.

As for the R-T instability, material ablation on the unstable surface is expected to reduce the growth rate as it will remove the perturbation away from the surface^[2]. The R-T instability has been observed in the x-ray driven ablation^[3]. But for direct-drive experiments, care must be paid not to be dominated by initial imprinting. We will present the first imprint-free observation of the linear R-T growth rate in the target irradiated directly by laser.

Rippled shock wave: The polystyrene targets were uniformly irradiated by partially coherent light (PCL) at an intensity of 4×10^{13} W/cm². The perturbation wavelengths were either 60 or 100 μ m. Thicknesses and amplitudes of the targets were 25-160 μ m and 2-10 μ m, respectively. The following three quantities were measured: ripples of the shock front, perturbation of the areal density, and the perturbation of the laser-irradiated surface. The experiments have shown that the areal-density perturbations grow as a result of the damped oscillation of the rippled shock front, whereas the perturbations on the ablation front do not.

Imprint: The high irradiation uniformity of the PCL beams enables us to make a single-wavelength modulation on the beam pattern as the other Fourier components are significantly suppressed. Flat polystyrene targets with a 16- μ m thickness were irradiated with the PCL beam that consists of a foot pulse with a 1.8-ns width and a 5×10^{12} W/cm² intensity followed by a main pulse with the same width and a 1×10^{14} W/cm² intensity. The intensity modulation was imposed only on the foot pulse. The wavelength of the imposed modulation was 100 μ m and the amplitude was varied from 40% to 0% (no modulation) of the average intensity. The small imprint amplitude was amplified to be visible by the subsequent R-T instability driven by the uniform main pulse. Temporal evolution of the areal-density perturbation was observed by the face-on backlighting (see Fig. 1). For the 40% modulation case, the imprint amplitude was directly observed to be 0.7 μ m at the time of the first shock breakout. For the 10% modulation case, the amplitude was determined to be 0.3 μ m from the perturbation grown by the R-T instability.

Rayleigh-Taylor instability: The experimental conditions are very similar to those for the imprint experiment except for the un-modulated foot pulse and the modulated target.

The initial perturbation wavelength was fixed to be $60 \mu\text{m}$ and only the initial amplitude was varied. We measured areal-density perturbation growth by face-on backlighting. Growth factors for the small initial amplitude case, 0.1 and $0.3 \mu\text{m}$, are well fitted to an exponential curve with 1.2 ns^{-1} . On the other hand, classical growth rate of the R-T instability is calculated to be $(kg)^{1/2} = 2.3 \text{ ns}^{-1}$, where k is the wave number of initial perturbation and $g (= 5.1 \times 10^{15} \text{ cm/s}^2)$ is the acceleration measured with the side-on x-ray backlighting. The observed growth rate is reduced to about 50% of the classical growth rate.

1. Endo, T., et al., "Dynamic Behaviour of Rippled Shock Waves and Subsequently Induced Areal-Density-Perturbation Growth in Laser-Irradiated Foils", Phys. Rev. Lett. 74 (1995) 3608.
2. Takabe, H., et al., "Self-consistent growth rate of the Rayleigh-Taylor instability in an ablatively accelerated plasma", Phys. Fluids 28 (1985) 3676.
3. Remington, B., et al., "Large Growth Rayleigh-Taylor Experiments Using Shaped Laser Pulses", Phys. Rev. Lett. 67 (1991) 3259.

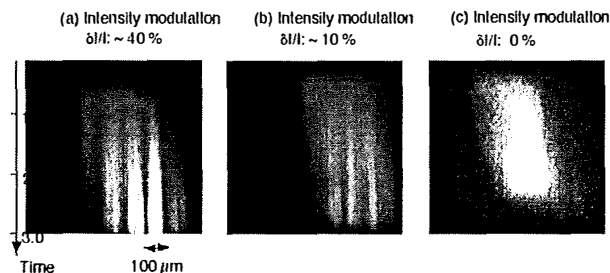


Fig. 1 Streaked x-ray backlighting images of the accelerated plastic planar targets irradiated with a sinusoidally modulated laser beam of (a) 40%, (b) 10% , and (c) 0% modulation depth.

Laser Imprinting Studies Using Multiple-UV-Beam Irradiation of Planar Targets

T.R. Boehly, D.D. Meyerhofer, J.P. Knauer, D. K. Bradley, R. L. Keck,
J.A. Delettrez, V.A. Smalyuk, J.M. Soures, and P. Verdon

*Laboratory for Laser Energetics, University of Rochester, 250 East River Road,
Rochester, NY 14623-1299*

The stability of direct-drive ICF implosions is determined by acceleration-driven growth of perturbations that are initially seeded by target imperfections and irradiation nonuniformities. At early times, before sufficient plasma is formed, the laser interacts directly with the target surface, and drive nonuniformities can "imprint" the target with perturbations. To design future drivers and targets, it is important to determine the times and intensities over which imprinting affects the target.

We report on multibeam, planar-target experiments that produce deliberate nonuniformities in drive to simulate various aspects of imprinting. To produce a relatively smooth drive, targets were irradiated at 2×10^{14} W/cm² with 5 to 10 UV beams (without DPP's) focused to 1- μ m spots. A smaller beam (400- μ m diam) was added at various times to simulate different types of irradiation perturbations. The energy and uniformity of the perturbing beam were also varied. Growth of the resulting perturbations is observed by using time-gated, pinhole photographs of -1.5-keV x-rays from a backlighter—a standard technique for stability experiments.

We report on results of experiments where the perturbing beam intensity is varied from 0, 0.1, 0.25, and 1.0 times the overall drive, and the delay of the perturbing beam is -150, 0, and +300 ps with respect to the smooth drive. Most of these experiments were performed with laser beams having no uniformity enhancements; however, one shot with a DPP and SSD on the perturbing beam showed a marked reduction in the growth of nonuniformities. We review plans for extending this technique to configurations employing DPP's and finer control of the perturbed beam.

* This work was supported by the U.S. Department of Energy Office of Inertial Confinement Fusion under Cooperative Agreement No. DE-FC03-92SF19460, the University of Rochester, and the New York State Energy Research and Development Authority. The support of DOE does not constitute an endorsement by DOE of the views expressed in this article.

Measurements of Laser Imprint in a Thin Foil Using An X-ray Laser for XUV Radiography*

D.H. Kalantar, L.B. DaSilva, S.G. Glendinning, F. Weber, B.A. Remington, S.V. Weber
Lawrence Livermore National Laboratory

M.H. Key, D. Neely, E. Wolfrum
Rutherford Appleton Laboratory, U.K.

A. Demir, J. Lin, R. Smith, G.J. Tallents
Essex Univeristy, U.K.

N.S. Kim, J.S. Wark, J. Zhang
Oxford University, U.K.

C.L.S. Lewis, A. McPhee, J. Warwick
Queens University, U.K.

J.P. Knauer
Laboratory for Laser Energetics, University of Rochester

For direct drive ICF, a capsule is imploded by directly illuminating the surface with laser light. Beam smoothing and uniformity of illumination affect the seeding of instabilities at the ablation front. We have used an x-ray laser backlighter to measure the imprinted modulation in a thin foil by XUV radiography. We use multilayer XUV optics to image the foil modulation in optical depth onto a CCD camera. This technique allows us to measure small fractional variations in the foil thickness. We measured the modulation due to imprint and subsequent Rayleigh-Taylor growth due to a low intensity $0.35\ \mu\text{m}$ drive beam incident on a $3\ \mu\text{m}$ Si foil using an yttrium x-ray laser on Nova.

We used a similar technique to measure the imprinted modulation and growth due to a low intensity $0.53\ \mu\text{m}$ drive beam incident on a $2\ \mu\text{m}$ Al foil using a germanium x-ray laser at the Vulcan facility. We present measurements of the modulation due to static RPP and SSD smoothed speckle patterns at both $0.35\ \mu\text{m}$ and $0.53\ \mu\text{m}$ irradiation. We also present measurements using ISI smoothing, as well as results from two overlapping beam speckle patterns at $0.53\ \mu\text{m}$ irradiation. We compare the results with the modulation due to a single mode optical imprint at $15\text{-}30\ \mu\text{m}$ wavelength generated by a narrow slit interference pattern at the thin foil target.

* Work was performed under the auspices of the U.S. Department of Energy by the Lawrence Livermore National Laboratory under Contract No. W-7405-ENG-48.

Multimode Classical Rayleigh-Taylor Experiments at Nova

K.S. Budil, B.A. Remington, A.M. Rubenchik, M. Berning, W.M. Wood-Vasey,
P.L. Miller, T.S. Perry, T.A. Peyser, and K.O. Mikaelian
Lawrence Livermore National Laboratory, P.O. Box 808, Livermore, CA 94551

The evolution of the Rayleigh-Taylor (RT) instability at an ablation front has been studied extensively due to its potential impact on inertial confinement fusion. Recent work showed strong growth of short wavelength modes ($\leq 10 \mu\text{m}$) at an embedded, classical interface in marked contrast to observations at the ablation front.^[1] This work has been extended to the study of multimode perturbations at an embedded interface to investigate the prediction of an *inverse cascade*, or trend toward progressively longer wavelength structures dominating the flow, as first predicted by Sharp and Wheeler.^[2]

As the growth of the initial modes enters the nonlinear regime, ($\kappa\eta > 0.1$), an initially sinusoidal perturbation assumes the characteristic "bubble and spike" shape and the initial modes begin to *couple* producing the beat modes $k_1 \pm k_2 = k_{\pm}$. Results will be presented for the growth of perturbations consisting of two, ten, and twenty modes with various amplitudes superposed in phase. The targets consisted of $40 \mu\text{m}$ of brominated plastic ($\text{C}_{50}\text{H}_{47}\text{Br}_3$, $\rho = 1.26 \text{ g/cm}^3$) backed with a $15 \mu\text{m}$ titanium ablator ($\rho = 4.5 \text{ g/cm}^3$) mounted across a hole on a 3 mm long by 1.6 mm diameter gold hohlraum. The perturbation is placed at the CH(Br)-Ti boundary, effectively isolated from the effects of ablation. Eight Nova beams at $\lambda = .351 \mu\text{m}$ are used to generate a 3.5 or 4.5 ns shaped, low-adiabat drive. The ablatively accelerated target is back-illuminated with $6.7 \text{ keV He} - \alpha$ x-rays generated by the remaining two Nova beams at $\lambda = .528 \mu\text{m}$ impinging on an iron foil. A gated x-ray imager (FXI) is utilized to record the images which are then converted to $\ln(\text{exposure}) - \text{OD} = - \int \rho \kappa dz$, where ρ is density and κ is opacity, and analyzed by Fourier decomposition.

For several of the targets studied, the wavelengths of the initial modes were below the experimental resolution ($\sim 7 \mu\text{m}$ at $12 \times$ magnification). The growth of these subresolution modes is diagnosed by observing the appearance of the coupled beat modes and then using 1D calculations to infer the growth of the initial modes.

1. K.S. Budil et al., "Classical Rayleigh-Taylor Experiments at Nova", in press, Phys. Rev. Lett. (1996).
2. D.H. Sharp and J.A. Wheeler, "Late Stage of Rayleigh-Taylor Instability", Institute for Defense Analyses, unpublished report (1961); J. Glimm et al., "A Numerical Study of Bubble Interactions in Rayleigh-Taylor Instability for Compressible Fluids", Phys. Fluids A, 2, 2046 (1990).

* This work was performed under the auspices of the U.S. Department of Energy by the Lawrence Livermore National Laboratory under Contract No. W-7405-ENG-48.

Modeling of Mix Due to the Rayleigh-Taylor Instability in Burnthrough Experiments Using the One-Dimensional Hydrodynamic Code *LILAC*

J.A. Delettrez, D.K. Bradley, and C.P. Verdon

*Laboratory for Laser Energetics, University of Rochester, 250 East River Road,
Rochester, NY 14623-1299*

We are presenting simulations with a mix model of the first spherical burnthrough experiments carried out on the 30-kJ OMEGA laser at the University of Rochester's Laboratory for Laser Energetics. The burnthrough experiments, in which a signature layer is buried under several microns of parylene (CH), are the first series of an experimental program to study mix in directly driven imploding spherical targets. The mix model is an integral part of the one-dimensional hydrodynamics code *LILAC*. In this model the Lagrangian grid is distorted according to the results of an analytic multimode model^[1] of the growth of the Rayleigh-Taylor instability. The electron temperature is then obtained over the distorted grid. As a result of grid distortion and heat conduction, the signature layer material in the spikes is heated to temperatures higher than those that would be reached in the absence of the instability. This leads to the early x-ray emission that characterizes the burnthrough experiments^[2] carried out on the 24-beam OMEGA laser. The burnthrough experiments serve as a check on the validity of the mix model.

1. S. W. Haan. Phys. Rev. A 39, 5812 (1989).
2. J. Delettrez, D. K. Bradley, and C. P. Verdon, Phys. Plasmas 1, 2342 (1994).

* This work was supported by the U.S. Department of Energy Office of Inertial Confinement Fusion under Cooperative Agreement No. DE-FC03-92SF19460, the University of Rochester, and the New York State Energy Research and Development Authority. The support of DOE does not constitute an endorsement by DOE of the views expressed in this article.

NOVA Feed-out/Feed-in Experiments

D.P. Smitherman, N.M. Hoffman, R.E. Chrien, G.R. Magelssen, D.C. Wilson

Los Alamos National Laboratory, Los Alamos, New Mexico 87545

Feed-out is defined as the communication of a perturbation from the cold side of an inertial fusion target to the ablation front. The perturbation is thought to be carried to the ablation surface by a reflected rarefaction from a shock wave hitting the perturbation on the back. At the ablation surface, the rarefaction imprint is thought to seed the Rayleigh-Taylor instability and grow. Likewise, feed-in, or feedthrough, is the communication of the perturbation on the ablation surface into the target payload. As the perturbation grows at the surface, it expands into the target.

A computational and experimental campaign to study feed-out in planar targets has begun. Four targets have been shot on NOVA. Two single material targets composed of aluminum, of 32 and 87 μm in thickness, and two aluminum/beryllium composite targets. 10 μm Be was on the back of both of the composite targets, with 25 and 80 μm of Al as an ablator. All the targets were given a 50 μm wavelength, 4 μm amplitude perturbation on the cold side, and were driven with hohlraum radiation from pulse shape 26. A 6.7 keV Fe backlighter was used for the thicker targets, and a 4.7 keV Ti for the thinner targets. Perturbation growth was observed using either a gated X-ray imager (GXI) or an FXI using face-on radiography. Comparisons of computational results will be compared with experimental data.

Dynamic Stability and Linear Feedthrough in ICF Implosions

R. Betti, R. Epstein, V.N. Goncharov, R.L. McCrory, and C.P. Verdon

*Laboratory for Laser Energetics, University of Rochester, 250 East River Road,
Rochester, NY 14623-1299*

The linear stability analyses of accelerated ablation fronts are often carried out for steady equilibrium configurations when the laser intensity, acceleration, and ablation velocity are approximately constant. Furthermore, little attention has been devoted to determining the magnitude of the perturbation feeding through the target and producing the seed for the Rayleigh-Taylor instability that occurs in the deceleration phase of the implosion (when the acceleration reverses its sign). To determine the evolution of the perturbation on the inner surface, we have developed a simple, sharp boundary model that includes the ablation of the outer surface and the finite target thickness (d). The target thickness and the acceleration depend on time, and the perturbation of the inner and outer surfaces are related by two coupled, ordinary differential equations. Such equations are numerically solved, and the magnitude of the feedthrough is related to the dimensionless wave number $\epsilon_d \equiv kd$ (k is the wave number) and the effective Froude number $Fr_d = V_a^2/gd$ (V_a is the ablation velocity and g is the acceleration). In addition, such a simple model is also applied to the case of an oscillating acceleration induced by the periodic modulation of the laser intensity. Although the oscillating acceleration is expected to induce the dynamic stabilization of the R-T instability on the ablation surface, it may also significantly alter the stability of the inner surface during the acceleration phase. However, by using the one-dimensional code *LILAC*, we have found that the oscillations are spatially localized near the ablation surface and their effect on the inner surface is (probably) negligible.

* This work was supported by the U.S. Department of Energy Office of Inertial Confinement Fusion under Cooperative Agreement No. DE-FC03-92SF19460. the University of Rochester and the New York State Energy Research and Development Authority. The support of DOE does not constitute an endorsement by DOE of the views expressed in this article.

Simulations of Foam-Buffered Laser-Target Interactions*

Rodney J. Mason, Roger A. Kopp, and Hoahn X. Vu
Los Alamos National Laboratory, Los Alamos, NM 87545

The use of foam buffer layers on foil targets has been shown to mitigate significantly the effects of direct drive laser nonuniformities. Experiments⁽¹⁾ on LANL's TRIDENT and Imperial College's VULCAN laser have demonstrated a substantial reduction of beam perturbations of frequency doubled 1.4×10^{14} W/cm² light. We have been using LASNEX to study this smoothing phenomenology. Typically, we have modeled 10 μ m thick CH foils, covered with 50 μ m of 50 mg/cm³ C₁₀H₈O₄ foams plus a 200 Å gold overlayer and exposed to a 1 ns flat pulses with additional 100 ps rise and fall-off times. We find that results are sensitive to the radiation transport modeling. NLTE physics predicts substantially smaller CH shell decompression than does LTE. We have propagated the light with refracting laser rays. The hydrodynamics has been modeled with a combined of Lagrangian and Eulerian method for maximum accuracy and minimal mesh tangling. The electron thermal flux limiter f_e has ranged from 0.03 to 0.6, but typically $f_e = 0.05$ was used.

With a 30 μ m, 60% laser perturbation imposed and no foam layer, the foils are violently disrupted by 1.2 ns. When the layer is added, foil integrity prevails beyond 3.0 ns. We find that for stability the very earliest light (< 10 ps) must be stopped at the foam surface by the gold or by "opaque" foam, otherwise light penetration of transparent foams seed instability. We have determined that primarily the electron thermal conductivity is responsible for the smoothing. When the foam conductivity is reduced by only a factor of ten violent foil disruption ensues. Our simulations have confirmed the general rule that the foam thickness should exceed the wavelength of the intensity perturbations. This has been demonstrated for parameter studies with foams lengths from 20 μ m to 400 μ m and disturbance lengths spanning 10 μ m to 300 μ m. Stabilization becomes more difficult as the laser intensity is reduced. At 1.6×10^{15} W/cm² the shells maintain integrity (with density variations no larger than 30%) beyond 5.5 ns, while at 3.2×10^{12} W/cm² integrity is lost after only 750 ps.

We find that mitigation is more difficult to achieve at shorter laser wavelengths, with 30% instability evident after 2 ns at 3ω . But, stability is returned if the foam thickness is increased to 200 μ m, or the intensity is doubled. Preliminary studies show minimal mitigation with lower density, 10 mg/cm³ foams. We cannot yet fully certify the value of a gold outer layer for fully effective disturbance mitigation. The gold can induce decompression of the plastic, discouraging ultimate high compression of the full target. However, simulations of structured foam targets—either picket fences or fibers—point toward hastened conversion of solid foam to plasma and to greater disturbance mitigation with the addition of the gold layer.

1. M. Dunne, M. Borghesi, A. Iwase, M.W. Jones, R. Taylor, O. Willi, R. Gibson, S.R. Goldman, J. Mack, and R. Watt, "Evaluation of a Foam Buffer Target Design for Spatially Uniform Ablation of Laser Irradiated Plasmas," *Phys. Rev. Lett.* **75**, 3858 (1995).

* Work supported by the USDOE.

Fokker-Planck Simulations of Foam-Buffered Targets

R.P.J. Town, R.W. Short, and C.P. Verdon

*Laboratory for Laser Energetics, University of Rochester, 250 East River Road,
Rochester, NY 14623-1299*

The Rayleigh-Taylor (RT) instability has a potentially deleterious effect on the final implosion conditions of a direct-drive inertial confinement fusion target. The RT instability can be seeded by nonuniformities in target fabrication and laser illumination. Techniques, such as SSD and ISI, have improved the time-integrated laser illumination; however, preliminary calculations indicate that these techniques may be limited in effectiveness during the initial "startup" phase. During this phase the nonuniform laser irradiation is imprinted on the target surface. Recent experiments¹ have been performed using foam-buffered targets that show a substantial reduction in the growth of the RT instability. The presence of the foam layer increases the standoff distance between the critical and ablation surfaces at early times, thus increasing the amount of smoothing of the instantaneous nonuniformities compared to conventional "bare" targets. This paper will examine the role of nonlocal heat transport on foam-buffered targets. Comparisons between *LILAC* and *SPARK* will be presented.

1. M. Dunne *et al.* Phys. Rev. Lett. 75, 3858 (1995).

* This work was supported by the U.S. Department of Energy Office of Inertial Confinement Fusion under Cooperative Agreement No. DE-FC03-92SF19460, the University of Rochester, and the New York State Energy Research and Development Authority. The support of DOE does not constitute an endorsement by DOE of the views expressed in this article.

Time and Space-Resolved Optical Probing of Femtosecond Laser-driven Shock Waves in Aluminum

J.-C. Gauthier, P. Audebert, and J.-P. Geindre

Laboratoire pour l'Utilisation des Lasers Intenses, Ecole Polytechnique, 91128 Palaiseau, France

R. Evans, A.D. Badger, F. Fallies, M. Mahdih, and T.A. Hall
Physics Department, University of Essex, Colchester, Essex, U.K.

A. Mysyrowicz, G. Grillon, and A. Antonetti
Laboratoire d'Optique Appliquee, Batterie de l'Yvette, 91120 Palaiseau, France

We present the first measurements of particle velocity histories at the interface between an aluminum sample shocked by a 120fs laser-driven pressure pulse and a fused silica window. Frequency-domain interferometry is used to provide space- and time-resolved measurements of the phase shift of a pair of probe pulses backscattered at the shocked interface. Pressures of 1-3 Mbar are inferred from the simultaneous measurement of the particle and shock velocities along the aluminum Hugoniot curve for 10^{14} W/cm² laser irradiances.

Shock and interface velocities are accurately predicted by hydrodynamic simulations using a standard equation-of-state for Al and SiO₂. Due to the very short pressure load involved in subpicosecond laser-produced plasmas, the study of the dynamic properties of dense, low temperature (1 eV) plasmas is readily feasible.

Time-Averaging of Irradiation Nonuniformity in Laser-Driven Plasmas Due to Target Ablation

R. Epstein

*Laboratory for Laser Energetics, University of Rochester, 250 East River Road,
Rochester, NY 14623-1299*

In experiments in inertial confinement fusion (ICF), irradiation uniformity is improved by passing laser beams through distributed phase plates (DPP's), which produce focused intensity profiles with well-controlled and reproducible envelopes modulated by fine random speckle.¹ A uniformly ablating plasma atmosphere acts to reduce the contribution of the speckle to the time-averaged irradiation nonuniformity by causing the intensity distribution to move relative to the absorption layer of the plasma. This occurs most directly as the absorption layer in the plasma moves with the ablation-driven flow, but it is shown that the effect of the accumulating ablated plasma on the phase of the laser light also makes a quantitatively significant contribution. Analytical results are obtained using the paraxial approximation applied to the beam propagation, and a simple statistical model is assumed for the properties of DPP's. The reduction in the time-averaged spatial spectrum of the speckle due to these effects is shown to be quantitatively significant within time intervals characteristic of atmospheric hydrodynamics under typical ICF conditions.

1. C. B. Burckhardt, *Appl. Opt.* 9, 695 (1970); Y. Kato and K. Mima, *Appl. Phys. B* 29, 186 (1982); Y. Kato, K. Mima, N. Miyanaga, S. Arinaga, Y. Kitigawa, M. Nakatsuka, and C. Yamanaka, *Phys. Rev. Lett.* 53, 1057 (1984); Laboratory for Laser Energetics LLE Review 33, NTIS document No. DOEIDP/40200-65, 1987 (unpublished), p. 1; and Laboratory for Laser Energetics LLE Review 63, NTIS document No. DOE/SF/19460-91, 1995 (unpublished), p. 1.

* This work was supported by the U.S. Department of Energy Office of Inertial Confinement Fusion under Cooperative Agreement No. DE-FC03-92SF19460, the University of Rochester, and the New York State Energy Research and Development Authority. The support of DOE does not constitute an endorsement by DOE of the views expressed in this article.

Diagnosing High- ρR Implosions Using Elastically Scattered DT Neutrons

S. Cremer and S. Skupsky

*Laboratory for Laser Energetics, University of Rochester, 250 East River Road,
Rochester, NY 14623-1299*

Future cryogenic ICF implosions are expected to achieve values of ρR in excess of 200 mg/cm^2 , which is beyond the range that can be diagnosed using charged particle knock-ons from (n,D) and (n,T) elastic scattering in the fuel. As an alternative, we have examined the possibility of using the elastically scattered neutron itself as the diagnostic signal. If these scattered neutrons can be distinguished from the other neutrons produced in the target, this technique will permit the measurement of ρR over the entire range of interest, for both OMEGA and NIF experiments, in a model independent way. The elastically scattered neutrons are produced in a continuous spectrum from 1.6 to 14.1 MeV. Additional neutrons are produced in the target in this energy range by the primary reactions $DD \rightarrow {}^3\text{He} + n$ (2.45 MeV) and $TT \rightarrow \alpha + 2n$ (up to 9.44 MeV), by the inelastic scattering $(n,D) \rightarrow p + 2n$ (up to 11.86 MeV) and by the thermal broadening of the 14.1-MeV DT neutron source itself (down to ~ 13 MeV, for temperatures up to 20 to 30 keV). Above 10 MeV, the $(n,D)_{\text{inel}}$ contribution is negligible compared to that of the elastically scattered neutrons, and we left with a "safe" window in the spectrum between 10 to 13 MeV, which is completely dominated by the elastically scattered neutrons. The number of neutrons in this window will give an unambiguous measurement of fuel ρR . It remains to develop an experimental technique that can clearly separate this part of the neutron spectrum from background scattered neutrons produced in the diagnostic apparatus itself.

* This work was supported by the U.S. Department of Energy Office of Inertial Confinement Fusion under Cooperative Agreement No. DE-FC03-92SF19460, the University of Rochester, and the New York State Energy Research and Development Authority. The support of DOE does not constitute an endorsement by DOE of the views expressed in this article.

Tuesday

INVITED TALK

7:30 – 8:30 PM

David Montgomery

Bedros Afeyan, Session Chair

Laser-Plasma Interaction Experiments in Gas-Filled Targets

David S. Montgomery

Los Alamos National Laboratory, Los Alamos, NM 87545

Stimulated Raman scattering (SRS) and stimulated Brillouin scattering (SBS) are major concerns in inertial confinement fusion (ICF) experiments since these instabilities can significantly reduce the laser absorption in large scale plasmas. Recent experimental efforts have used gas-filled targets in either an open geometry (LLNL gasbags), or in a closed geometry (LANL and LLNL hohlraums) to produce large plasmas with scale lengths ~ 2 mm, Te 3 keV, and electron densities $n_e / n_{cr} = 0.06 - 0.15$. Gas-filled targets provide the unique capability of systematically controlling the plasma electron density and ion Landau damping by appropriately choosing the initial gas pressure and species. These plasma experiments have allowed us to observe interesting features in the growth and saturation of SRS and SBS.

In the first two sets of experiments, both the LLNL gasbag and LANL gas hohlraum targets are used with high-Z, Xe gas fills, and C_5H_{12} dopant is added in various amounts to systematically increase the ion Landau damping. The saturated SRS reflectivity is found to *increase* with higher ion Landau damping, which is consistent with models of SRS saturation via Langmuir decay instability (LDI) or electromagnetic decay instability (EDI). Additional experiments performed by LANL using CF_4 , C_5D_{12} , and C_5H_{12} show similar trends as the high-Z experiments.

In the last set of experiments, LLNL gasbags are filled with different mixtures of either C_3H_8/C_5H_{12} , or CO_2/CF_4 . The electron density is varied between $n_e/n_{cr} = 0.06 - 0.15$, and the ion Landau damping rate is roughly constant for each gas species mixture as n_e / n_{cr} varies. Both strongly damped (with hydrogen) and weakly damped (no hydrogen) regimes are studied. As n_e / n_{cr} decreases, SRS is found to decrease, as expected from linear theory since electron Landau damping increases. However, SBS actually *increases* with decreasing n_e / n_{cr} , and is anti-correlated with the SRS, in contrast to simple theory. One explanation which invokes the growth of SBS and LDI in the presence of fluctuations may explain these data. Other possible explanations will be discussed.

* This work was supported by the U.S. Department of Energy.

Tuesday

POSTER SESSIONS
8:30 – 10:30 PM

Improvements to Busquet's Non LTE Algorithm in NRL's Hydro Code

Marcel Klapisch

ARTEP, Inc. Columbia, MD 21045

Denis Colombant

Plasma Physics Division, Naval Research Laboratory, Washington, DC 20375

The implementation of M. Busquet's Radiation Dependent Ionization Model (RADIOM)¹ in NRL's RAD2D Hydro code in conservative form was reported previously². While the results were satisfactory, the algorithm was slow and not always converging.

We describe here modifications that address the latter two shortcomings. The fitting of the function $\text{frad}(u)$ is now performed by orthogonal polynomials. In addition to being quicker and more stable than inverting a matrix, this method gives information about the validity of the fitting. It turns out that the number and distribution of groups in the multigroup diffusion opacity tables—a basis for the computation of radiation effects in the ionization balance in RADIOM—has a large influence on the robustness of the algorithm.

These modifications also helped us to gain some insight in the meaning of the algorithm, and to check that the obtained average charge state is the true average.

In addition, code optimization resulted in greatly reduced computing time: The ratio of Non LTE to LTE computing times being now between 1.5 and 2.

1. M. Busquet, *Phys. Fluids B*, 5, 4191 (1993).
2. M. Klapisch, D. Colombant, J. P. Dahlburg, J. H. Gardner, A. J. Schmitt and D. A. Garren, *Bull. Am. Phys. Soc.*, 40, 1806 (1995), and 25th Anomalous Absorption Conference, Aspen CO (1995).

* Supported by U.S. Dept of Energy.

Preheating Effects in Laser Driven Shock Waves

J.J. Honrubia, R. Dezulian
Instituto de Fusion Nuclear, UPM, Madrid

M. Koenig, A. Benuzzi, J. Krishnan
*Laboratoire pour l'Utilisation des Laser Intenses (CNRS), Ecole Polytechnique, 91128
Palaiseau, France*

N. Grandjouan
*Laboratoire Physique Milieux Ionisés (CNRS), Ecole Polytechnique, 91128 Palaiseau,
France*

T.A. Hall, M. Mahdiah
University of Essex, Dept. of Physics, Wivenhoe Park, 504 3SQ Colchester, UK

D. Batani, S. Bossi, D. Beretta
University of Milan, Dept. of Physics, via Celoria 16, 20133 Milan, Italy

Th. Löwer
Max Planck Institut für Quantenoptik, Garching, Munich, Germany

The experiments have been performed at the LULI laboratory of the Ecole Polytechnique using the LULI laser at $0.53 \mu\text{m}$ with an average intensity $I_L < 10^{14} \text{ W/cm}^2$ and FWHM = 600 ps. The targets were aluminium foils (thicknesses 5 - 25 μm) and aluminium - gold foils (Au thickness 1000 Å). In order to check preheating effects we analyzed the time behavior of the target rear side emissivity (recorded with a streak camera). Here we present experimental results compared with numerical calculations. Simulations were performed with the SARA and MULTI 1D multigroup radiation codes.

Foam Buffered Direct Drive Implosion Experiments at 527 nm

D.C. Wilson, R.G. Watt, R. Hollis, P. Gobby, R. Chrien, R. Mason, R. Kopp
Los Alamos National Laboratory

R. Lerche, M. Nelson, B. MacGowan, D. Kalantar
Lawrence Livermore Laboratory

J. Knauer, P. McKenty, C.P. Verdon
Laboratory for Laser Energetics

O. Willi
Imperial College of Science and Technology

A serious concern for directly driven ICF implosions is the asymmetry imparted to the capsule by laser drive non-uniformities, particularly the “early time imprint” remaining after the laser speckle pattern is averaged over several coherence times by SSD. The use of a foam buffer has been proposed as a means to reduce this imprint, and studied experimentally in several planar and cylindrical experiments at 527 nm. Preliminary implosion tests of the concept using a polystyrene foam were performed at the NOVA laser. This first test of foam buffering in spherical geometry was compared the yield and imploded core symmetry of capsules with and without foam buffering to that calculated in 1D without any degradation. The laser irradiation non-uniformity was complex. The ten overlapped f/4.3 Nova beams produced low irradiance at the poles and equator. In addition each had a 400 μm hole in the center (for tangent focus on a 1600 μm diameter, foam coated capsule). The targets consisted of a central glass microballoon (GMB) 1230 to 1350 μm diameter, approximately 4 μm thick, filled to 20 atm pressure of DT. The DT neutron yield was measured by Cu activation. The time of the neutron yield and the ion temperature measurements used time of flight detectors and a large single hit detector array (Tion), respectively. The neutron burn history was measured using a scintillator streak camera system with <100 ps time resolution. 1D Lasnex calculations of each target provided the undegraded yield and minimum shell size for comparison with the measurements.

One GMB was irradiated with full laser energy at 351 nm, and two at 527 nm to test the ability to model both laser wavelengths. The calculated implosion times generally agreed with measurements, indicating that laser absorption and hydrodynamics were correctly modeled. Two GMBs, covered with 200 μm of 0.045 g/cc polystyrene foam and 25 nm of Au gave 2.3% and 4.6% of clean calculated yield. Another three comparison targets were imploded to reach similar fuel conditions as the foam targets. To reach a similar convergence ratio and implosion time the laser energy had to be reduced on the comparison targets. To test targets with a similar mass to the foam targets, two microballoons were covered with 10 μm of full density CH and irradiated with 21 kJ. One target, coated with 75 nm of Al, gave 0.3% of calculated. The other, with the usual 25 nm of Au, gave 0.1%. One GMB driven with 9 kJ to produce similar convergence and yield as the foam targets, gave 1.1%.

The minimum shell diameter was the same as the foam (246 μm) and less than calculated (360 μm). Calculations for all of the foam and comparison capsules show two peaks in the neutron yield, with various relative strengths. The first peak is caused by compression and heating when the first shock reaches capsule center. The second peak is from the DT burn at the time of peak shell compression. In general, the neutron production during stagnation is degraded more than during the shock induced pulse. The temperature of the burning DT is higher during the first shock peak than in the later final compression. Since most of the experimentally observed yield comes from the first shock heating, we expect, and find in most cases, that the observed temperatures are higher than those calculated with full yield. These results suggest that foam buffering reduces the yield degradation. Experiments with and without a controlled asymmetry are needed. Such experiments, using very high quality incident drive beams, are being proposed for the Omega Upgrade laser system.

The Effect of Dopants on Direct Drive ICF Target Design

John H. Gardner, Lee S. Phillips

LCP&FD, Naval Research Laboratory, Washington, DC

Marcel Klapisch, Denis G. Colombant, Andrew J. Schmitt,

Jill P. Dahlburg, and Stephen E. Bodner

Plasma Physics Division, Naval Research Laboratory, Washington, DC

We report the results of calculations aimed at elucidating the effects of using dopants in the outer layer to control the seed and the growth of the Rayleigh-Taylor instability in direct drive laser fusion targets. We investigate the use of a thin overcoating of plastic doped with Hi Z material and compare with undoped low-isentrope target designs. In each simulation, the target is accelerated with a $1/4 \mu\text{m}$ laser light with peak intensity in the mid- 10^{14}W/cm^2 range, and intensity temporal profiles developed for moderately high-gain direct-drive KrF designs with contrast ratios between the foot and the main pulse on the order of one hundred.^[1]

For these calculations we use a multigroup, variable Eddington radiation transport model with STA opacities and the non-LTE model of Busquet^[2] coupled to our FAST2D laser matter interaction code. Multiple materials are tracked by a volume fraction model. Laser energy is deposited by means of a ray trace algorithm that emulates the effects of ISI optics, and is absorbed by inverse bremsstrahlung. The ISI speckle is modelled by Gaussian-Distributed random field amplitudes. The laser energy is transported to the target surface by two different physical processes. Classical thermal conduction dominates the outer region, transporting the energy to a region of higher density where some fraction of the energy is converted to soft x-rays. The x rays are then transported further towards the target by the multigroup transport process to a second absorption front dominated by x-ray absorption. Our goal is to manipulate transport processes in the second region of absorption, to reduce the effects of imprinting and Rayleigh-Taylor growth while maintaining a low enough isentrope target to test the viability of high-gain with direct-drive pellets on KrF systems.

1. A. J. Schmitt, et al., 25th Anomalous Absorption Conference.
2. M. Busquet, Physics. Fluids B5 (4190) 1993.

* Work supported by USDOE and ONR.

Studies of the Temporally and Spatially Resolved Front and Rear Side Light Emission from Laser Irradiated Targets

E.A. McLean, S.P. Obenschain, J.A. Stamper, A.J. Schmitt, J.D. Sethian, K.A. Gerber, C.J. Pawley, V. Serlin, R.H. Lehmberg, S.E. Bodner, C.A. Sullivan, M.S. Pronko, A.N. Mostovych, J.P. Dahlburg, and D.G. Colombant
Plasma Physics Division, Naval Research Laboratory, Washington, DC

A.V. Deniz, T. Lehecka, L-Y. Chan, and N. Metzler
Science Applications International Corporation, McLean, VA

J.H. Gardner
Laboratory for Computational Physics and Fluid Dynamics, NRL

M. Klapisch
ARTEP Incorporated, Columbia, MD

The NRL Nike laser is a 56-beam, multiplexed KrF laser at 248 nm designed for flat-target experiments. The beams have ISI beam smoothing such that the RMS spatial variations of a single 4-ns beam has been measured to be $\sim 1\%$. The net smoothing is expected to be much better than this when up to 44 beams at ~ 2 kJ are overlapped on a target. Targets are typically irradiated with laser pulses having intensities of $\sim 10^{14}$ W/cm². Calibrated time-resolved measurements of the absolute intensity of the target rear and front surface visible emission allows brightness temperatures to be inferred. Streak camera recording of the rear surface light intensity with a time-resolution of ~ 30 ps gives the timing and uniformity of the shock breakout, and with intensity calibration can give brightness temperature with better time resolution than can be achieved with photomultipliers. Data will be included with and without a 2–3 ns, $\sim 3\%$ amplitude foot preceding the main laser pulse. The temporal intensity variations in light emission between transparent and opaque targets are observed and will be discussed. A comparison of some of these measurements with hydrodynamic simulations will be made.

* This work was supported by the U. S. Department of Energy.

Electron Density Measurement of a Colliding Plasma Using Soft X-ray Laser Interferometry

A.S. Wan, C.A. Back, T.W. Barbee, Jr., R. Cauble, P. Celliers, L.B. DaSilva, S. Glenzer,
J.C. Moreno, P.W. Rambo, G.F. Stone, J.E. Trebes, and F. Weber

Lawrence Livermore National Laboratory, P. O. Box 808, Livermore CA 94550

The understanding of the collision and subsequent interaction of counter-streaming high-density plasmas is important for the design of indirectly-driven inertial confinement fusion (ICF) hohlraums. We have employed a soft x-ray Mach-Zehnder interferometer, using a Ne-like Y x-ray laser at 155 Å as the probe source, to study interpenetration and stagnation of two colliding plasmas. We observed a peaked density profile at the symmetry axis with a wide stagnation region with width of order 100 μm. We compare the measured density profile with density profiles calculated by the radiation hydrodynamic code LASNEX and a multi-specie fluid code which allows for interpenetration. The measured density profile falls in between the calculated profiles using collisionless and fluid approximations. By using different target materials and irradiation configurations, we can vary the collisionality of the plasma. We hope to use the soft x-ray laser interferometry as a mechanism to validate and benchmark our numerical codes used for the design and analysis of high-energy-density physics experiments.

Three-Dimensional Simulations of National Ignition Facility Capsule Implosions

M.M. Marinak, S.W. Haan, R.E. Tipton, G.B. Zimmerman
Lawrence Livermore National Laboratory, Livermore, CA 94551

Hydrodynamic instabilities on ignition targets designed for the National Ignition Facility have been modeled previously using weakly nonlinear saturation analysis and two-dimensional single mode and multimode LASNEX simulations. We present here the first three-dimensional simulations of the NIF point design capsule, performed with the HYDRA radiation hydrodynamics code. These examine the growth of multimode perturbations seeded by roughness on both the inner and outer surfaces. The spectrum of modes, simulated over a portion of the capsule, extends up to values equivalent to spherical harmonic mode number $l = 120$. Simulations show that perturbation growth progresses well into the nonlinear regime, underscoring the importance of an accurate treatment of saturation effects. The greatest threat presented by short wavelength modes is to the integrity of the capsule shell during the implosion phase. Intermediate wavelength perturbations also develop into spikes of cold fuel which could quench the hot spot. We compare simulations performed using a variety of surface perturbations having different spectrum shapes and amplitudes. Results indicate that spikes can penetrate up to $10 \mu\text{m}$ into the $30 \mu\text{m}$ radius hot spot before ignition is quenched. Yields of up to 12 MJ have been obtained in simulations with realistic surface roughnesses. Perturbation growth will be compared with predictions of the weakly nonlinear saturation model. We will examine how convergence influences nonlinear evolution.

* Worked performed under the auspices of the U.S. Department of Energy by the Lawrence Livermore National Laboratory under Contract W-7405-ENG-48.

Laser Cooling for Heavy-Fusion

D.D.M. Ho, S.T. Brandon, and Y.T. Lee
Lawrence Livermore National Laboratory

One of the critical requirements for heavy-ion fusion (HIF) is the ability to focus space-charge dominated beams onto a millimeter-size spot. However, momentum spread along the beam causes chromatic aberration which can result in a substantial fraction of the beam ions falling outside the desired spot radius. Because of the space-charge force, the remedy for correcting the chromatic aberration using sextuple magnets proves to be impractical.¹ Novel correcting schemes should therefore be sought for. Recent success in laser cooling of low-current ion beams in storage rings^{2,3} leads us to explore the possibility of applying laser cooling to HIF.

Basic Scheme — After the beams have been accelerated to the desired energy by the recirculating induction linac,⁴ we let the beams coast around at constant energy by turning the recirculator into a storage ring. The particular method used here for the HIF recirculator consists of at least two lasers (both are in the direction of beam propagation) tuned to the resonant frequency with the ion beam near the tail of the ion velocity distribution to provide the last force F_L . In addition, there is an auxiliary force F_a , which is in the opposition direction of F_L , provided by the induction cores of the recirculator. The momentum spread along the beam can therefore be compressed by F_L and F_a in velocity space. After the compression is completed, the momentum spread is reduced.

Laser Requirement — For efficient interaction between the laser and the beam ions, we use Ba^+ . We use two different lasers to pump the two transitions in the Ba^+ (P to S at 493 nm and P to D at 650 nm). Furthermore, the lasers will operate at a few times of the saturation intensity in order to increase the spread of the laser force in velocity space so that the laser can interact with a larger fraction of the beam particles.

In this paper, we will present estimates for the laser power requirements and the cooling time, and preliminary PIC simulations using the 2-1/2-D PIC code CONDOR. Potential difficulties caused by velocity space instabilities will be discussed.

1. D.D.-M. Ho et al., "Sextupole Correction of Second-Order Chromatic Aberration for High-Current Heavy-Ion Beam," Linear Accelerator Conference, Ottawa, Canada, Aug. 1992.
2. S. Schroder et al., Phys. Rev. Lett., vol. 64, no. 24, 1990, p. 2901.
3. J.S. Hangst et al., Phys. Rev. Lett., vol. 67, no. 10, 1991, p. 1238.
4. J.J. Barnard et al., Study of Recirculating Induction Accelerators as Drivers for Heavy Ion Fusion, Lawrence Livermore National Laboratory, UCRL-LR-108095, 1991.

* Work performed under the auspices of the U.S. Department of Energy by the Lawrence Livermore National Laboratory under Contract W-7405-ENG-48.

Shocked Witness Foam-Ball Drive Diagnostic at Target Center

P. Amendt, S.G. Glendinning, B.A. Hammel, O. Landen and L.J. Suter
University of California, Lawrence Livermore National Laboratory

Backlighting of low density SiO_2 aerogel balls in NOVA Au (empty) hohlraums enables indirect imaging of the ablatively-driven shock trajectory versus time. The transmissivity inflection point contour is actually imaged in the experiments, which we show from analysis and simulations to correlate well with the radiation-driven shock trajectory. An advantage in using this surrogate target technique is that the drive near target center can be directly inferred in contrast to witness plates and Dante x-ray PIN diode arrays which are tailored to measure drive near the hohlraum wall. Such a distinction is critical for Nova hohlraums fitted with axial Au discs or P_2 -shields which can give rise to a significant local enhancement in drive temperature near target center. We provide experimental corroboration for a predicted 20 eV (40%) increase in peak drive temperature (x-ray flux) using a flattop 1 ns pulse. Lower order flux asymmetry is negligibly small implying nearly uniform enhancement of drive around the surrogate target. Simple analytic estimates of the peak radiation temperature with and without P_2 -shields show excellent agreement with radiation-hydrodynamic simulations.

*Work performed under the auspices of the U.S. Department of Energy by the Lawrence Livermore National Laboratory under Contract W-7405-ENG-48.

Energetics of Small, High-Temperature Laser-Driven Hohlraums

T. J. Orzechowski, B. Afeyan, R.L. Berger, R.K. Kirkwood, W.L. Kruer, B.J. MacGowan,
L.V. Powers, P.S. Springer, M.D. Rosen, J.D. Moody, and L.J. Suter
Lawrence Livermore National Laboratory, P. O. Box 808, Livermore, CA 94550

M.A. Blain
CEA Limeil-Valenton, Villeneuve-St-Georges, France

Hohlraums provide a source of thermal radiation corresponding to temperatures ~ 100 's of eV. This radiation is generated by the interaction of intense laser radiation with the interior of a high-Z (e. g. gold) cavity. The temperature inside the cavity is a function of the laser power and the dimensions of the cavity; higher temperatures correspond to higher laser power and smaller hohlraum dimensions. For a fixed laser power, higher radiation temperatures are achieved with smaller hohlraum dimensions. The radiation in the cavity ablates the hohlraum wall creating a high-Z plasma inside the cavity. Furthermore, the smaller the cavity, the higher the laser intensity on the hohlraum wall (i. e. the laser must be more tightly focused in order to propagate into the smaller cavity). In the conventional "scale-1" Nova hohlraum ($L_h = 2700 \mu\text{m}$, $\phi_h = 1600 \mu\text{m}$) with the laser focus $1000 \mu\text{m}$ outside of the laser entrance holes (LEHs), the laser intensity on the hohlraum wall is $\sim 2 \times 10^{15} \text{ W/cm}^2$. In a scale-3/4 hohlraum with laser focus in the LEH the intensity is about $6 \times 10^{15} \text{ W/cm}^2$. In the scale-5/8 hohlraum, the intensity on the hohlraum wall approaches 10^{16} W/cm^2 . These higher intensities can affect both the x-ray conversion efficiency and the absorbed laser power. In this paper we report the measured hohlraum temperatures and the inferred absorbed laser power as a function of the hohlraum size and laser intensity. We compare the measurements with Lasnex and LIP calculations. We also present the results of beam smoothing on the backscattered radiation and the implications for improved hohlraum drive.

* This work was performed under the auspices of the U. S. DOE by the Lawrence Livermore National Laboratory under Contract No. W-7405-Eng-48.

Radiation Temperature Scaling in Hohltraums for Nova and NIF

L.V. Powers, R.L. Berger, R.K. Kirkwood, W.L. Kruer, A.B. Langdon, B.J. MacGowan,
T.J. Orzechowski, M.D. Rosen, P.T. Springer, C.H. Still, L.J. Suter and E.A. Williams

Lawrence Livermore National Laboratory

Establishing the practical limit on achievable radiation temperature in high-Z hohltraums is of interest both for ignition targets¹ for proposed high-power lasers such as the National Ignition Facility (NIF), and for x-ray physics experiments². Two related efforts are underway to define the physics issues of high energy density hohlraum targets: 1) experiments on the Nova laser in small scale hohltraums to establish and understand the practical limits on radiation temperature in Nova hohltraums, and 2) design calculations for high-temperature hohltraums for the NIF and related experiments.

Nova experiments are underway to evaluate the effects of the high laser intensity and fill density typical of small vacuum hohltraums on radiation physics and parametric instabilities. Modeling and analysis of these experiments tests our understanding of physics effects that may determine the practical limits for hohlraum temperatures with NIF. Modeling results for the Nova experiments will be presented, and issues and scalings relevant to NIF hohlraum design calculations will be discussed.

1. S.M. Haan, et al., Phys. Plasmas 2, 2480 (1995).
2. S.B. Libby, Energy and Technology Review, UCRL-52000-94-12, 23 (1994).

* Work performed under the auspices of the U.S. Department of Energy by Lawrence Livermore National Laboratory under contract number W-7405-ENG-48

Mesoscale Modeling of Laser-Plasma Instabilities in Macroscopic Sized Systems

Alfred Hanssen

University of Tromso, Norway

D.F. DuBois

Los Alamos National Laboratory and Lodestar Research Corp.

Harvey A. Rose

Los Alamos National Laboratory

David Russell

Lodestar Research Corp.

The numerical modeling of the nonlinear evolution of laser-plasma instabilities at the microscopic level, in large plasmas (mm's) over long times (ns) relevant to NIF applications, is impossible today even with the largest massively parallel computers. A modeling procedure is proposed which is based on the large separation of space and time scales between the macro scales and the microscopic correlation lengths of the induced Langmuir turbulence excited by instabilities such as SRS, TPD and IADI. Physically interesting behavior related to the envelopes of light waves and the density profile evolves on spatial scales such as gain lengths and speckle or filament dimensions and times such as ion acoustic transit times. These intermediate—or mesoscale—phenomena may be modelled in a large system using information on certain integral properties of the underlying induced turbulence obtained from small scale, homogeneous, quasi steady state, plasma simulations. As a first example we have modeled in 1D the propagation of the pump wave and the modification of the initially linear density profile by the turbulence induced near critical density by the IADI (ion acoustic decay instability) and the related modulational insatiability. The spatial scale of the pump envelope is like an Airy length which is much greater than turbulence correlation lengths. The effect of the induced turbulence on the equation for the pump propagation is reduced to an effective (or anomalous) absorption coefficient and a frequency shift parameter. These depend nonlinearly on the local pump intensity and the local (perturbed) density. This dependence can be obtained from a series of small homogeneous simulations. The density profile is perturbed in space and time by the ponderomotive pressure of the pump and the much larger ponderomotive pressure of the induced turbulence. The latter can also be obtained as a function of the local heater intensity and density from homogeneous simulations. Solution of the resulting mesoscale equations shows a dramatic, time dependent, alteration of the usual linear Airy profile. An application to SRS is proposed in which the standard coupled 3 wave envelope equations are altered by the coupling to the Langmuir turbulence, via the Langmuir decay instability, of the daughter Langmuir wave. The equation for the latter is again modified by turbulence-induced anomalous absorption and frequency shift parameters which, along with the LW energy density, whose ponderomotive pressure modifies the density profile, can be obtained from homogeneous simulations.

* Research supported by the USDOE and by NSF grant #ATM-9503147

Eigenmode Structure of Convective and Absolute Parametric Instabilities Near the Critical Density in Inhomogeneous Ionospheric and Laboratory Plasmas

D.L. Newman and M.V. Goldman*

APAS Dept., Campus Box 391, University of Colorado, Boulder CO 80309

B.B. Afeyan, and W.L. Kruert†

Lawrence Livermore National Laboratory, L-418, Livermore CA 94551

The parametric decay of a homogeneous pump wave into daughter Langmuir and ion acoustic waves is numerically studied for a plasma with a 1-D background density inhomogeneity. By varying parameters, the pump field can be interpreted as either the HF heater in ionospheric-modification experiments or as the laser field in laboratory laser-plasma interactions. The amplification of a stationary Langmuir source, which is localized along the direction of the gradient and taken to have a single (nonzero) wave number perpendicular to the gradient, is computed as a function of the source frequency. For sufficiently weak pumps, the amplitude of the steady-state response is finite (i.e., the system is absolutely stable), and spatially confined (by Landau damping at large wave numbers) to the linear region of the background density perturbation (which is assumed to be sinusoidal on the largest scales for numerical simplicity). In this regime, convective gain profiles can be determined. For more intense pumps, absolutely unstable eigen frequencies and eigen states are found. The transition from convective to absolute instability is examined in terms of the topology of the normal mode structure in complex frequency space. Examples from both the laboratory and ionospheric environments will be presented:

1. Convective amplification of Langmuir waves is studied for an HF irradiated “artificial barium ionosphere” produced during a chemical release over Arecibo. Here, the density scale length (~ 5 km) is short compared to that of the natural ionosphere. The influence of the background geomagnetic field is also included.
2. Parametric instabilities farther from the critical density are considered for conditions relevant to laser-generated high-Z plasmas in high temperature (smaller scale) hohlraums. A new regime of instability results due to the marked reduction in Landau damping of high-t Langmuir waves in the presence of modified electron distributions, which have depleted tails and flattened cores relative to Maxwellians.

* Work supported under by NSF Atmospheric Physics Grant ATM-9314409.

† Work supported by DoE contract No. W-7405-ENG-48.

Persistent Anti-Correlation of Stimulated Raman Scattering and Stimulated Brillouin Scattering in Gasbag Plasmas

D.S. Montgomery[†], B.J. MacGowan, R.K. Kirkwood, J.D. Moody, C.A. Back, S.H. Glenzer, G.F. Stone, B.B. Afeyan, R.L. Berger, W.L. Kruer, B.F. Lasinski, D.H. Munro, and E.A. Williams

Lawrence Livermore National Laboratory, Livermore, California 94551

D. Desenne and C. Rousseaux

Commissariat a l'Energie Atomique, Centre d'Etudes de Limeil-Valenton, 94195 Villeneuve-St-Georges Cedex, France

Persistent anti-correlation between the levels of stimulated Brillouin scattering (SBS) and stimulated Raman scattering (SRS) is observed in laser plasma experiments where the electron density n_e and the acoustic wave damping ν_{ia} are systematically varied. Gasbag targets are irradiated by nine beams of the Nova laser to create ≥ 2 mm size, 3 keV plasmas. A 351 nm interaction laser is used with beam smoothing to drive SRS and SBS with a fixed average intensity of $\sim 2 \times 10^{15}$ W/cm². The electron density n_e is varied between 0.06 - 0.15 n_{cr} using mixtures of C₃H₈/C₅H₁₂ (high ν_{ia}) or CO₂/CF₄ (low ν_{ia}). The estimated electron plasma wave damping increases a factor of 20 as density decreases, and the observed SRS levels decrease as expected. The estimated SBS gain decreases as the electron density decreases. However, observed SBS levels actually increase for lower density and are anti-correlated with the observed SRS levels. These experimental results will be presented and possible mechanisms for the anti-correlation will be discussed.

* Work performed under the auspices of the U.S. Department of Energy by the Lawrence Livermore National Laboratory under Contract No. W-7405-ENG-48.

† Present address Los Alamos National Laboratory, Los Alamos, New Mexico 87545

Spatiotemporal Evolution of Stimulated Raman Scattering

E.J. Turano and C.J. McKinstrie

*Laboratory for Laser Energetics, University of Rochester, 250 East River Road,
Rochester, NY 14623-1299*

We have solved the SRS equations analytically for boundary and initial conditions that are representative of a laser pulse convecting into fresh plasma.^[1] These solutions allow us to study forward, sideward, and backward SRS within a unified framework, and to follow the evolution of these instabilities as a laser pulse of arbitrary length enters into, propagates across, and exits from the plasma.

Unless the laser pulse is much longer than the plasma, SRS is a convective instability for all scattering angles. Regions of distinct spatiotemporal growth are delineated, and saturation times that account for both convection and damping are determined.

1. C. J. McKinstrie, R. Betti, R. E. Giacone, T. Kolber and E. J. Turano, Phys. Rev. E 51, 3752 (1995).

* This work was supported by the U.S. Department of Energy Office of Inertial Confinement Fusion under Cooperative Agreement No. DE-FC03-92SF19460, the University of Rochester, and the New York State Energy Research and Development Authority. The support of DOE does not constitute an endorsement by DOE of the views expressed in this article.

Deflection of an Unsmoothed Laser Beam by a Transverse Flowing Plasma

B. Bezzerides

Los Alamos National Laboratory, Los Alamos, New Mexico 87545

Results of gas-filled hohlraum experiments indicate that the laser beam is deflected towards the laser entrance hole[1]. Theoretical efforts to understand this phenomena invoke the model of filamented light guided by a transverse plasma flow[2-3]. In this paper, with experimental lineouts of the beam intensity profile for an *unsmoothed* NOVA beam, we calculate significant rates of deflection throughout the entire beam waist region. Thus, even in the absence of filamentation the beam can experience sizeable net deflection. One may draw some preliminary conclusions from this result. Beam smoothing may be a viable approach to reduce the deflection of the beam if strong filamentation is not present[4]. However at high enough intensities, even the smoothed beam is susceptible to hot spot induced filaments, and therefore merely smoothing the beam is not sufficient to remove the deflection in a general sense.

1. N.D. Delamater, et al., *Bull. Am. Phys.* **40**, 1831 (1995).
2. H.A. Rose, *Phys. Plasmas* **3**, 1709 (1996).
3. E.A. Williams and D.E. Hinkle, *Bull. Am. Phys.* **40** 1824 (1995).
4. J.D. Moody, et al., *Bull. Am. Phys.* **40**, 1824 (1995).

Laser Light Smoothing and Filamentation in Plasmas with Transverse and Axial Flows

D.E. Hinkel, C.H. Still, R.L. Berger, A.B. Langdon, E.A. Williams

Lawrence Livermore National Laboratory, University of California, Livermore, CA 94550

We have constructed a three-dimensional code (F3D) with nonlinear hydrodynamics¹ to study filamentation instabilities driven by nonuniform laser beams. In previous work with linearized hydrodynamics, we have shown that both supersonic and subsonic transverse flow “steers” the laser beam in the direction of the flow². In agreement with analytic estimates³, we have also observed in 3D simulations that, in homogeneous, initially stationary plasma, the laser beam hotspots move in time such that the time averaged laser intensity is smoother than the instantaneous pattern. This naturally occurring smoothing is compared to the smoothing obtained with imposed schemes such as SSD. The addition of axial flow has been shown to have dramatic effects on the filamentation process in 2D simulations⁴. The influence of three dimensional beam structure on filamentation and beam smoothing will be examined with and without axial flow.

1. C. H. Still, BAPS Louisville, Ky. , Nov. 1995
2. D. E. Hinkel et al., accepted to PRL, Jan 1996
3. D. E. Hinkel and E. A. Williams, BAPS 37, 1376, November 1992
4. A. Schmitt and B. B. Afeyan, BAPS Louisville, Ky., Nov. 1995

* This work was performed under the auspices of the United States Department of Energy by the Lawrence Livermore National Laboratory under Contract No. W-7405-ENG-48.

Interaction of Two Neighboring Hot Spots Taking Into Account the Effects of Plasma Dynamics

S. Hüller, Ph. Mounaix, D. Pesme, V.T. Tikhonchuk*
CPHT and LULI, Ecole Polytechnique, Palaiseau, France

D. Mourenas, M. Casanova
CEA Limeil-Valenton, Villeneuve-St. Georges, France

We present results of our code⁽¹⁾ KOLIBRI which models the interaction of intense electromagnetic beams with the low-frequency dynamics of the plasma fluid in two or three spatial dimensions. The light propagation is treated without the restriction of the paraxial optics approximation.

We have investigated the case of two focussed beams interacting with each other in a hot underdense homogeneous plasma. This can be considered as a reduced model for multiple hot spot interaction in optically smoothed laser beams. The superposition of the two beams gives rise to a strong interaction if the distance between the beams is smaller than the diameter of a single one in the focal region. This interaction produces the merging of the beams into a single density channel even though the incident power is below the self-focussing critical power. In high intensity regimes, this single channel formation is enforced by strong gradients in the light intensity caused by SBS near the entrance edge of the plasma. SBS remains unaffected by the long-wavelength density modifications caused by the beam merging. On the other hand, the SBS reflectivity is highly sensitive to the inter-beam distance.

1. S. Huller, Ph. Mounaix, D. Pesme, to be published in *Physica Scripta* (1996).

* On leave from Lebedev Physics Institute, Moscow, Russia.

Spot and Speckle Motion in SSD Illumination

A.B. Langdon and E.A. Williams

Lawrence Livermore National Laboratory, Livermore, CA 94550

We present analytic and computer results on laser spot motion due to SSD, at and below critical dispersion, and during "beam fill". Within the spot, we contrast time domain and frequency domain views of speckle structure, motion and lifetime. The results are of interest regarding laser-plasma phenomena that evolve on a time scale that is very short compared to the period of the frequency modulation.

Saturation of Stimulated Brillouin Scattering by Hydrodynamic and Kinetic Nonlinearities

A.V. Maximov, W. Rozmus and V.T. Tikhonchuk*

Department of Physics, University of Alberta, Edmonton, Canada

C.E. Capjack

Department of Electrical Engineering, University of Alberta, Edmonton, Canada

S.C. Wilks, W.L. Kruer

Lawrence Livermore National Laboratory, Livermore, USA

This work is concerned with a nonlinear evolution of stimulated Brillouin scattering (SBS) in one spatial dimension. We have studied effects of particle trapping and plasma inhomogeneity produced by the ponderomotive force of a single hot spot on the saturation of SBS. These studies involve particle-in-cell code and fully nonlinear hydrodynamical code.

The focussed laser light in a single hot spot exerts pressure on the background plasma producing velocity gradient which can saturate SBS for small f /numbers. The effect of ion trapping was accounted for in the hydrodynamical code by adding extra terms in the Poisson equation. The form of these additional contributions which are responsible for the ion acoustic frequency shift is based on the analytical theory of Ref. [1]. We were able to obtain very similar results to PIC code from hydrodynamical model with these extra terms and therefore we can include kinetic effects on the long spatial and time scales affordable in hydrodynamical modeling. The scaling of SBS reflectivity has been derived and compared with PIC simulations.

1. A. A. Andreev, V. T. Tikhonchuk, *Sov. Phys. JETP*, 68, 1135 (1989).

* On leave from Russian Academy of Sciences, Moscow, Russia.

Saturation of Stimulated Brillouin Scatter by Self Consistent Flow Profile Modification in Laser Hot Spots

Harvey A. Rose

Los Alamos National Laboratory, Los Alamos, NM 87545

Scattering instabilities, such as Stimulated Brillouin Scatter and Stimulated Raman Scatter, transfer momentum to the plasma which leads to flow inhomogeneities in laser hot spots that may significantly reduce the level of SBS. Simple estimates and simulations show that the magnitude of flow fluctuations can reach Mach numbers of order unity in a time scale of 100's of picoseconds. Temporal beam smoothing, such as SSD, does not necessarily eliminate this effect.

Hybrid PIC Simulations of Stimulated Brillouin Scattering Including Ion-Ion Collisions

P.W. Rambo, S.C. Wilks and W.L. Kruer

University of California, Lawrence Livermore National Laboratory

We investigate the role of Coulomb collisions in non-linear saturation and heating due to stimulated Brillouin scattering (SBS) in laser heated plasmas. Ion-ion collisions are particularly relevant to SBS from high-Z plasmas, where the collision rate of heated ions can be appreciable compared to the acoustic frequency. Our kinetic modeling makes use of particle-in-cell (PIC) techniques with binary Monte Carlo (MC) particle-particle collisions that are equivalent to the Fokker-Planck collision operator. For plasmas composed of high and low-Z ion mixtures (e.g. Au-Be), simulations show that collisions can maintain near-linear damping for finite amplitude waves by reducing the population of trapped ions. Inclusion of collisions reduces SBS compared to collisionless simulations due to modifications to the nonlinearly heated distribution function. For single species plasmas (e.g. Au), collisions reduce the heat flow compared to free-streaming conduction, locally decreasing $2 T_e T_i$ which in turn reduces SBS at late time compared to collisionless simulation. We note that similar effects with regard to electron-ion collisions may effect stimulated Raman scattering. We also present results on numerical heating in hybrid simulations, which is particularly severe for plasmas with large ratio of sound speed to ion-thermal speed, $2 T_e T_i \gg 1$; we have investigated the effect of smoothing, particle number, and particle-grid interpolation on this numerical heating.

* This work was performed under the auspices of the U. S. Department of Energy by Lawrence Livermore National Laboratory under Contract No. W-7405-Eng48.

Yield and Emission Line Ratios from ICF Target Implosions with Multi-Mode Rayleigh-Taylor Perturbations

Steven H. Langer, Chris Keane, Howard A. Scott

Lawrence Livermore National Laboratory, Livermore, CA 94551

In this paper we report results of detailed spectral postprocessing calculations of indirectly driven ICF implosions. We use Lasnex to simulate a two-dimensional capsule with surface perturbations covering a range of wavelengths. The perturbations grow during the Rayleigh-Taylor unstable phases of the implosion. The Lasnex hydrodynamic simulations are postprocessed using detailed atomic kinetics models to produce simulated spectra of argon and titanium. Argon is mixed with the fuel and its emission line ratios are used to diagnose fuel temperature. The titanium placed as a dopant in the inner regions of the plastic shell and its line emission is used to diagnose the mixing of fuel and pusher material. The models are run for several values of capsule surface roughness. We compare the yield and line emission as a function of surface roughness. Our results are compared to the predictions of Haan's mix model, which computes a mix depth based on Lasnex runs with single wavelength Rayleigh-Taylor perturbations.

* Worked performed under the auspices of the U.S. Department of Energy by the Lawrence Livermore National Laboratory under Contract W-7405-ENG-48.

Reflective Probing of the Electrical Conductivity of Hot Aluminum in the Solid, Liquid, and Plasma Phases

Andrew N. Mostovych and Yung Chan

*Laser Plasma Branch, Plasma Physics Division, U.S. Naval Research Laboratory,
Washington, D.C. 20375*

For most metals, experimental measurements of the electrical and thermal properties are limited to the low temperature ($< 2,000$ K) near-solid density ($N \sim N_{\text{solid}}$) condensed state or to the high temperature ($> 10,000$ K), low-density ($N \ll N_{\text{solid}}$) gas and plasma states. Theoretical models for calculating these transport properties are similarly restricted to very much the same parameter space. Calculations in the ordered solid phase and the highly disordered gas phase lend themselves to simplifying assumptions whereas calculations in the liquid phase at elevated temperatures and in the transition liquid-gas, liquid-plasma, and metal-insulator regions are difficult and there is little experimental data to test the theory. In this transitional regime, dense hot matter is typically degenerate and strongly coupled.

We report on experiments with tamped laser-heated aluminum which is in the transitional regime ($N \sim 0.6-1.0$ ns, $T \sim 0.3-1.0$ eV) and at sufficiently high pressure such that the samples are below the predicted critical point and boiling curve for aluminum. The electrical conductivity is measured by reflective probing and we find that the conductivity falls sharply as the aluminum is heated above 0.3-0.4 eV, substantially less than extrapolations of liquid-metal theory but greater than recent predictions of strongly coupled plasma theory for fully ionized plasmas.

* Supported by the Office of Naval Research

Spectroscopy of Thin Foils Heated With Ultra Short Laser Pulses

Ronnie Shepherd, Bruce Young, Dwight Price, A.L. Osterheld, Rosemary Walling,
Gary Guethlein, Richard More, and Richard Stewart
Lawrence Livermore National Laboratory, Livermore CA 94550

Takato Kato
National Institute for Fusion Studies, Nagoya, Japan

The technique of creating high energy-density plasmas using short pulse laser solid interaction is a developing field. A common goal of many researchers is producing the highest possible temperature with little or no material expansion. A significant limiting effect on the maximum temperature achieved in the interaction is the cooling rate. In the present set of experiments, we examine the competing cooling due to expansion versus thermal conduction.

The experiment is done using thin aluminum foils of successive thickness ranging from 250 Å to 1250 Å . The foils were heated with a 400 nm, 150 fs (FWHM) ultra short pulse laser. The laser energy was approximately 200 mJ and was focused to a spot size of 3 m, resulting in a peak intensity of 1.9×10^{19} W/cm². The prepulse to main pulse contrast was determined to be better than 10^{-7} . The $1s^2-1s2p$, $1s^2-1s3p$ transitions in He-like aluminum and the $1s-2p$ transition in H-like aluminum were temporally resolved using a 900 fs x-ray streak camera. Additionally, the Li-like and He-like satellites were temporally resolved. Using these data, the effect of target thickness (and hence thermal conduction) is used to examine the rate of cooling in the plasma. A simple model is used to interpret the experiment. We present the data and the preliminary findings from this study.

Investigation of the Conversion of Laser Energy to Relativistic Electrons at Intensities of 10^{20} W/cm²

K. Wharton, Y. Zakharenkov, C. Brown, B. Hammel, C. Joshi, J. Moody, A. Offenberger, M. Perry, S. Wilks, and V. Yanovsky

Lawrence Livermore National Laboratory, Livermore, CA 94550

We report on experiments using the 100 TW laser at LLNL (40 J, 400 fs, 10^{20} W/cm² focal intensity) and planar multi-layer targets (Mo/Sn) to study the generation and transport of electrons with MeV energies. Such fast electrons are of prime importance to many proposed applications, e.g., the fast ignitor fusion concept. X-ray emission spectroscopy is used to study the electron transport. Characteristic K- α photon emission produced by the fast electrons in the front (Mo) and rear (Sn) layers of the target is measured with a CCD detector (single photon counting mode) to infer the electron energy deposition. The electron energy spectrum is measured by varying the thickness of the Mo layer to attenuate the electrons by different amounts. In addition, penumbral imaging of the K- α emission is used to give information about the angular distribution of the fast electron emission. Comparisons with monte-carlo simulations reveal that the high-energy electrons contain over 10% of the incident laser energy.

Observation of Relativistic Electrons Produced in the Interaction of a 400-fs Laser Pulse With a Solid Target

G. Malka, C. Rousseaux, E. Lefebvre and J.L. Miquel
CEA-Limeil/Valenton, 94195 Villeneuve Saint-Georges Cedex, France

Relativistic electrons (0.5-20 MeV) produced by the interaction of a short 400-fs, 1.06- μm laser pulse on solid target, in the 3×10^{17} to 2×10^{19} W/cm² intensity range, have been measured. The results demonstrate the role of the ponderomotive force via the $\mathbf{J} \times \mathbf{B}$ effect: the hot temperature T_h of electrons accelerated along the laser axis is equal to the electron oscillation energy in the laser field, $T_h \sim (\gamma_{\text{osc}} - 1)mc^2$. For electrons emitted at 22° and 135°, T_h scales as $I^{1/3}$, X-ray spectroscopic measurements and numerical simulation show that the plasma is characterized by a step (a few microns) density gradient near the critical density. These data are compared with 1D PIC simulations.

In recent experiments, at a laser wavelength of 0.53 μm , the number of hot electrons sharply decreases as compared with the 1.06 μm experiments, and a cut-off appears in the hot electron distribution tail, due to interaction with dense plasma characterized by a very short gradient scale length ($L < \lambda$).

(Ref: "Experimental Confirmation of Ponderomotive-Force Electrons Produced by an Ultra Relativistic Laser Pulse on a Solid Target," G. Malka and J.L. Miquel, accepted for publication to Phys. Rev. Lett. May 96).

Absorption Mechanisms for Ultra-Intense Laser-Plasma and Solid Target Interactions

Scott C. Wilks and William L. Kruer

X-Division, Lawrence Livermore National Laboratory, Livermore, CA 94550

We present a comprehensive study of various absorption mechanisms present for the interaction of an ultra-intense laser interacting with an overdense plasma, which may be produced by shining the laser onto a solid. We concentrate on the absorption mechanisms that result in hot electrons. We will also mention absorption mechanisms that may occur in the underdense plasma in front of the solid, assuming the presence of a pre-pulse. Other absorption mechanisms, such as ion acceleration and shock formation will also be studied. Applications to the fast ignitor fusion scheme will be discussed.

* Work performed under the auspices of the United States Department of Energy by the Lawrence Livermore National Laboratory under contract number W-7405-ENG-48.

Electron/Ion Heating in the Interaction of an Ultra-Intense Laser Pulse with an Overdense Plasma

Erik Lefebvre, Catherine Toupin, Guy Bonnaud

CEA, Centre d'Etudes de L'imeil-Valenton, DPTA, 94195 Villeneuve-Saint-Georges, France

We address the electron/ion heating caused by the interaction of an ultra-intense laser pulse with an overdense plasma. The irradiance and plasma density values are such that no self-induced transparency^[1] occurs and thus the laser pulse only interacts with the plasma surface. The results come from the 1.5 D particle-in-cell fully-relativistic EUTERPE code. The laser irradiance I_0 and the density are in the respective ranges $[10^{18}—10^{20}]$ W/cm² and $[2—100]$ critical density n_c . The hot electron temperature is shown to be strongly dependent on the plasma density and the density gradient at the plasma edge. The higher the density, the lower the temperature increase. The temperature is observed to be much lower than the usual ponderomotive potential^[2]. Reducing the density gradient causes the temperature to increase.

The ion heating has been examined; the analysis of the ion trajectories has evidenced that ion heating can be due to both ion crossing in some kind of wave-breaking at the plasma surface, and collisionless shock deeper in the plasma^[3]. The domain of existence in the (irradiance, density) parameter space for such scenarii is given and kinetic energies are provided as well.

1. E. Lefebvre and G. Bonnaud, Transparency/opacity of an overdense plasma impinged by a ultra-intense laser pulse, *Phys. Rev. Lett.* 74, 2002 (1995).
2. S.C. Wilks, W.L. Kruer, M. Tabak, A.B. Langdon, Absorption of ultra-intense laser pulses, *Phys. Rev. Lett.* 69, 1383 (1992).
3. J. Denavit, Absorption of high-intensity subpicosecond lasers on solid density targets, *Phys. Rev. Lett.* 69, 3052 (1992).

Designs for Hole-Boring and Integrated Fast Ignitor Experiments

S.P. Hatchett, J.D. Moody, J.H. Hammer and M. Tabak

Lawrence Livermore National Laboratory, Livermore CA, 94551

With experiments on laser systems combining Nova with the 100-terawatt and the Petawatt short-pulse lasers we plan to test several elements of the "Fast Ignitor" technique. This is a proposed, novel technique for achieving inertial fusion in which the fuel is assembled, but not ignited, in a relatively cold implosion. A powerful and very short laser pulse, $I > 10^{19}$ W cm⁻², then ignites a spot on one side of the dense imploded material. In order for the high-intensity pulse to reach the dense matter, a longer, less intense laser pulse must first bore a hole or channel through the ablated plasma.

We present a design for an integrated implosion/hole-boring/high-intensity-energy-deposition experiment using the Petawatt/Nova-10-beam system. For that experiment we present computational studies addressing several design issues, especially the hole-boring element.

We present our designs, based on those studies, for early tests of the hole-boring element using the 100-terawatt/Nova-2-beam laser system. In these proposed experiments Nova beams illuminate one or two sides of a low-Z foil, creating an ablated blowoff plasma similar to that expected in the integrated experiments. A hole through the blowoff plasma and through/into the remaining high density material is produced by the 100-terawatt laser with a ~ 160 ps pulse at $I \sim 10^{17}$ W cm⁻². We discuss and model proposed diagnostic techniques for these experiments including interferometry and transmitted light.

*Worked performed under the auspices of the U.S. Department of Energy by the Lawrence Livermore National Laboratory under Contract W-7405-ENG-48.

Femtosecond Optical Probe Measurements of the Propagation of Terawatt Laser Pulses in Underdense Gas Targets

R. Fedosejevs¹, X.F. Wang² and G.D. Tsakiris

Max Planck Institut fur Quantenoptik, D-85748, Garching, Germany

Optical investigations have been undertaken of the interaction of a terawatt Ti:Sapphire laser pulse with underdense plasmas created from high density gas targets. The laser system delivers TW pulses with a duration of 250 fs and energy of 100 mJ to the target. These were focussed by an off axis parabola at a peak intensity of 3×10^{17} W/cm² into a high density gas jet capable of generating densities up to a few tenths critical density in the ionized gas. An optical probe pulse was generated by frequency doubling 4% of the main pulse and this was used together with a CCD camera imaging system to take time resolved shadowgraphic images of the interaction region in a transverse direction. The time integrated self emission and scattered radiation were also imaged onto the same CCD camera system. A separate CCD camera system viewed an image of the transmitted radiation. The electron densities explored in the present investigation ranged from 0.05 to 0.25 n_c using the gases: hydrogen, helium, and nitrogen. Various features of the interaction process are observed including the refraction of the leading edge of the pulse from the ionization induced electron density gradients, the self Thomson scattering of the fundamental radiation from the center of the plasma, and the emission of second harmonic radiation. Evidence for the onset of self focussing is observed for hydrogen at the critical power for relativistic self focussing. The results will be presented and discussed in terms of the expected behaviour at the threshold for relativistic self focussing.

¹ Permanent address: Department of Electrical Engineering, University of Alberta, Edmonton, Alberta T6G 2G7, Canada.

² Permanent address: Shanghai Institute of Optics and Fine Mechanics, Shanghai, P.R., China.

Interaction of a Chirped Picosecond Laser Pulse With He Gas: Time-Resolved Ionization-Induced Refraction and Compton Back-Scattering

E. DeWispelaere, V. Malka, J.R. Marqués, F. Arniranoff, F. Dorchies

**Laboratoire pour l'Utilisation des Lasers Intenses, Ecole Polytechnique, 91128 Palaiseau Cedex, FRANCE.*

P. Chessa, P. Mora, Ph. Mounaix

Centre de Physique Theorique, Ecole Polytechnique, 91128 Palaiseau Cedex, FRANCE

G. Grillon, G. Hamoniaux

**Laboratoire d'Optique Applique'e, Ecole Nationale Supérieure des Techniques Avancées, FRANCE*

Laboratoires associés aux Centre National de la Recherche Scientifique.

We present an experimental study of the interaction of a chirped laser pulse (1.5 ps) with helium gas. By using long chirped pulses, we obtain some new informations on ionization-induced refraction and Compton backscattering.

A comparison between the angular-resolved transmitted spectra in the case of positive and negative chirp is used to resolve in time the importance of refraction. This comparison shows that the rising part of the pulse is unmodified by the propagation while the end is refracted at large angles, except on the axis, where the spectrum keeps its initial aspect. These results are compared with 2D numerical simulations.

Concerning the Compton instability, we present the intensity and wavelength behaviour of the backscattered satellite as function of the gas pressure and of the sign of the chirp.

Second Harmonic Generation in the Interaction of a Short-Pulse Laser with Underdense Plasma

V. Malka

Ecole Polytechnique, Palaiseau, FRANCE

A. Modena, Z. Najmudin and A.E. Dangor
Imperial College, London, U.K.

C.E. Clayton, K.A. Marsh and C. Joshi
UCLA, Los Angeles, USA

C.N. Danson, D. Neely and F.N. Walsh
Rutherford Appleton Lab., Oxon. U.K.

In an experiment using the VULCAN CPA laser at the Rutherford Appleton Laboratory we observed very high efficiency ($>10^{-3}$) of second harmonic generation in the interaction of a short pulse intense laser with underdense plasma. Second harmonic spectra observed in the forward direction show Stokes and anti-Stokes satellites. This is a signature of the presence of large amplitude relativistic plasma waves interacting with the second harmonic light. Second harmonic images were also taken at 30° from the propagation axis and show that the light is generated over few times the Rayleigh length. The creation of the second harmonic emission is most probably due to radial density gradients which are caused by different ionization stages boundaries and by depletion of electrons due to the radial ponderomotive force.

Suppression of Cavitation by the Occurrence of RFS^{1*}

K.-C. Tzeng[†] and W.B. Mori^{††}

*Departments of Physics and Astronomy, and Electrical Engineering
University of California, Los Angeles, CA 90095*

The evolution of a short-pulse laser in an underdense plasma has been a topic of active research due to its importance to laser plasma accelerators, the fast ignitor fusion concept, and the nonlinear optics of plasmas at relativistic intensities. Such laser pulses are susceptible to a variety of instabilities, one of which, relativistic self-focusing can cause electrons near the center to be completely evacuated due to the increased light pressure. This complete evacuation of electrons is called cavitation. We have previously presented PIC simulations^[1] which show Raman Forward Scattering (RFS) dominates in these regimes and no evidence of cavitation was observed. The simulations were done in 2D slab geometry which reduces the intensity enhancement caused by self-focusing. In this paper, however, we show using PIC simulations in which RFS is artificially suppressed that, for initially wide spot sizes, cavitation can occur even in 2D slab geometry. Therefore the occurrence of RFS definitely reduces the tendency for cavitation. We will also discuss the competition between cavitation, self-focusing, and RFS for parameters relevant to several recent short-pulse laser-plasma experiments.

1. K.-C. Tzeng, W.B. Mori, and C.D. Decker, Phys. Rev. Lett., 76, 3332 (1996).

* Work supported by LLNL# 4-444025-DA-26⁹⁵5 and DOE# DE-FG03-92ER40727.

† Email Address: tzeng@physics.ucla.edu

†† Email Address: mori@physics.ucla.edu

Wednesday

ORAL PRESENTATIONS

8:30 AM – 12:30 PM

Short Pulse Laser

Chris Clayton, Session Chair

Long Pulse Laser

Colin McKinstrie, Session Chair

Foil-Terminated Free Wave Acceleration

Scott C. Wilks, R. Freeman, F. Hartmann, A. Kerman, A.B. Langdon, and J. Woodworth
X- Division, Lawrence Livermore National Laboratory, Livermore, CA 94550

We present theoretical and simulation results on a modification of the free wave accelerator concept.^[1] It is well known that real acceleration of a charged particle in the presence of an electromagnetic wave is impossible, if all the criteria of the Lawson-Woodward theorem are satisfied. However, if one or more of the criteria are broken, it may be possible to use intense laser beams to accelerate charged particles to very high energies. We present a scheme in which the criterion requiring vacuum EM wave propagation is broken. In particular, a thin foil is placed at the focus of the laser beam. Particles are accelerated on their way to the foil, obtaining maximum energy near the focus. If the foil is not present, the particles would then lose their energy back to the EM wave, as they pass through the focus. However, we place the thin foil at the focus to disrupt the laser beam. In this manner, the particle preserves the energy it has gained on its way to the focus, since there is no EM field present behind the foil. Many questions about this scheme have been addressed via particle in cell simulations. Namely, effects of the reflected wave on the particles on energy gain and emittance, as well as various configurations of the EM wave will be discussed.

1. See for example, E. Esarey et al., this conference, or W. B. Mori and T. Katsouleas Proceedings of the Advanced Accelerator Concepts, AIP, Lake Geneva, WI, editor P. Schoessow (1995).

* Work performed under the auspices of the United States Department of Energy by the Lawrence Livermore National Laboratory under contract number W-7405-ENG-48.

Electron Acceleration by a Laser Pulse in a Plasma

E.A. Startsev and C.J. McKinstrie

*Laboratory for Laser Energetics, University of Rochester, 250 East River Road,
Rochester, NY 14623-1299*

The motion of a charged particle in an electromagnetic field is a well-known paradigm of physics. Suppose that the field is associated with a laser pulse of finite extent propagating in a vacuum. As the pulse overtakes the particle, the particle gains energy and momentum. At the peak of an intense pulse, the particle has considerable momentum in the propagation direction of the pulse. However, the oscillatory energy of the particle is wasted, and it is difficult to extract the particle from the middle of the pulse.

We have found an exact analytic solution for the motion of an electron under the influence of a circularly polarized laser pulse in a plasma. This solution shows that a pre-accelerated electron can be accelerated efficiently and extracted easily. Although the pulse tends to generate a plasma wake, to which it loses energy, one can eliminate the wake by choosing the duration of the pulse judiciously. The effects of finite pulse width will be discussed briefly.

* This work was supported by the U.S. Department of Energy Office of Inertial Confinement Fusion under Cooperative Agreement No. DE-FC03-92SF19460, the University of Rochester, and the New York State Energy Research and Development Authority. The support of DOE does not constitute an endorsement by DOE of the views expressed in this article.

Multiple-Scale Derivation of the Relativistic Ponderomotive Force

C.J. McKinstrie and E.A. Startsev

*Laboratory for Laser Energetics, University of Rochester, 250 East River Road,
Rochester, NY 14623-1299*

Although the ponderomotive term^[1] that appears in the Eulerian formulation of the electron-fluid momentum equation has the units of a force, it is not the actual force felt by a single electron or a Lagrangian element of the electron fluid. In the nonrelativistic limit, the ponderomotive force on a single particle is $\nabla(A_0^2/4)$, where $A_0 = v_0/c$ is the quiver velocity of the particle oscillating in the high-frequency electromagnetic field. Some authors have generalized this result by replacing the nonrelativistic quiver velocity v_0/c with the relativistic quiver momentum p_0/m_0c . This generalization is incorrect.

By using multiple-scale analysis, we have shown that for an electromagnetic wave in a vacuum.[2]

$$d_{\tau\tau}^2 X_\mu = \partial_\mu (A_0^2/4),$$

where X_μ is the slowly varying position four-vector of the particle, τ is its proper time and A_0 is its quiver momentum. Thus, the common generalization is the spatial component of the ponderomotive four-force. To determine correctly the averaged particle motion, one needs to determine also the slowly varying time X_0 and plot X_j as a function of X_0 . Some consequences of the ponderomotive force for experiments with terawatt laser beams will be discussed briefly.

1. C. J. McKinstrie and D. F. DuBois, Phys. Fluids 31, 278 (1988).
2. E. A. Startsev and C. J. McKinstrie, Bull Am. Phys. Soc. 40, 1723 (1995).

* This work was supported by the U.S. Department of Energy Office of Inertial Confinement Fusion under Cooperative Agreement No. DE-FC03-92SF19460, the University of Rochester, and the New York State Energy Research and Development Authority. The support of DOE does not constitute an endorsement by DOE of the views expressed in this article.

Stabilities of Intense Laser Propagating in Underdense Plasma Channels

T.C. Chiou, T. Katsouleas

*Department of Electrical Engineering-Electrophysics, University of Southern California
Los Angeles, CA 90089-0484*

W. B. Mori

University of California, Los Angeles, CA 90024

The stability of intense laser pulses ($I \lesssim 10^{18} \text{W/cm}^2$) that are propagating in and guided by underdense plasma channels is investigated both analytically and through Particle-In-Cell (PIC) simulations.

In a plasma channel with parabolic radial profile matched to a Gaussian laser profile, the laser evolves into a one-dimensional (1-D) like Raman forward scattering (RFS) or laser hosing instability depending on the noise source for the instabilities. In a partially filled channel where the radial plasma density is a step function with lower density inside and higher density outside, the laser hosing instability can be suppressed by reducing the channel radius such that the channel can guide only one mode. However, the laser can still undergo 1-D like RFS. In a hollow channel where the plasma is totally evacuated from the channel center, the 3-wave and 4-wave growth rates of RFS are derived. The laser hosing can be suppressed by making it a single mode channel as in the partially filled channel case. The analytic expressions also show that even the RFS can be completely suppressed if $a < 0.6c/\omega_p$ where a is the channel radius and ω_p is the plasma frequency. The PIC simulations are performed and shown to agree with these analytical predictions.

These results suggest that hollow plasma channels may be effective in transporting ultra-intense lasers over many Rayleigh lengths.

An Experimental Demonstration of the Laser Wakefield “Photon Accelerator”: Longitudinal Interferometric Diagnostics for Plasma Based Accelerators

¹C.W. Siders, S.P. LeBlanc, D. Fisher, T. Tajima, M.C. Downer,
²A. Babine, A. Stepanov, A. Sergeev

¹*Department of Physics, The Institute of Applied Physics, University of Texas at Austin,
Austin, Texas;* ²*The Institute of Applied Physics, Nizhny Novgorod, Russia*

Because the electrostatic fields present in plasma waves exceed those in conventional accelerators and approach atomic scale (500 GV/m), plasma based accelerators have received considerable attention as compact sources of high-energy electron pulses^[1]. Although stimulated Raman scattering^[2] or terahertz radiation at Up^[3] provided spatially averaged evidence of the plasma wave's existence, new diagnostic techniques are needed to map the temporal and spatial plasma wave structure. In this paper, we report femtosecond time resolved measurements of the longitudinal structure of laser wakefield oscillations using an all-optical technique known as photon acceleration^[4].

In these experiments, a probe pulse co-propagates behind an intense pump pulse ($I = 3 \times 10^{17}$ W/cm², $A = 0.8$ μ m, $T = 100$ fs) tightly focused ($f\# = 4.2$) in helium gas. As the pump ionizes the gas and exerts ponderomotive pressure on the resulting plasma, the probe pulse experiences electron density gradients behind the pump pulse which cause both DC phase shifts and blue/red shifting of the probe pulse frequency spectrum. To detect the small changes in frequency and phase with femtosecond resolution, our diagnostic uses multiple, temporally separated probe pulses in a longitudinal (i.e. frequency domain) interferometric configuration^[5].

Two experiments were conducted to temporally resolve the wakefield oscillations. In the first, probe pulses propagated in front of and behind the pump pulse and the pump-probe delay was varied. Figure 1 shows measured phase shifts in 4.8 (2.7) Torr helium oscillating with a period of 220 ± 25 (270 ± 10) fs, to be compared with the linear values of 200 (267) fs, and an amplitude of 7(5) mrad. Under these conditions, we detect wakefield oscillations 3-5 (4-5) cycles behind the pump pulse. From the amplitude of the phase modulation in Figure 1, we estimate that the amplitude of the wakefield density oscillation, $\delta n_e/n_e$, is of order unity. This amplitude is larger than a simple one (longitudinal) dimension estimation as the radial component of the ponderomotive force is order ten times larger than the axial component. The peak longitudinal electric field is estimated as ~ 10 GV/m. The second, pressure scan, experiment confirmed that the oscillatory phase measured originated from plasma density oscillations (see Siders et al. in [5]).

To model the experimental results, numerical simulations were performed with a two-dimensional, fully relativistic, cold fluid model. The simulation in Figure 2 shows the excitation of nonlinear plasma waves near the focus with significant density peaking and a peak $\delta n_e/n_e \sim 5$. In the intense focus, the wakefield oscillations are strongly steepened on a length scale shorter than the probe pulse. Thus, density peaking is not directly resolved by

the probe pulse, though a small nonlinear decrease in ω_p is seen in the simulations, consistent with the observed periods.

1. T. Tajima et al., Phys. Rev. Lett. 43, 267 (1979); P. Sprangle, W. M. Wood et al., Phys. Rev. Lett. 67, 3523 (1991). et al., Phys. Fluids B 4, 2241 (1992).
2. C. E. Clayton et al., Phys. Rev. Lett. 54, 2343 (1985), et al., Opt. Lett. 17, 1131 (1992); J. P. Geindre et al., Opt.
3. H. Hamster et al., Phys. Rev. E 49, 671 (1994), Lett. 19, 1997 (1994); Siders et al., IEEE Trans. Plasma Sci. 24, 301 (1996); Siders et al., Phys. Rev. Lett. 76, 3,70 (1996).
4. S. C. Wilks et al., Phys. Rev. Lett. 62, 2600 (1989).
5. Reynaud et al., Opt. Lett. 14, 275 (1989); E. Tokunaga et al.

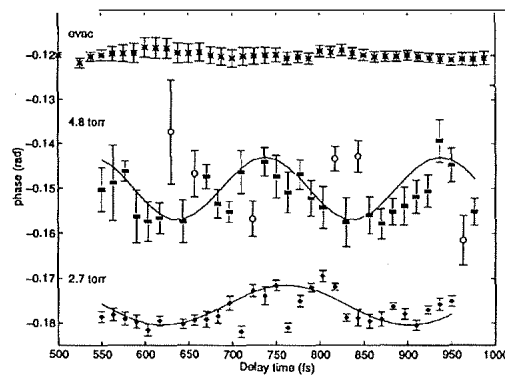


Figure 1. Wakefield oscillations in He. For 4.8 Torr, the two probes were separated by 2.2 ps about the pump. In the 2.7 Torr data (offset from zero and shifted by -400 fs) the probes trail the pump with 415 fs separation. The e^{-1} intensity radius was 3.6 (5.0) μm . Solid lines show the calculated phase shift from the wakefield. The top set of data corresponds to an evacuated gas chamber.

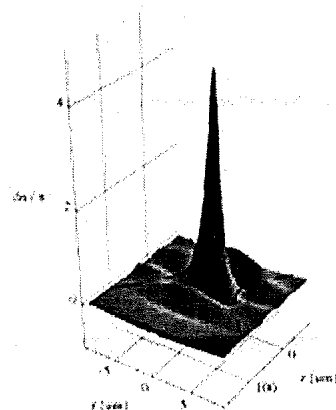


Figure 2. Two-dimensional simulation of $\delta n_e/n_e$ corresponding to $E = 10$ mJ, 3.6 μm spot radius, $\tau = 100$ fs, $n_e = 3 \times 10^{17}$ cm^{-3} . The figure shows the electron density oscillations within the tight focus. The pump pulse (centered at $z = 111$ μm) is moving in the positive z direction, but is not shown. The heavy line represents the e^{-1} intensity contour of the laser focus.

Laser Wakefield: First Temporal and Spatial Measurement of the Electron Density Oscillation

J.R. Marques, F. Dorchies, F. Amiranoff, P. Audebert, J.-P. Geindre, J.-C. Gauthier
LULI, Ecole Polytechnique - CNRS, 91128 Palaiseau, France

A. Antonetti, G. Grillon
LOA, ENSTA, Ecole Polytechnique - CNRS, 91120 Palaiseau, France

The plasma electron density oscillation produced in the wake of an ultra-short laser pulse is measured for the first time with a temporal resolution much better than the electron plasma period, and a high spatial resolution along the laser focal spot diameter. The relative amplitude of the density oscillation goes from 10 to 100%. Numerical simulations show a good agreement with the observed oscillation period, amplitude and lifetime.

Exploded Foil Transmission Experiments with an Ultra-Intense Laser

J.A. Cobble, R.P. Johnson, R.J. Mason

Los Alamos National Laboratory

The fast ignitor is an exciting new concept¹ for the ignition of laser fusion capsules. It relies on conventional compression to assemble a fuel mass to high density after which a high intensity laser beam (irradiance $> 10^{18}$ W/cm²) achieves point ignition at the fuel surface. The "surface" is the boundary between the critical density and the density profile steepened² by the ponderomotive force of the ultra-intense beam. The first issue for the success of the fast ignitor is whether the high intensity beam can, in fact, penetrate³ the sub-critical corona surrounding the high density fuel.

We have used an exploding foil as a surrogate corona plasma target which we have probed at irradiances $1 - 7 \times 10^{18}$ W/cm². The beam transmission, the integrity of its intensity profile, and the SBS backscatter have been measured. We find that the majority of the light is transmitted through densities below $\sim 5\%$ critical where the plasma scale length is > 300 Elm. The f number of this component of the beam approximately doubles as was the case⁴ on a H₂ gas jet with no prelude. This tendency for beam collimation is very encouraging for the fast ignitor. We also observe less than a few percent SBS backscatter. The SRS backscatter from comparable densities has been measured elsewhere⁵ as saturating at no more than 20%. If these trends continue in experiments where the probe climbs the density gradient, it means the fast ignitor has passed the first test.

1. M. Tabak, J. Hammer, M. E. Glinsky, W. L. Kruer, S. C. Wilks, J. Woodworth, E. M. Campbell, M. D. Perry, R. J. Mason, *Phys. Plasmas* 1, 1626 (1994).
2. W. L. Kruer, **The Physics of Laser Plasma Interactions**, AddisonWesley, 1988, chap. 10.
3. P. E. Young, M. E. Foord, J. H. Hammer, W. L. Kruer, M. Tabak, S. C. Wilks, *Phys. Rev. Lett.* 76, 1082 (1995).
4. P. Monot, T. Auguste, P. Gibbon, F. Jakober, G. Mainfray, *Phys. Rev. E* 52, R5780.
5. C. Rousseaux, G. Malka, J. L. Miquel, *Phys. Rev. Lett.* 74, 4655 (1995).

Development of an Ultrafast, High Energy Pulse CO₂ Laser

Jochen Meyer and Michael KY. Hughes

Dept. of Physics, University of British Columbia

In recent years a rapid advance has taken place in the development of compact laser systems capable of generating subpicosecond multi TW pulses in the UV to near IR spectral region. This in turn has opened up new frontiers in laser-matter interaction physics. There exist however a class of problems, including ponderomotive confinement of surface plasmas, tunneling ionization effects etc. which would much better be investigated using ultrashort pulses in the mid IR spectral region. To this end we have developed a unique CO₂ laser system capable of generating 0.1 J pulses of Alps duration at a rate of 1 Hz. The gain medium consists of a 15 atm TE-fast discharge module of 1.5 cm diameter aperture. Due to pressure broadening of the rotational lines the bandwidth of the complete vibrational gain spectrum of either the R-branch centered around 9.4 μm or the Q-branch around 10.6 μm can support the short pulses. The gain module is positioned in a 1.5 m long telescopic unstable resonator. Sub ps CO₂ laser pulses are injected into the resonator from a special semiconductor wafer positioned at Brewster angle to the cavity and by optical switching from a cw-beam. After regenerative amplification in 10 round trips the pulse is dumped from the cavity by a second optically activated Brewster angle GaAs wafer to provide the output. The injection switch is activated by a 200 fs pulse from an amplified synchronously mode locked dye laser generating an ultrashort lifetime free carrier mirror. Details of the development of this fast switch will be discussed. The cavity dump is activated by the output from a frequency doubled Nd:YAG regenerative amplifier which also pumps the dye amplifier. Successful operation of the system required the development of accurate timing technology for the various components and proper optical beam geometry. To analyze the output from this system we have developed a novel cross correlation technique which permits the measurement of the pulse power as function of time at 100 fs resolution. The technique and its application will be described. Plans for further amplification and pre pulse control with a high pressure CO₂ hot cell will also be discussed.

Dependence of Stimulated Raman Scattering on Ion Acoustic Damping*

Juan C. Fernandez¹, J.A. Cobble¹, Bruce H. Failor³, Donald F. DuBois¹,
David S. Montgomery^{2**}, Harvey A. Rose¹, Hoanh X. Vu¹, Bernhard H. Wilde,
Mark D. Wilke¹ and Robert E. Chrien¹

¹*Los Alamos National Laboratory, Los Alamos, NM, USA*

²*Lawrence Livermore National Laboratory, Livermore, CA, USA*

³*Physics International, San Leandro, CA, USA*

The reflectivity of a laser due to Stimulated Raman scattering (SRS) has been recently studied in Nova hohlraum plasmas with scale lengths approaching those expected in ignition hohlraum plasmas. It is found that the SRS reflectivity depends approximately linearly on the damping rate of ion acoustic waves normalized to the real acoustic frequency (ν_i/ω_i). This is consistent with SRS saturation by parametric decay processes of the SRS Langmuir wave involving ion acoustic waves. In addition to the time-integrated reflectivity data, we show in this paper the time evolution of the reflected SRS power, which is consistent with the evolution of ν_i/ω_i predicted by radiation-hydrodynamic simulations of these hohlraums using the LASNEX computer code.

* This work sponsored by the US DOE.

** Present address: Los Alamos National Laboratory, Los Alamos, NM

Study of SRS and SBS from NOVA Targets Using the Axial Imager

Wm. Monty Wood, Juan C. Fernandez

Los Alamos National Laboratory, Los Alamos, NM 87544

Time-resolved images of SRS and SBS, looking down the axis of NOVA hohlraum targets, have been collected and analyzed. Images have resolution of smaller than 10 microns, with depth of field between 0.5 and 1.0 mm. Time resolution varies between integrated time steps of 0.3 ns to 0.5 ns. Monitoring SRS, the evolution of different plasma density regions has been followed with integrated time steps of approximately 0.3 ns. Evidence of effects due to window ablation and target wall ablation and expansion have been observed. Images have been compared to the expected plasma density and temperatures from modeling of the hohlraum targets. Monitoring SBS, evidence of scattering from regions smaller than 25 microns in diameter has been observed. Asymmetries in images also give an indication of beam steering.

Saturation of SRS by the Stimulation of Ion Waves in Ignition Relevant Plasmas*

R.K. Kirkwood, B.B. Afeyan, C.A. Back, M.A. Blain, R.L. Berger, D.E. Desenne,
K.G. Estabrook, S.H. Glenzer, W.L. Kruer, B.F. Lasinski, B.J. MacGowan,
D.S. Montgomery, J.D. Moody, R. Wallace and E.A. Williams

*Lawrence Livermore National Laboratory, University of California, L-473 P.O. Box 808,
Livermore California 94550, U.S.A*

**Centre D'Etudes de Limeil-Valenton, France*

A series of experiments has been performed that demonstrate the dependence of stimulated Raman scattering (SRS) on ion wave damping in the high Z plasmas found in ignition scale targets. This dependence has been observed in two types of targets shot on Nova that simulate the conditions of the National Ignition Facility and is consistent with a model in which growth of the Langmuir wave is impeded by a secondary decay involving an ion acoustic wave. In the high Z plasmas formed in both CH filled 'scale-1' hohlraums, and Xe filled gas bags, the ion wave damping is varied by varying the concentration of a low Z impurity in the high Z material. The impurity is introduced in the Au wall of the hohlraum by placing a patch of alternating layers of Au/Be (110 Å per layer pair, 5000 Å thick) over a hole cut in the hohlraum wall at the point at which one of the laser beams is incident. A strong dependence of SRS reflectivity on the atomic fraction of Be is observed even with as little as 20 % Be. It is further demonstrated using the well characterized plasmas formed with a Xe filled gas bag target, that the SRS reflectivity is linearly proportional to the ion wave damping rate and has a magnitude consistent with secondary decay mechanisms that involve ion waves. In these experiments the SRS reflectivity is proportional to the concentration of a C₅H₁₂ impurity when the impurity concentration is low, while other plasma properties such as Te and ne are essentially constant. The reflectivity is interpreted as a Thomson scattering measurement of the amplitude of the Langmuir wave. Both the wave amplitude and its linear dependence on impurity concentration are consistent with the growth of the Langmuir wave being impeded by either Langmuir decay instability (LDI) and the electromagnetic decay instability (EDI), or both. In these instabilities the SRS driven Langmuir wave decays into an ion acoustic wave and a secondary Langmuir wave or electromagnetic wave, transferring energy from the resonant SRS wave to waves with different frequency and wave number.

* This work was performed under the auspices of the United States Department of Energy by the Lawrence Livermore National Laboratory under Contract No. W7405-ENG-48.

Saturation of SRS by Excitation of Langmuir Turbulence*

David Russell

Lodestar Research Corporation

D.F. DuBois and Harvey A. Rose

Los Alamos National Laboratory

Recent NIF emulation experiments using gas bag¹ and hohlraum targets² have found a roughly linear dependence on the ion acoustic damping ratio. Such a dependence has been predicted theoretically³ and from 1D reduced model simulations^{4,5} which take into account the Langmuir decay instability (LDI) of the primary SRS Langmuir wave (LW) into another LW and an ion acoustic wave. (The decay LWs from LDI were recently observed by Thomson scattering⁶). The proportionality of the LW power threshold for LDI on leads⁷ to the dependence of the SRS reflectivity. Here we report preliminary results from a new 2D reduced model code. The code includes RPP hot spot structure of the pump field and plasma inhomogeneity. Results are found for regimes high temperatures (>3 keV) and low Z and density where LDI is predicted to be the control valve for saturation. Nonlinear processes which play a role in the saturated state, in addition to LDI, include Langmuir collapse and density profile modification, the latter being dominated by the ponderomotive pressure of the induced Langmuir turbulence. The dependence of the reflectivity on and the level of long wavelength velocity fluctuations driven up by the Langmuir turbulence are studied. The latter arise from ponderomotive beats of nearby wave vectors in the primary LW spectrum. It is of interest to determine whether these long wave length fluctuation are strong enough to suppress SBS⁸.

1. Kirkwood et al., submitted to PRL 1996.
2. Fernandez et al., submitted to PRL 1996.
3. Heikkinen and Kartunnen, Phys. Fluids, **29**, 1291, (1986).
4. Bezzerides, DuBois, and Rose, Phys. Rev. Lett. **70**, 2569 (1993).
5. Kolber, Rozmus, and Tikhonchuk, Phys. Fluids **B6**, 138 (1993).
6. K. Baker, Thesis 1996, UCD.
7. Drake and Batha, Phys. Fluids **B3**, 2936 (1991).
8. Maximov, Rozmus, Tikhonchuk, DuBois, Rose and Rubenchik, Phys. Plasmas, **3**, 1689, (1996).

* Research supported by the USDOE.

Saturation of SRS in Regimes Where Secondary Langmuir Decay is Inaccessible*

D.F. DuBois and Harvey Rose
Los Alamos National Laboratory

David Russell
Lodestar Research Corp.

For a wide range of densities, temperatures, and laser parameters predicted for NIF plasmas for which there is appreciable SRS gain, the Langmuir decay instability (LDI) is the controlling instability leading to saturation as discussed in the preceding paper. This is particularly true for high Z regimes in which the electron velocity distribution is modified in such a way as to lower the Langmuir wave (LW) Landau damping compared to that for a Maxwellian distribution^{1,2}. Another secondary instability sometimes called the electromagnetic decay instability (EDI)³ in which the SRS LW decays into an electromagnetic wave (EMW) and an ion acoustic wave (IAW), can also occur. The EMW is excited most strongly in directions perpendicular to the laser axis. Its damping threshold is proportional to the EMW collisional damping whereas that for the LDI is proportional to the LW Landau damping in regimes where this damping is strong and the LDI has a higher damping threshold. (In such high Landau damping regimes the effective EDI threshold is raised above its damping threshold because of the broad bandwidth of the LW pump. The thresholds for both processes are proportional to the IAW damping parameter V_i). Even though its threshold may be higher, in regimes where both instabilities are allowed, LDI will control the saturation because the convective gain rate of EDI is so low. However for low Z plasmas there are high temperature, moderate density regimes (e.g. $I_0 = 2 \times 10^{15}$ W/cm², $T_e > 3$ keV, $n/n_c > 0.1$, for $V_i = 0.1, f/4$) where the LDI is inaccessible⁴ because of strong Landau damping while the SRS critical gain threshold⁵ is still exceeded. For comparable SRS linear convective gain the reflectivity is expected to be higher in regimes where LDI is prohibited. In such regimes a high LW saturation level resulting from the weak EDI is expected. Theoretical arguments leading to these conjectures will be presented and preliminary results from a 2D reduced model simulation code which models both LDI and EDI will be presented.

1. Langdon (1980), Alaterre, Matte, and Lamoureux (1985) and others.
2. Afeyan, Chou, and Kruer, 1996 private communication.
3. Kevin Baker, 1966 thesis UCD; Kirkwood et al. 1996 submitted to PRL.
4. Fernandez et al. 1996 submitted to PRL
5. Rose and DuBois (1994), in the strong damping limit the critical intensity for SRS is calculated the same way as for SBS.

*Research supported by the USDOE

135

Electron Plasma and Ion Acoustic Waves in Flat Top Electron Velocity Distributions

Bedros B. Afeyan¹, Albert E. Chou² and W.L. Kruer

¹*Lawrence Livermore National Laboratory*

²*University of California, Los Angeles*

We have calculated the complex frequencies of electron plasma waves and ion acoustic waves in non-Maxwellian electron distribution functions that occur in high Z plasmas illuminated by high intensity lasers. The palpable reduction in electron Landau damping and large modification in the sound speed and damping of ion waves have significant consequences for Raman and Brillouin scattering in such plasmas. We explore these ramifications highlighting the changed angular distribution of SRS and the curtailment of long interaction lengths for SBS due to changes in the acoustic speed caused by hot spots in high Z plasmas. This work is motivated by Xe gas bag as well as high temperature hohlraum experiments recently conducted on NOVA at LLNL.

* Work performed under the auspices of the U.S. DoE by LLNL under contract No. W-7405-ENG-48.

Raman Scattering in Gas-Filled Hohlräume and Gasbags

Albert Simon

*Laboratory for Laser Energetics, University of Rochester, 250 East River Road,
Rochester, NY 14623-1299*

There seem to be two distinct types of Raman scattering in hohlraums and gasbags. In Nova Scale-1 hohlraums,^[1] where n_c and $n_c/4$ surfaces abound, the Raman scattering is dominated by very short wavelengths concentrated near $\lambda = 470$ nm. A weaker narrow component is seen above 550 nm. The situation is reversed in gasbags.^[2] The narrow component near 550 nm dominates. A weak short- λ component is seen transiently. We propose that the narrow component is the "real" SRS, while the short- λ radiation is incoherent Thomson scattering from very-enhanced plasma waves created by electron beams originating at n_c or $n_c/4$ surfaces.^[3,4] Alternative explanations of the short- λ radiation based on SRS or SCS face serious difficulties, which we will discuss. Explanations based on filaments have much difficulty producing the observed spectrum, while this spectrum arises more readily in the Thomson beam model. The transient short- λ in gasbags may be due to chunks of n_c or $n_c/4$ being illuminated by the interaction beam, since conditions may not be as uniform as LASNEX predicts.^[5] RPP strongly reduces the electron beam production mechanism at n_c or $n_c/4$ yet has only a small effect on the real SRS. Adding SSD further reduces the real SRS. "Occam's Razor" will also be discussed.

1. B. MacGowan, presented at the Laboratory for Laser Energetics, University of Rochester, Rochester, NY, 22 September 1995.
2. D. S. Montgomery *et al.*, presented at the 25th Annual Anomalous Absorption Conference, Aspen, CO, 27 May-1 June 1995. paper 109.
3. A. Simon and R. W. Short, Phys. Rev. Lett. 53, 1912 (1984).
4. A. Simon, W. Seka, L. M. Goldman, and R. W. Short, Phys. Fluids 29, 1704 (1986).
5. J. C. Fernandez *et al.*, Phys. Rev. E 53, 2747 (1996).

* This work was supported by the U.S. Department of Energy Office of Inertial Confinement Fusion under Cooperative Agreement No. DE-FC03-92SF19460, the University of Rochester, and the New York State Energy Research and Development Authority. The support of DOE does not constitute an endorsement by DOE of the views expressed in this article.

Thursday

ORAL PRESENTATIONS
8:30 AM – 12:30 PM

Hohlraum Physics
Larry Suter, Session Chair

Hydrodynamics
Doug Wilson, Session Chair

138

Indirect-Drive Proof-of-Principle Experiments on OMEGA

T.J. Murphy, J. Wallace, J.A. Oertel, Cris W. Barnes, N.D. Delamater, P. Gobby,
A.A. Hauer, G. Magelssen, J.B. Moore, and R. Watt
Los Alamos National Laboratory, Los Alamos, NM

O.L. Landen, R.E. Turner, P. Amendt, C. Decker, L.J. Suter, B.A. Hammel, and R.J. Wallace
Lawrence Livermore National Laboratory, Livermore, CA

J. Knauer, F.J. Marshall, D. Bradley, R.S. Craxton, R. Keck, J. Kelly, R. Kremens,
W. Seka, J.M. Soures, and C.P. Verdon
Laboratory for Laser Energetics, University of Rochester, N.Y.

M.D. Cable

Lawrence Livermore National Laboratory, Livermore, CA
Laboratory for Laser Energetics, University of Rochester, N.Y.

Two weeks of experiments are planned on the OMEGA laser facility at the University of Rochester to establish the usefulness of this facility for conducting indirect-drive experiments. The plan is to use up to forty beams of OMEGA to shoot Nova-type hohlraum targets. The goals of this campaign, in order of decreasing priority, are to:

- Verify ability to perform indirect drive (hohlraum) experiments on OMEGA
 - Ability to align hohlraum targets
 - Ability to point beams accurately for hohlraum targets
- “Touch base” with Nova experience
 - Implosion symmetry predictable as in vacuum hohlraums on Nova
 - Radiation temperature scales as expected
- Demonstrate new capabilities
 - Implosions with several rings of illumination
 - $m=5/m=15$ azimuthal symmetry comparison

The beams will be arranged in three beam cones on each side of the hohlraum, consisting of five, five, and ten beams per cone centered on a pentagonal diagnostic port. The half angles of the beam cones, relative to the hohlraum axis, are 21.4°, 42.0°, and 58.8°. (A fourth beam cone, half angle of 81.2°, is not useful for these experiments, since the beams are too steep and cannot make it through the laser entrance hole for cylindrical hohlraums.) To reduce high-Z debris loading on the OMEGA optics, thin-wall hohlraums will be used. These will consist of a 2- μm -thick gold hohlraum supported by a 100- μm -thick epoxy wall. The thin gold wall will allow imaging of the laser spots using x-ray framing cameras and pinhole cameras. Hohlraums will be mounted with the hohlraum axis 63.4° from vertical. Radiation temperature will be measured with the absolutely calibrated and filtered diode array (Dante) routinely used at Nova. Time-integrated hohlraum symmetry will be determined from the shape of imploded-core images recorded with x-ray framing cameras. The effect of increased azimuthal symmetry will be monitored by observing neutron

yield and by x-ray imaging of the imploded core along the hohlraum axis for a set of implosions, and by observing the reemission of x rays from a bismuth-coated capsule placed at the center of a hohlraum, as the beam pointing is changed from an $m=15$ symmetry to an $m=5$ symmetry. The results of these experiments will be presented and their implications for indirect drive experiments on OMEGA will be discussed.

* This work was performed under the auspices of the U. S. Department of Energy by the Los Alamos National Laboratory under contract W-7405-ENG-36, by the Lawrence Livermore National Laboratory under contract W-7405-ENG-48, and by the University of Rochester under Cooperative Agreement No. DE-FC03-92SF19460.

Design and Modeling of Hohlraum Experiments at Omega*

J.M. Wallace

Los Alamos National Laboratory, Los Alamos, New Mexico 87545

We shall discuss the design and modeling of early Hohlraum experiments to be fielded on the Omega-Upgrade laser facility at the University of Rochester. The general features of indirect-drive targets for this driver will be described, considering similarities and differences with respect to current NOVA targets. Included will be results for 1) thin-wall imaging targets to determine beam pointing and spot motion over the laser pulse duration, 2) capsule-implosion simulations with multiring irradiation of the hohlraum; and 3) implosion symmetry dependence on beam pointing.

* Work supported by the U.S. Department of Energy.

Observations of Beam Deflection in Laser Heated Gas-Filled Thin-Wall Hohlräum Experiments at NOVA*

N.D. Delamater*, T.J. Murphy*, A.A. Hauer*, R.L. Kauffman[†], A.L. Richard**, E.L. Lindman*, G.R. Magelssen*, B.A. Failor^Δ, J.M. Wallace*, L.V. Powers[‡], L.J. Suter[‡], G. Glendinning[‡], H.A. Rose*, J.B. Moore*, M.A. Salazar* and K. Gifford*

*Los Alamos National Laboratory, MS E-526, Los Alamos, NM. 87545

[‡]Lawrence Livermore National Laboratory, Livermore, CA 94551

[†]General Atomics, San Diego, CA

**Centre D'Etudes De Limeil-Valenton, France

^ΔPhysics International, San Leandro, CA

Modeling and execution of drive symmetry experiments in gas-filled hohlraums at NOVA are being pursued to verify the accuracy of the design tools which are used to predict target performance for the National Ignition Facility (NIF)^{1,2}. We report on the results of a series of experiments performed at the Nova laser facility at Lawrence Livermore National Laboratory with the goal of understanding radiation drive symmetry in laser-heated gas-filled hohlraums. Results of combined capsule symmetry and laser spot motion measurements using thin wall gas-filled hohlraums are discussed. Our results show that the implosion symmetry in gas differs from vacuum results with similar laser pointing, indicating an axial shift in beam position on the hohlraum wall. This shift causes a hotter drive at the capsule's poles and weaker drive at the equator. The thin wall hohlraum provides a means of observing laser spots in high energy x-rays directly through the gold wall of the hohlraum. Thus, time resolved measurements of laser spot positions in the hohlraum can be obtained. The thin wall measurements of laser spot positions in gas-filled hohlraums show evidence of an axial shift in spot position which is consistent with the shift deduced from the implosion results. These results are consistent with a recently proposed theory³ to explain the observed shift as a plasma physics effect: beam deflection due to filamentation or beam aberrations in the presence of transverse plasma flows.

1. "Symmetry experiments in gas filled hohlraums at Nova", N.D. Delamater, T.J. Murphy, A.A. Hauer, et. al., *Physics of Plasmas*, 3, 2002, May, 1996.
2. "Modeling of drive symmetry experiments in gas-filled hohlraums at Nova", E.L. Lindman, N.D. Delamater, et.al., in *Laser Interaction and Related Plasma Phenomena, Proceedings of the 12th International Conference*, AIP press, 1996.
3. "Laser beam deflection by flow and nonlinear self-focusing", H.A. Rose, *Physics of Plasmas*, 3, 1709, 1996.

* Work performed under auspices of the U.S. D.O.E. under contract no. W-7405-ENG-36.

Early Time Laser Beam Motion Suggested by Time Dependent Symmetry Measurements in Methane-filled Hohiraums

G.R. Magelssen, N.D. Delamater, E.L. Lindman, A.A. Hauer, M.R. Clover,
J.L. Collins, C.W. Cranfill, and W.J. Powers

Los Alamos National Laboratory, Los Alamos, New Mexico 87545

Assuming laser beam motion toward the laser entrance hole is causing the observed early-time symmetry shift in methane-filled hohlraums¹, Reemission Ball² (Reemit) and Symmetry Capsule³ (SymCap) techniques were used to determine the time dependence of the laser beam shift. The imploded core images from SymCap data were used to find the time integrated symmetry over the first nanosecond. These capsules had an initial shell thickness of 20 to 22 microns. The Reemit data was used to determine the time dependence of the symmetry over the same time period. LASNEX calculations have been done that reproduce both the Reemit and SymCap data. These calculations were done by adjusting the motion of the laser beams with time. We will present the Reemit and SymCap data as well as the suggested time dependent beam motion.

1. N. D. Delamater et al., Physics of Plasmas, in press, May 1996.
2. N. D. Delamater et al., Phys. Rev. E 53, 1, 1996.
3. Harris et al., Bull. Am. Phys. Soc. 38, 1885, 1993.

Modeling the Effects of Laser Plasma Interactions on Drive Symmetry in Gas-Filled Hohltraums at Nova

E.L. Lindman, G.R. Magelssen, J.M. Wallace, N.D. Delamater,
B.H. Failor and M.D. Wilke
Los Alamos National Laboratory, Los Alamos, NM 87545, USA

S.M. Pollaine and T.D. Shepard
Lawrence Livermore National Laboratory, Livermore, CA 94551, USA

Drive symmetry experiments in gas filled hohltraums at Nova are currently being pursued to verify the accuracy of the design tools which are used to predict target performance for the National Ignition Facility (NIF). Since the current point design for the NIF uses gas fill to reduce hohlraum wall motion and, hence, spot motion, experiments are being carried out in gas filled hohltraums.

The experiments are being carried out in scale 1 hohltraums (1650 μm in diameter with lengths between 2000 and 2700 μm) filled with 1 atmosphere of methane or propane. The pointing of the laser beams is adjusted so they enter the hohlraum at the center of the laser entrance holes (diameter 0.75 of the hohlraum diameter) located at the ends of the hohlraum. The gas is held in the hohlraum with 0.35 μm thick polyamide windows. The experiments are driven with shaped pulses consisting of a 1 to 2 ns foot followed by a 1 ns main pulse with a contrast ratio between 2 and 3 and a total energy of 25 to 30 kJ.

X-ray images of an imploded standard capsule (220 μm fuel radius with a 55 μm thick plastic wall) are used to examine the time integrated symmetry over the whole laser pulse. In order to monitor the location of the laser spots on the wall of the hohlraum without perturbing the radiation transport or the plasma flow, thin wall hohltraums have been used in recent experiments. In a thin wall hohlraum the 25 μm thick gold cylinder is replaced with a 150 μm thick epoxy cylinder that has a 2 μm thick gold layer deposited on the inside. LASNEX integrated calculations of these experiments include the propagation of the laser through the window and gas and the energy deposition in the hohlraum walls and its reradiation as x rays. Also included are the dynamics of the window, gas, hohlraum walls and capsule. In addition, when SRS and SBS losses are included along with plasma induced beam steering, excellent agreement with experiment is obtained.

* Work performed under the auspices of the U. S. Department of Energy under Contract No. W 7405 ENG 36 at the Los Alamos National Laboratory and under Contract No. W7405 ENG-48 at the Lawrence Livermore National Laboratory.

Effects of Beam Conditioning on Wall Emission from Gas-Filled Hohltraums*

R.L. Kauffman, S.G. Glendinning, L.V. Powers, R.L. Berger, D.E. Hinkel, O.L. Landen,
D. Ress, L.J. Suter, T.D. Shepard, and E.A. Williams

Lawrence Livermore National Laboratory, Livermore, California 94551

A.L. Richard and M.A. Blain

Centre d'Etudes de Limeil-Valenton, Villeneuve-St. Georges FRANCE

P2 radiation symmetry for indirect drive implosions using the Nova laser is controlled by varying the beam pointing on the hohlraum wall. The measured pointing for optimal symmetry in gas-filled hohltraums is shifted by $\sim 150 \mu\text{m}$ from the calculated optimal pointing and from empty hohltraums for implosion experiments using $0.35 \mu\text{m}$ light in a 2.2 ns shaped pulse with a contrast ratio of $\sim 3:1$ (PS22).¹ In experiments reported here, measurements of the wall emission indicate that the beam is deflected from the initial pointing position by $\sim 100 \mu\text{m}$ for CH_4 -filled hohltraums and $\sim 200 \mu\text{m}$ for C_3H_8 -filled hohltraums early in time. After about 1 ns, the shift is reduced and, for CH_4 -filled hohltraums, the shift is comparable to empty hohltraums. At later times enhanced wall emission is observed near the end of the hohlraum toward the LEH. This also can contribute to the observed pointing shift for implosions. Single beam experiments with an RPP beam indicate that the shift is nearly eliminated for CH_4 -filled hohltraums and in agreement with calculations. The shift is also much reduced for C_3H_8 -filled hohltraums. These results can be understood at least qualitatively by filamentation and refraction of the beam due to transverse flow as it traverses the sonic point near the laser entrance hole.^{2,3} A Nova beam without beam conditioning is more likely to filament and refract since a significant higher fraction of the beam is at higher intensity than with an RPP and the spatial scales of the hotspots also differ. In addition, the RPP reduces the scattered light from SBS and SRS consistent with the RPP reducing the fraction of the beam at higher intensity. More recent experiments using KPP confirm that the beam shift and spatial emission profile is closer to calculated than for an unsmoothed beams. KPP's are planned for all 10 of Nova's beams to perform implosion experiments.

1. N. Delameter, et al., Phys. Plasmas 3, 2022 (1996).
2. H. A. Rose, Phys. Plasmas 3, 1709 (1996).
3. D. E. Hinkel, E. A. Williams, and C. H. Still, submitted to Phys. Rev. Lett.

* Work performed under the auspices of the United States Department of Energy by the Lawrence Livermore National Laboratory under contract number W-7405-ENG-48.

Selection of Beam Angles for the National Ignition Facility (NIF)

S.M. Pollaine and S.W. Haan

Lawrence Livermore National Laboratory, Livermore, California

The NIF has 192 beamlets arranged in 48 groups of 4. These 48 beams are arranged in 10 rings at $\theta = \{23.5, 30, 44.5, 50, 77.45, 102.55, 130, 135.5, 150, 156.5\}$. Indirect drive will have $\{4,4,8,8,0,0,8,8,4,4\}$ beams, respectively, in each ring; direct drive will have $\{4,0,8,0,12,12,0,8,0,4\}$ beams, respectively, and tetrahedral hohlraums for indirect drive will have $\{4,4,8,0,8,8,0,8,4,4\}$ in each ring.

The angles 23.5, 30, 44.5 and 50 and their supplementary angles were chosen to maximize flexibility in indirect drive, so that both a 2-ring and a 3-ring hohlraum configuration could be shot. In the two-ring configuration, the 23.5 and 30 degree beams combine to form an inner ring at the hohlraum waist, and the 44.5 degree beams are moved out 190 microns to form one outer ring with the 50 degree beams. In the three-ring configuration, the 44.5 degree rings are moved in 300 microns to form a middle ring, with the 50 degree beams forming an outer ring inside the hohlraum.

The beam angles of 77.45 and 102.55 degrees were chosen to eliminate the Y20 component for directly-driven capsules; the direct-drive beam angles obey the relation $4*P2(23.5) + 8*P2(44.5) + 12*P2(77.45) = 0$. Other moments are small, so that the rms of about 1% is dominated by errors from beam pointing and power balance.

Because both direct-drive and standard indirect drive capsules are insensitive to the azimuthal angles j , the azimuthal angles were chosen to optimize the indirect-drive tetrahedral hohlraums. These hohlraums have potential symmetry advantages over standard indirect-drive hohlraums in that P2 through P5 can be eliminated with suitably placed beams. Although compromises with design requirements for direct and indirect drive hohlraums have reduced some of these advantages, tetrahedral hohlraums remains a third option for NIF.

Tetrahedral Hohltraums—A Way to Achieve time-Independent Uniformity on the NIF?

R.S. Craxton and J.D. Schnittman

*Laboratory for Laser Energetics, University of Rochester, 250 East River Road,
Rochester, NY 14623-1299*

Tetrahedral hohltraums, i.e., spherical hohltraums with four laser entrance holes (LEH's) placed at or near the vertices of a tetrahedron, are advocated as a means of achieving a high degree of uniformity on the NIF in a time-independent way. All but four of the 48 NIF beams can irradiate a tetrahedral hohlraum, given the latest selection of port angles for the NIF.

The key feature of the tetrahedral hohlraum is that the laser-beam spots are spread fairly uniformly over the hohlraum wall. Thus, unlike the case of the cylindrical hohlraum, the nonuniformity pattern on the capsule is to lowest order independent of whether the laser spots dominate (early time) or the case dominates (late time). The rms nonuniformity is close to 2% at all times, and is dominated by the primary (Y_{32}) tetrahedral mode. If the capsule is shimmed with a small (~2%) thickness perturbation in this same mode, it may be possible to accomplish better than 1% nonuniformity at all times. Little if any time-dependent beam "phasing" is needed, and it should be possible to deliver somewhere between 1.37 and 1.65 MJ (out of the nominal 1.8 MJ) into the hohlraum.

Three issues, all relating to clearances, are critical. The incident angles through the LEH's must be big enough so that the capsule plasma is not directly irradiated; they must be small enough that the beams can enter unimpeded by wall plasma; and the beams must not irradiate the hohlraum wall too close to other LEH's. For the most part, these issues appear to be not greatly different from similar issues faced by cylindrical hohltraums.

* This work was supported by the U.S. Department of Energy Office of Inertial Confinement Fusion under Cooperative Agreement No. DE-FC03-92SF19460. the University of Rochester, and the New York State Energy Research and Development Authority. The support of DOE does not constitute an endorsement by DOE of the views expressed in this article.

Compression of a High-Z Foil by Hydrodynamic Pressure of Radiatively Heated Matter*

T.D. Shepard, O.L. Landen, J.D. Lindl, M.D. Rosen, L.J. Suter

Lawrence Livermore National Laboratory, Livermore, CA

The radiation field from a laser-heated hohlraum can drive a supersonic Marshak wave through low-density material such as a foam buffer placed between the radiation source and the foil sample. When the radiation wavefront arrives at the foil/foam interface, pressure is applied to the foil by the radiatively heated and ionized buffer material. Because the opacity of the high-Z foil impedes the flow of radiation, the foil is not volumetrically heated and hence does not develop a back-pressure. The foil is accelerated by the resulting pressure imbalance. A rarefaction wave propagates behind the radiation wavefront, and the material pressure applied to the sample drops when the rarefaction wave reaches it.

Using laser facilities such as the proposed NIF (National Ignition Facility) and HU (Helen Upgrade), and perhaps Nova, pressures of order tens (HU) to hundreds (NIF) of Mbar can be generated and sustained for several nanoseconds. For the same radiation drive, this method generates typically double the pressure that would be generated if the sample were ablatively accelerated, at the expense of requiring additional energy to heat the buffer material.

The design parameters that can be varied to tailor the pressure pulse include the applied radiation field intensity and pulse length, the density and opacity of the buffer material, the thickness of the buffer material, and the density and opacity of the foil. We will present Lasnex simulations of experimental designs that could be fielded on HU, NIF, and maybe Nova.

* This technique was first described to us by researchers from AWE, Aldermaston, UK.

Scaling Laws for Rayleigh-Taylor and Richtmyer-Meshkov Instability Based on Bubble and Vortex Competition Models

Uri Alon, Dror Ofer, Dan Oron, Avi Rekanati, Yanai Yedov, Dov Shvarts
Physics Department, N.R.C.N, Israel

Theoretical models for the Rayleigh Taylor and Richtmyer-Meshkov instabilities single mode and multi mode mixing fronts are presented. The late time mixing zone penetration is modeled by a statistical bubble merger model. The bubble merger rates for the $A=1$ case are derived from a potential Layzer-type flow model. The RM instability in the limit of two fluids of similar densities ($A \rightarrow 0$) is treated by the motion of point potential vortices. Two bubble merger is demonstrated and bubble competition rates are calculated. Similar scaling law for the RM case, predicting that the bubble front evolves as $t^{0.4}$, are obtained for both the high and the low Atwood number limits, in good agreement with simulations and experiments. The construction of an effective mixing model based on these scaling laws will be presented.

Scaling of the Rayleigh-Taylor Nonlinear Evolution in Ablatively Driven ICF

Dov Shvarts, Dan Oron, Uri Alon, Dror Ofer, Yanai Yedov

Physics Department, N.R.C.N, Israel

A theoretical model for the ablatively driven Rayleigh-Taylor instability single mode and multi-mode mixing fronts are presented. The effects of ablation are approximately included in a Layzer-type potential flow model, yielding the description of both the single mode evolution and the two bubble nonlinear competition. The ablation stabilization of the linear growth rate obtained in the model is similar to the Takabe formula. The single bubble terminal velocity is found to be reduced by ablation, in good agreement with numerical simulations. Two bubble competition is than calculated, and a statistical model for multi-bubble fronts is presented. The asymptotic ablation correction to the classical $RT\alpha \times gt^2$ law is derived. The effect of this correction to the ablation front mixing zone evolution in an ICF target and its effect on the allowed in-flight aspect ratio is presented. Possible effects of the non-planar geometry on the nonlinear evolution stage are discussed.

Hybrid Guiding Center/Paraxial Model for Laser Propagation in Prescribed Density Profiles

H.X. Vu, R.A. Kopp, and B. Bezzerides

Los Alamos National Laboratory, Los Alamos, New Mexico 87545

In radiation-hydrodynamics simulations of Inertial Confinement Fusion (ICF) targets, the laser is universally modeled by ray-tracing. For most ICF applications, the ray-trace model is adequate for describing the laser's propagation through, and interaction with, plasmas. However, for ICF applications in which a small perturbation in the laser deposition (due to statistical noise inherent to ray-tracing) can affect the outcome of the simulation significantly, it is desirable to have an alternative model that permits smoother laser deposition. In this paper, a preliminary investigation of such an alternative model is reported. Our approach here to construct a hybrid model that combines features of both the ray-trace and the paraxial models. The details of this model, and test simulations of a gaussian beam propagating through: (a) a uniform background density, (b) a cylindrically symmetric hollow density profile, and (c) a hollow density profile with an axial dependence such that the laser beam is deflected, will be presented. The goal of this paper is to assess the feasibility of implementing this hybrid guiding center/paraxial model into a radiation-hydrodynamics simulation code.

ICF Ignition Criteria and Critical Profiles Using Self-Similar Solutions to the Burn Wave Propagation Problem

Roy Kishony, Dov Shvarts and Eli Waxman*

Physics Department, N.R.C.N, Israel

The ignition conditions, under which a thermonuclear burn wave propagates from an initial hot spot, and the features of the propagating burn wave are investigated using a new family of self similar solutions. The self similar solutions will be shown to provide a natural ignition criterion and critical profiles of the hot spot at ignition. The trajectories of the propagating hot spot in the ρ R-T plane are shown to be closely related to the self similar Ignition Line. The distance of these trajectories from the Ignition Line in the ρ R-T plane is derived. Very good agreement between the new self similar solutions with full numerical simulations will be shown.

* Presently at the Institute for Advance Studies, Princeton.

Computational Design of the Radiatively Driven Cylindrical Implosion Experiments

J. Bradley Beck*, Warren W. Hsing*, Cris W. Barnes*,
Nelson M. Hoffman*, and Chan K. Choi†

**Los Alamos National Laboratory, Los Alamos, NM 87545*

†School of Nuclear Engineering, Purdue University, West Lafayette, Indiana 47907

The implosion of an inertial-confinement-fusion (ICF) capsule is most efficient if the imploding flow is exactly spherically symmetric. It is well known, however, that real ICF flows are subject to a variety of fluid instabilities that destroy spherical symmetry. Of specific concern is the ablation-surface instability, where the ablation of the outer shell of the capsule creates a situation analogous to the classical Rayleigh-Taylor instability. The study of perturbation growth at this surface is experimentally difficult in spherical geometry, while planar geometry experiments neglect the effects of convergence. For these reasons, this study examined the growth of unstable perturbations at the ablation front of an imploding cylinder. This enabled the effects of convergence to be seen while still maintaining a direct diagnostic line-of-sight access.

Due to the convergent nature that exists in cylindrical geometry, a theoretical growth rate for the Rayleigh-Taylor instability was first derived. This growth rate showed two effects due to convergent geometry. First, the growth rate was enhanced over the classical growth rate in planar geometry due to the fact that the wavelength decreases as the cylinder implodes. Second, the derivation predicted that perturbations can grow in convergent geometry in the absence of acceleration. With the use of this theory and results from a one-dimensional computational code, the amount of perturbation growth could be predicted for specific cylindrical designs.

Two separate cylindrical designs were experimentally used to test our theories. The first design was a low-perturbation growth design, while the second design utilized high-Z doped materials to increase the amount of perturbation growth. In both designs, a central, highly opaque marker layer is placed upon the inner surface of the cylinder. The perturbations placed upon the outer surface of the ablator will grow due to the ablation-surface instability and then “feed-in” to this marker layer. A gated x-ray camera was used to obtain time-dependent analysis of the growth upon the marker layer. The results from these experiments will be compared to the theoretically predicted results, with the theoretical results showing the reasons why the amount of perturbation growth is different for the separate designs.

Thursday

INVITED TALK
7:30 – 8:30 PM

Mike Sulzer
Al Wong, Session Chair

Experiments on EM Wave Interactions with the Ionosphere

Michael P. Sulzer

Arecibo Observatory

The combination of an HF modification facility, an incoherent scatter radar, and various other optical and radio diagnostics is a very powerful tool for studying plasma physics and for studying the ionosphere itself. An upcoming experiment for studying the thermal balance in the ionosphere is described, with the motivation of showing how an incoherent scatter radar is used. It is pointed out that getting useful results from this experiment requires a good understanding of the physics which describes the interaction of a powerful HF wave with the ionospheric plasma. The rest of this paper describes some of this physics and how experiments involving powerful HF waves and various diagnostics can be useful.

The basic physics related to ionospheric modification is introduced by beginning with a description of some of the early experiments. The interpretation of results in terms of theories then current is discussed, and it is shown how a few simple ideas could explain many of the complex observational results. The parametric instabilities that result from analytic solutions to the relatively simple equations encountered with the weak turbulence approximation are attractive for observational study because they have a number of characteristics that can be verified. They are relatively easily observable with a sensitive incoherent scatter radar when excited with a moderately powered ionospheric modification facility. However, almost from the earliest observations there were some unexplained characteristics.

Most observers at the time would have likened these to a few missing bricks in an almost completed building, but now many would say that the foundation was resting on soft ground, and that a considerable amount of digging was necessary to get to the rock beneath. The Zacharov equations which predict the effects of strong Langmuir turbulence are not easy to solve, but they produce a powerful and coherent explanation for the observed results, and they have had the satisfying effect of pointing the way towards more detailed observations and additional verification between simulations and observations. The observations often require the use of new techniques. Observations during the earliest time after turning on the heater are described in detail because the agreement with the theory is very good on this time scale.

Thursday

POSTER SESSIONS
8:30 – 10:30 PM

Chirped Pulse Reflectometry for High-Precision Measurements of Shock Velocity

D.M. Gold, A. Sullivan, R. Shepherd, J. Dunn, and R. Stewart
Lawrence Livermore National Laboratory, Livermore, CA

We present results of a high-precision, optical technique for measurement of megabar shock velocities in laser-driven materials. Chirped Pulse Reflectometry (CPR) uses a chirped laser probe pulse to detect the time at which a strong (ionizing) shock wave breaks out of a target. The chirp encodes the pulse spectrum with a proportional time history. A reflectivity change from ionization during shock breakout gates and modulates the spectrum, producing interference fringes which act as sub-100 fs time fiducials for the shock breakout time. Measuring breakout times in a stepped target with different thicknesses gives the velocity of the shock in that material. Accurate equation-of-state (EOS) data for many materials can be obtained by impedance-matching experiments¹ relative to a standard material, e.g. Al, with a known EOS.

CPR was tested by using an aluminum target ionized by a 100 fs, 10^{15} - 10^{16} W/cm² pulse to simulate the reflectivity change (~50% at $T_e = 1$ -10 eV) produced by a ionizing shock breakout. A 100 fs, 800 nm probe pulse chirped in a grating pair stretcher to ~20 ps and reflected from the plasma was imaged onto a spectrometer slit. Spectral interference fringes produced by the reflective gating provided timing fiducials accurate to <100 fs. Breakout times are spatially resolved along one dimension of the plasma by imaging onto the spectrometer entrance slit. The measured >3000:1 signal-to-noise ratio allows Fourier inversion of spectral results for a complete shock breakout time history. Application of CPR measurements to megabar shocks produced by the 1 ns Janus laser facility will also be discussed.

The current capability of shock velocity measurements relies on direct viewing or interferometric techniques² with fast optical or x-ray streak cameras. Streak cameras have practical time resolutions of a few picoseconds, are typically noisy, of limited sensitivity and dynamic range, and have nonlinear distortions in sweep speed which must be characterized on a shot-by-shot basis. CPR would avoid these problems, while increasing the precision of shock velocity measurements by more than one order of magnitude. This would allow sensitive discrimination between EOS models³ used in hydrodynamic and thermodynamic codes.

1. M. Koenig, et al., Phys. Rev. Lett. 74, 2260 (1995).
2. M. Koenig, et al., Phys. Rev. Lett. 74, 2260 (1995); A. Ng, D. Parfeniuk, P. Celliers, and L. DaSilva, Phys. Rev. Lett. 57, 1595 (1986); J.R. Asay and L.M. Barker, J. App. Phys. 45, 2540 (1974).
3. B.I. Bennett et al., LANL Report No. LA-7130, 1978 (unpublished); T-4 Handbook of Material Properties Data Bases: Vol. Ic, Equations of State, edited by K.S. Holian LANL Report No. LA-10160-MS, UC-34, 1984 (unpublished); R.M. More, K.H. Warren, D.A. Young, and G.B. Zimmerman, Phys. Fluids 31, 3059 (1988).

An Improved Pinhole Spatial Filter

Kent Estabrook, Peter Celliers, Jim Murray, Russel Wallace, Gary Stone,
Bruno Van Wouterghem, Brian MacGowan, John Hunt and Ken Manes

Lawrence Livermore National Laboratory, University of California, Livermore, CA 94551

Lasers generate phase aberrated light that can damage laser glass, frequency conversion crystals, lenses and mirror coatings and can also reduce extractable energy and power. Spatial pinhole filters^{1,2} can partly eliminate such "hot spots." Problems are that the pinhole closes during the laser pulse and has to be made too large initially to avoid being too small at the end of the pulse. Debris from the pinhole can damage spatial filter lenses. This paper presents a novel design for a more robust pinhole filter. Phase distorted (hot spot) light is refracted at grazing incidence by plasma on the wall of a funnel shaped filter resulting in less absorption and debris.

Refracted light is dumped at low intensities on the vacuum wall. We present two dimensional hydrodynamic computer simulations comparing the two types of filters with experimental results. We present simulations of NIF spatial filters.

We are happy to acknowledge valuable conversations with Fred Mayer, Mike Campbell, Roger Haas, E.S. Bliss and Harry Kornblum. This work was performed under the auspices of the U.S. Department of Energy under Contract No. W-7405-ENG-448.

1. W. W. Simons, S. Guch, Jr., F. Rainer, and J. E. Murray, "A High Energy Spatial Filter for Removal of Small Scale Beam Instabilities in High Power Solid State Lasers," Lawrence Livermore Laboratory Report UCRL-76873 (May 1975). IEEE J. Quant. Elect. QE-11, 30D (1975).
2. J. S. Pearlman and J. P. Anthes, Applied Optics 16, 2328 (1977).

On the Effects of Fine-Scale Structure in Foam-Buffering Calculations

R.A. Kopp, S.R. Goldman, J.L. Collins, and R.J. Mason
Los Alamos National Laboratory, Los Alamos, NM 87545

We examine the microdynamics of a low-density (although slightly overdense) acrylate foam medium, such as is currently being used in various ICF experiments to study foam-buffering as a possible candidate for smoothing laser nonuniformities. The foam is assumed to consist of an assemblage of solid-density fibers, illuminated by a 2ω laser with an intensity of $\sim 2 \times 10^{14} \text{W/cm}^2$. Initially the laser light can penetrate and deposit energy deep within the foam, by propagating and scattering amongst the fibers. However, preferential heating and ablation of the laserward "tips" of the fibers very quickly (within a few ps) fills the voids between the fibers near the foam "surface", and this ablated fiber plasma subsequently stops the laser beam as it first enters the foam.

Once the interfiber voids have been thus filled at shallow depths, the laser absorption region rapidly evolves to become a nearly planar surface. Thermal transport of the absorbed laser energy inward from this surface then becomes the primary agent by which deeper segments of the fibers are heated and vaporized. This occurs at a rate sufficient to maintain an overdense absorption region. As the conductive flux reaches these greater depths, it gets channeled by the most recently ablated (but still nonuniform) plasma into the still-cool remnants of the original fibril structures. This gives rise to a geometrical restriction of the heat flux caused by the inhomogeneous fibril structure of the foam. The magnitude of the reduction factor is evaluated for a few cases as a function of the areal "filling factor" of the foam. We argue that such a reduction factor should be routinely used in fluid simulations of foam-target scenarios, in order to describe correctly the heating and dynamics of low-density foam plasmas.

* Work supported by the US DOE under Contract No. W-7405-Eng-36.

Ablative Rayleigh-Taylor Instability: Applications of the Linear Theory to Target Designs Relevant to Inertial Confinement Fusion

V.N. Goncharov, R. Betti, R.L. McCrory, and C.P. Verdon

*Laboratory for Laser Energetics, University of Rochester, 250 East River Road,
Rochester, NY 14623-1299*

The linear theory of the ablative Rayleigh-Taylor instability (based on the isobaric model) is used to determine the growth rate of unstable modes in targets relevant to inertial confinement fusion (ICF). The analytic growth rate depends on the Froude number ($Fr = V_a^2/gL_0$), where g is the acceleration, V_a is the ablation velocity, and L_0 is the characteristic width of ablation front] and the power index for thermal conduction, ν ($\kappa \sim T^\nu$). The parameters Fr and ν are determined by fitting the hydrodynamic profiles (density, pressure) obtained in one-dimensional numerical simulations (including multigroup radiation transport models) with the theoretical profiles. A simple formula for the growth rate, $\gamma^{fit} = \alpha \sqrt{k g} - \beta k V_a$, is proposed to describe the evolution of the perturbations. The coefficients α and β are functions of Fr and ν . It is found that α is approximately a constant over a wide range of Fr and ν ; and β can be approximated by power law, $\beta = Fr^\mu$, with negative values of μ for $Fr < 1$ and positive values of μ for $Fr > 1$.

* This work was supported by the U.S. Department of Energy Office of Inertial Confinement Fusion under Cooperative Agreement No. DE-FC03-92SF19460, the University of Rochester, and the New York State Energy Research and Development Authority. The support of DOE does not constitute an endorsement by DOE of the views expressed in this article.

160

Simulation of Indirectly Driven Implosions Using a Gas-Filled Hohlraum Heated by KPP-Smoothed Laser Beams

T.D. Shepard, L.V. Powers

Lawrence Livermore National Laboratory, Livermore, CA

Smoothing of all 10 Nova beams using kinoform phase plates (KPP) is planned as a method for reducing the effects of laser-plasma instabilities in indirectly-driven gas-hohlraum implosion experiments. We have developed a method to mock up the behavior of KPP beams using the Lasnex ray-tracing package. This model includes realistic beam profiles both along and perpendicular to the beam axis. Smoothing by spectral dispersion (SSD) will also be implemented on Nova and is treated in our model by dynamically re-pointing each ray during the course of the calculation. SSD can produce an oscillation in the pointing of the beam-spot centroid at the modulation frequency. The oscillation can be eliminated if the SSD is critically dispersed and if the laser power is constant, but transient motion still occurs during the turn-on of the foot and peak of the shaped laser pulse typically used for indirect-drive implosions. The period of this oscillation is of order 400 ps and the largest amplitude of the motion of the spot on the hohlraum wall is of order ± 50 microns at turn-on of the foot for standard Nova implosion experiments. The SSD also modifies the shape of the beam spot even when critically dispersed. We will present results from Lasnex simulations to quantify the sensitivity of implosion symmetry to these effects.

A Non-Cryogenic Double-Shell Ignition Target

W.S. Varnum and D.B. Harris

Los Alamos National Laboratory, Los Alamos, NM 87545

Until recently it was assumed that the collision in a double-shell target would be too hydrodynamically unstable for an efficient National Ignition Facility (NIF) target. The reasoning was that the collision would not have the stabilizing density gradient and ablative smoothing mechanisms, and hence would be too unstable. However, we have not been able to calculate growth of multi-mode surface perturbations until the last few years.¹

We have designed a double-shell target for the NIF, which contains gaseous DT at high pressure instead of cryogenic DT, that is, in several ways, analogous to the NIF single-shell PT target design. We have performed both 2-D integrated (hohlraum plus capsule) and stand-alone 2-D capsule calculations with multi-mode surface perturbations. Results will be reported.

This is not presently an optimized target and is not intended to be a replacement for the PT target, but, rather, is complementary. The clean 1-D calculated yield is 2.6 MJ, which is considered an upper limit. Calculated yield with surface perturbations is about 1.6 MJ. Hence the target could produce an interesting fusion burn without the complicating issues of cryogenics and sophisticated pulse shaping.

1. N.M. Hoffman, D.C. Wilson, R.E. Chrien, and J.D. Colvin, presented at the 25th Anomalous Absorption Conference, The Aspen Institute, Aspen, Colorado, 27 May-1 June, 1995.

* Work supported by USDOE contract W-7405-ENG-36.

A Distributed Radiator Heavy Ion Target Design

Max Tabak and Darwin Ho

Lawrence Livermore National Laboratory

We describe the status of a novel distributed radiator heavy ion target design. In preliminary integrated calculation this target ignited and produced 335 MJ of yield when driven with about 7.5 MJ of 3-3.5 GeV Pb ions. The target has cylindrical symmetry in a 6 mm radius spot. We discuss the considerations which led to this design together with some previously unused design features: low density hohlraum walls in approximate pressure balance with internal low-Z fill materials, radiation symmetry determined by position of radiator materials and particle ranges, and early time pressure symmetry influenced by radiation shims.

Studies of Pulse Compression and Beat Wave Excitation in Ionospheric Heating

Steve Cowley and E. Valeo†

UCLA Physics Department, 405 Hilgard Avenue, Los Angeles, CA 90024

This paper will address the use of pulse compression and multiple frequencies in Ionospheric heating. In a recent publication (Geophysical Res. Lett. 20, 24319 (1993)) we showed how large intensities can be obtained by using the dielectric properties of the Ionosphere to compress pulses of radiation. Simulation of the nonlinear interaction of the compressed pulse with the plasma will be presented. The generation of high energy electrons will be discussed. The nonlinear degradation of the pulse compression is calculated. Factors that hinder the practical development of the pulse compression scheme will be addressed. Various plasma waves can be excited by beating two transparent waves together near the density maximum of the Ionosphere. The efficiency of the process is helped by the long scale length of the density in this region which allows the three wave conditions to be satisfied over a large region. We shall discuss the excitation of magnetized waves such as ion cyclotron and whistler waves.

† Permanent address, PPPL, PO Box 451, Princeton, NJ 08543.

* Work supported by ONR Grant N00014-92-J-1382.

Generation of Large Density Perturbations by Frequency Matching at the Peak of the Ionospheric Density Profile

A.Y. Wong, J. Pau, J. Villasenor

Department of Physics and HIPAS Observatory, University of California at Los Angeles

L.C. Tsai, T. Berkey

Utah State University

Using the HIPAS heating facility, we present the density perturbation generated by heating the region where the ionospheric density scale length was maximum (>80 km), the critical plasma frequency region. When the heater frequency approached the vicinity of this critical plasma frequency, we observed symmetric and asymmetric broadening in the frequency spectra and reduction of the reflected wave amplitude during o-mode heating. Furthermore, the frequency spectra show positive shifting during o-mode heating and negative during x-mode heating. We also observed a spreading of the echo returns in the ionograms during the matching period. The spreading extends to a vertical distance of 300 km.

The large reduction in the reflected wave amplitude suggests the possibility of the anomalous absorption. The frequency broadening of the order of electrostatic ion cyclotron frequencies indicates the modulation of electrostatic ion cyclotron waves. The broadening took approximately ten minutes to recover and has the scale size of the order of 10^3 m, which suggest the formation of thermal caviton.

2D/3D Simulations of Filamentation With Space/Time Beam Smoothing in ICF Context

Gilles Riazuelo, Pierre Zerlauth, Guy Bonnaud

*CEA, Centre d'Etudes de Limeil-Valenton, DPTA, 94195 Villeneuve-Saint-Georges,
France*

Results of simulations of the paraxial propagation of a laser beam inside an underdense plasma with ponderomotive non-linearity are presented. We first address the qualitative and quantitative differences between the results obtained in both 2D (slab and cylinder) and 3D geometries for the steady-state behavior of the laser beam. We compare the scenarios (self-focusing, filamentation), the peak intensities, the density depletions, the beam widths and the focal distances, for an initially gaussian-shaped laser beam.

Second, we analyze the unstationary situation of the coupling of the beam propagation equation to the ion-acoustic wave equation, within the context of a 2D slab geometry (less time-consuming). The time for steady state access is analyzed in terms of the observed scenario and the ion-acoustic damping. The reduction of beam filamentation by adding both space and time random irregularities in the initial beam is then analyzed. The results provide physical insight of the processes and preliminary scaling laws for beam smoothing.

Laser Filamentation Simulations With Nonlinear Hydrodynamics

C.H. Still, R.L. Berger, A.B. Langdon, L.V. Powers, E.A. Williams, P.E. Young
Lawrence Livermore National Laboratory, Livermore, California 94550.

Recent application of our laser filamentation code to high temperature hohlraums (e.g., $I = 10^{16} \text{W/cm}^2$, $T_e = 10 \text{ keV}$), or channeling experiments where nearly all of the mass is evacuated from a cavity, have motivated the development, and integration into F3d, of a 3D nonlinear eulerian hydrodynamics (Nh3).

The specifics of Nh3 and some applications to beam deflection were reported last year^(1,2). Since then, a linearized model for nonlocal thermal conduction has been added to Nh3, and the whole package integrated into the F3d code. Laser propagation is carried out by solving the paraxial wave equation. The hydrodynamics equations are solved using a split step method with 2nd order upwinding van Leer approximations. Nonlocal heat transport includes electron heating by inverse brehmsstrahlung, and allows simulating thermally driven, as well as ponderomotively driven, filamentation.

In this presentation, we will show F3d simulations for high temperature hohlraums where the filamentation gain per speckle is large, when an extremely tight focus in a plasma is achieved (similar to Peter Young's experiments on Janus⁽³⁾), and in channeling experiments where near vacuum is achieved.

1. C. H. Still, R. L. Berger, A. B. Langdon, E. A. Williams and D. S. Miller, "Nonlinear Eulerian Hydrodynamics in Three Dimensions and Applications to Beam Deflection," 25th Anomalous Absorption Conference, Aspen CO, 27 May - 1 June, 1995.
2. C. H. Still, R. L. Berger, A. B. Langdon, E. A. Williams and D. S. Miller, "3D Nonlinear Hydrodynamics with Beam Deflection Applications", APS Division of Plasma Physics Meeting, Louisville KY, 6-11 November, 1995.
3. P. E. Young, J. H. Hammer, S. C. Wilks and W. L. Kruer, "Laser beam propagation and channel formation in underdense plasmas", Phys. of Plasmas, 2 7 (1995).

* Work performed under the auspices of the United States Department of Energy by the Lawrence Livermore National Laboratory under contract number W-7405-ENG-48.

Changes in Filamentation Behavior Due to the Presence of Hydrodynamic Axial Coupling and Flow

Andrew J. Schmitt

Plasma Physics Division, Naval Research Laboratory, Washington, DC 20375

Bedros Afeyan†

Lawrence Livermore National Laboratory, Livermore CA 94551

The presence of axial (i.e., in the direction of laser propagation) flow and coupling is an important feature in ICF plasmas. However, because of computational constraints many earlier studies of filamentation in plasmas ignored this phenomena and assumed its effect was small^[1]. We find here that inclusion of axial hydrodynamic flow and coupling profoundly changes the nature and behavior of filamentation in plasmas.

A 2d Cartesian plasma hydrocode^[2] based on the flux-corrected-transport (FCT) algorithm and the parabolic wave laser propagation description¹ are used to model the relevant physics. We have used this code to study the filamentation behavior in both quasi-realistic and idealized plasma scenarios. Flow velocity, laser intensity, and hydrodynamic wave damping were varied to test their effects on filamentation.

The simulations show a fundamental change in the dynamics of filamentation: the presence of flow can delay or prevent the formation of steady-state filamentation behavior even in idealized homogeneous plasmas. More significantly, we have found substantial levels of spatial and temporal incoherence induced on the laser due to the axial flow and coupling. Applications of these results to the reduction of laser imprinting in direct drive targets and to the control of beam spreading and breakup in hohlraums will be discussed.

1. A.J. Schmitt, Phys. Fluids B3, 186 (1991); R. L. Berger, B. F. Lasinski, T. B. Kaiser, E. A. Williams, A. B. Langdon and B. I. Cohen, Phys. Fluids B5, 2243 (1993).
2. C. R. DeVore, Journal of Computational Physics 92, 142-160 (1991).

* Supported by U.S. Department of Energy.

† B.B.A.'s work at Livermore is performed under the auspices of the U.S. DoE by LLNL under contract No. W-7405-ENG-48.

Enhanced Scattering in Magnetized Laser-Produced Plasma

D. Mourenas

CEL-VCEA, 94195 Villeneuve St. Georges Cedex, France

A model of Bernstein modes parametric excitation near the electron plasma frequency in a magnetized (B in the megagauss range) subcritical laser-produced plasma is presented. It is shown that, when their group velocity vanishes, the threshold of such modes may become much smaller than the usually invoked convective Raman backscattering threshold. Special emphasis is placed on a simplified formulation of the growth rate and threshold intensity for parameters ranges of interest in laser fusion experiments. Predictions (such as lower threshold, higher reflectivity, spectral gap, scintillation in time) compare favorably with experimental observations.

Multi-Dimensional Evolution of Stimulated Scattering and Filamentation

R.L. Berger, C.H. Still, D.E. Hinkel, A.B. Langdon, E.A. Williams, R.K. Kirkwood,
B.J. MacGowan, and J.D. Moody

Lawrence Livermore National Laboratory, University of California, Livermore, CA 94550

D.S. Montgomery

Los Alamos National Laboratory

We have constructed a three-dimensional code (F3D) to study the interaction of stimulated back scattering and filamentation instabilities driven by laser beams that have large but statistically well-understood nonuniformity, e.g. at the focal plane of a laser with random phase plates (RPP). In support of gasbag experiments at LLNL with the Nova laser (and reported at this conference) in which the electron density is nearly 1/10 critical ($\sim 10^{21}$ cm⁻³), the electron temperature is $T_e \sim 3$ keV, and nearly constant over 1-2mm, we have studied the behavior of this competition and collaboration between instabilities as a function of laser intensity, laser f-number, ion acoustic damping rate, and electron density. The effects of laser beam smoothing produced with SSD are also examined. Simulations in plasmas with strong flow gradients that limit SBS growth but not filamentation will be compared to the uniform plasma simulations.

* This work was performed under the auspices of the United States Department of Energy by the Lawrence Livermore National Laboratory under Contract No. W-7405-ENG-48.

SOFTSTEP Simulations of Stimulated Raman Scattering in Inhomogeneous Plasmas Driven by Structured Laser Beams

Bedros B. Afeyan

Lawrence Livermore National Laboratory

Albert E. Chou

University of California, Los Angeles

The theory of stimulated Raman scattering in inhomogeneous and turbulent plasmas is investigated in the presence of laser beams with random phase plates. The growth rates and reflectivities of SRS at different densities and illumination conditions are calculated using a spectral technique to solve parabolic PDEs. The high frequency wave equations are not paraxialized but merely enveloped in time. SRS SOFTSTEP can examine multiple crossing laser beams, waves that reach their turning points, and filamenting pump waves. This work at low densities sheds light on SRS issues concerning the NIF and at higher densities addresses high temperature hohlraums.

* Work performed under the auspices of the U.S. DoE by LLNL under contract No. W-7405-ENG-48.

Heat Flux Inhibition by Electron Nonlocality and Ion Acoustic Turbulence in Laser-Produced Plasmas

J.P. Matte,¹ V. Yu. Bychenkov,¹ K. Estabrook,³ T.W. Johnston,¹
W. Rozmus,⁴ and V.T. Tikhonchuk²

¹*Institut National de la Recherche Scientifique Énergie, CP 1020, Varennes, Québec, Canada*

²*P.N. Lebedev Physics Institute, Russian Academy of Science, Moscow 117924, Russia*

³*Lawrence Livermore National Laboratory, University of California, Livermore, California 94551, USA*

⁴*Theoretical Physics Institute, Department of Physics, University of Alberta, Edmonton T6G 2J1, Alberta, Canada*

Fokker-Planck simulations of laser-produced plasmas which include the turbulence due to the return current-induced ion acoustic instability demonstrate significant modification of the transport phenomena as compared to the determined by Coulomb collisions alone. An inhomogeneous plasma was heated by the inverse bremsstrahlung absorption of the laser energy and for the first time the combined effect of two phenomena—the electron nonlocality and ion acoustic wave turbulence—on the electron energy transport has been studied self-consistently. Electrons have been treated kinetically and coupled to hydrodynamic ions and to the ion acoustic wave turbulence in a quasilinear approximation.

We found that the electron nonlocality and ion acoustic instability act constructively to enhance the electron flux inhibition. For a 1 μm laser beam of intensity 10^{14} - 10^{15} W/cm² the development of ion acoustic instability occurs in a 100 ps time scale and results in excitation of a broad spectrum of high level turbulence, with considerable energy density, $W/n_e T_e \sim 0.1$ very near the critical surface. It results in ion overheating and steepening of the electron temperature and density profiles in the vicinity of the critical density. A density plateau is also formed in the underdense region and propagates with a super-sonic velocity downstream. The implications of these effects for inertial confinement fusion and x-ray lasers will be discussed.

Stimulated Brillouin Scattering From a Smoothed Laser Beam in an Inhomogeneous Plasma

V.T. Tikhonchuk

P.N. Lebedev Physics Institute, Moscow, Russia

D. Pesme, Ph. Mounaix

LULI and CPHT, Ecole Polytechnique, Palaiseau, France

The theory of stimulated Brillouin (SBS) from a randomized laser beam propagating through an inhomogeneous plasma is developed. We consider the stationary SBS in the regime where the characteristic length of convective amplification is much less than the speckle. The “microscopic” SBS reflectivity from an individual speckle is calculated with the pump wave depletion taken into account. Then the statistical theory of distribution of hot spots in a focused laser beam applied for the calculation of the averaged, “macroscopic” SBS reflectivity from an inhomogeneous plasmas. This averaged SBS reflectivity is analyzed as a function of laser and plasma parameters and a simple analytical approximation for it is proposed.

We demonstrate that the domain of parameter of this theory corresponds well to many current interaction experiments with nanosecond laser pulses and it predicts a reasonable magnitude of SBS reflectivity without any additional assumptions.

Petawatt Laser System

D.M. Pennington, M.D. Perry, B.C. Stuart, R. Boyd, J.A. Britten, C.G. Brown,
S. Herman, J.L. Miller, H. Nguyen, W. Olsen, B. Shore, G. Tietbohl, V. Yanovsky

*Laser Program, Lawrence Livermore National Laboratory,
PO Box 808, L-439, Livermore, CA 94550*

We recently demonstrated the production of over a petawatt of peak power in the Nova/Petawatt Laser Facility, generating > 500 J in < 500 fs. The Petawatt Laser Project was initiated to develop the capability to test the fast ignitor concept for inertial confinement fusion (ICF), and to provide a unique capability in high energy density physics. The laser was designed to produce near kJ pulses with a pulse duration adjustable between 0.5 and 20 ps. At the shortest pulse lengths, this laser will surpass 10^{21} W/cm² when focused later this year.

The laser system begins with a Ti:sapphire chirped pulse amplification system operating at 1054 nm. The pulse is stretched to ~ 2 ns and is amplified up to 50 mJ in the titanium-sapphire section with minimal bandwidth narrowing. Further amplification in mixed phosphate glass rod amplifiers produces a spectrally-shaped 10 J pulse. This pulse is further amplified up to the kilojoule level by a series of disk amplifiers. Near diffraction-limited beam quality is achieved by utilizing only the central 80% of the disk amplifiers and the use of adaptive optics to correct any residual thermal or pump induced aberrations. Following amplification, the chirped nanosecond pulse is compressed to 480 fsec by a pair of large aperture (80 cm) diffraction gratings arranged in a single pass geometry. Pulse compression occurs in vacuum with a compressor throughput of 84%. Currently, this system is limited to 600 J pulses in a 46 cm beam. Expansion of the beam to 58 cm will enable 1 kJ operation.

Target experiments with petawatt pulses will be possible either integrated with Nova in the 10 beam target chamber or as a stand alone system in an independent, dedicated chamber. Focusing the beam onto a target will be accomplished using an on axis parabolic mirror. The focal spot will be diagnosed with an axial x-ray imaging camera. The design of a novel targeting system enabling the production of ultrahigh contrast pulses and an easily variable effective focal length will also be described.

* This work was performed under the auspices of the U.S. Department of Energy by the Lawrence Livermore National Laboratory under Contract No. W-7405-ENG-48.

Numerical Simulations Of Stimulated Brillouin Scattering In Two And Three Spatial Dimensions

R.E. Giacone, H.X. Vu

Los Alamos National Laboratory, Los Alamos, New Mexico 87545

The results arising from numerical simulations of stimulated Brillouin scattering (SBS) in two and three spatial dimensions using HERCULES, an adiabatic fluid-electron particle in cell code^[1], are presented. We compare the results of these simulations against the solutions of a linearized fluid model of SBS in homogeneous plasmas^[2]. Multidimensional effects on the angular dependence of SBS are studied. The results obtained from numerical simulations are in good agreement with the linear model comparisons of beam bending effects^[3] in two and three dimensions will be also presented.

1. H. X. Vu, J. Comput. Phys. 124, 417 (1996).
2. C. J. McKinstrie, R. Betti, R. E. Giacone, T. Kolber and J. S. Li, Phys. Rev. E 50, 2182 (1994).
3. H. A. Rose, Phys. Plasmas 3, 1709 (1996).

* Work performed under the auspices of the US Department of Energy.

Stimulated Brillouin Scatter In Pic-Fluid Simulations

B.F. Lasinski, B.I. Cohen, A.B. Langdon, and E.A. Williams

Lawrence Livermore National Laboratory Livermore, California 94550

BZOHAR studies of Stimulated Brillouin Scatter (SBS) in plasma parameter regimes appropriate to NOVA and planned NIF experiments are reported. We compare results from electromagnetic simulations to those with an imposed ponderomotive driver. In the latter simulations we more readily isolate and diagnose those effects associated with nonlinearities in the ion waves which contribute to the saturation of SBS and the resulting SBS reflectivity in the electromagnetic cases.

* Work performed under the auspices of the United States Department of Energy by the Lawrence Livermore National Laboratory under contract number W-7405-ENG-48.

Laser Interaction With Helium Gas Jet in the Nanosecond Pulse Regime

V. Malka, E. DeWispelaere, F. Amiranoff, R. Bonadio, C. Coulaud

**Laboratoire pour l'Utilisation des Lasers Intenses, Ecole Polytechnique, 91128 Palaiseau Cedex, FRANCE*

Ph. Mounaix, S. Hüller

Centre de Physique Théorique, Ecole Polytechnique, 91128 Palaiseau, FRANCE

A. Modena

Department of Physics, Blackett Laboratory, Imperial College of Science, Technology and Medicine, London SW7 2BZ, United Kingdom

D. Puissant, C. Stenz

**Groupe de Recherches sur l'Energétique des Milieux Ionisés, Université d'Orléans, 45067 Orléans Cedex 2, FRANCE*

Experimental studies on the interaction of a 0.53 μm laser pulse (600 ps) with a helium gas jet ($n_e \leq 5 \times 10^{19} \text{ cm}^{-3}$) are presented. Plasma creation and evolution were studied with various diagnostics. Time-resolved images obtained by Schlieren technique show the radial evolution of the plasma with structures which can be interpreted as shock wave reflection in cylindrical geometry. Electron density and temperature is measured by Thomson scattering. Time and space resolved spectra show the formation of a channel on the laser axis. Other results presented include: (i) Measurement of Stimulated Brillouin Backscatter (SBS) reflectivity which is shown to increase with laser intensity and saturate at 10% for laser intensity greater than $\approx 10^{14} \text{ W/cm}^2$, (ii) Stimulated Raman Backscatter (SRS) which is much less important (reflectivity $\approx 10^{-4}$) and is emitted during ≈ 100 ps, (iii) Anomalous features on the Thomson spectra which are presently being analyzed.

* Laboratoires associés au Centre National de la Recherche Scientifique.

A Detailed Configuration, Non-Lte Model For Gold

Christopher J. Fontes and Joseph Abdallah, Jr.

Los Alamos National Laboratory, Los Alamos, NM 87545

It is well known that an accurate description of the x-ray conversion occurring in the gold walls of ICF hohlraums requires a non-LTE treatment^[1]. However, the size of any reasonably complete gold model would be prohibitively large from a computational perspective and approximate methods are currently employed. Some examples of these methods include the average atom approach^[2] and the radiation dependent ionization model (RADIOM)^[3]. The current work explores yet another possibility for providing a more accurate, non-LTE gold model.

Our approach involves the use of configuration average atomic physics for each ion stage of interest. The model is then averaged down to a manageable number of composite states that could be used in a rad-hydro code such as LASNEX. Unresolved transition array (UTA) theory^[4] is used in conjunction with existing kinetics codes to calculate the necessary spectral quantities. We present preliminary results of these calculations for such quantities as the ionization balance and total radiated power over a range of electron temperatures and densities. Comparisons are made with existing theories when appropriate. Possible experiments that benchmark these models will also be discussed.

1. J. Lindl, *Physics of Plasmas* 2, 3933 (1995).
2. G. Pollak, Los Alamos Report No. LA-UR-90-2423 (1992).
3. M. Busquet, *Physics of Fluids B* 5, 4191 (1993).
4. D.P. Kilcrease, J. Abdallah, Jr., J.J. Keady, and R.E.H. Clark, *J. Phys. B* 26, L717 (1993).

NLTE Calculations of X-Ray Flux from Burnthrough Au Foils

D. Colombant, J. Dahlburg, M. Klapisch† and J. Gardner

*Plasma Physics Division and L.C.P.F.D., Naval Research Laboratory,
Washington, D.C. 20375*

The NLTE physics model developed at NRL and based on Busquet's model^[1] with STA-generated opacities is used to simulate burnthrough Au foil experiments. Among the simulation results discussed will be results from cases with parameters comparable to those used for exploding Au foil experiments^[2]. In those experiments, the x-ray flux for the non-irradiated rear side of the foil was measured for Au foils of various thicknesses, using 2W laser light. Code-computed rear-side x-ray flux will be compared with the experimentally measured values.

Computations are started with the foil already slightly expanded, with the initial mass of the foil present in the calculation. Sensitivity of the x-ray flux to initial conditions has been tested and will be shown. Two different regimes appear for the different foil thicknesses: a quick burnthrough for the thinner foils with a rapid thermalization of the front and back material, whereas a delayed burnthrough for the thicker foils, in agreement with the experimental observations.

1. M. Busquet, Phys. Fluids B 5, 4191 (1993)
2. C. Back et al., J.Q.R.S.T., 51, 19 (1994)

* Sponsored by DOE.

† Artep Inc., Columbia, MD 21045.

Electron Temperature and Density Measurements in Large Scale-Length Gasbag Plasmas by K-Shell Spectroscopy

K.G. Estabrook, S.H. Glenzer, C.A. Back, B.J. MacGowan, G.F. Stone,
J.D. Moody, and R.K. Kirkwood

Lawrence Livermore National Laboratory, P.O. Box 808 Livermore, CA 94551

D.S. Montgomery

Los Alamos National Laboratory

We present temporally and spatially resolved measurements of the K-shell emission from argon and chlorine dopants in laser-produced mm-size gasbag plasmas. Particularly useful for the diagnostics of these plasmas are the line intensity ratios of the He-like and H-like resonance lines to their respective Li- and He-like dielectronic satellite transitions. By Abel inverting the experimental spectra and applying time-dependent collisional-radiative modeling, local electron temperatures and densities are deduced. About 400ps after the beginning of the laser heating we observe a homogeneous plasma center which heats steadily until the end of the heating pulse. Although the heating is slower than predicted by the hydrodynamic code LASNEX, the experimental peak electron temperature of $T_e = 3$ KeV for neopentane filled gasbags is in agreement with the simulations. In addition, electron densities inferred from the line intensity ratio of the intercombination to the resonance line of helium like argon are 10^{21} cm⁻³ in the center of the bag. Further gas fillings have been investigated and lower temperatures with lower gas densities are found consistent with simulations.

* This work performed under the auspices of the U.S. Department of Energy by the Lawrence Livermore National Laboratory under Contract No. W-7405-ENG-48.

High-Intensity Interaction of a Sub-Picosecond Laser-Pulse with a Preformed Critical Plasma

C. Rousseaux¹, F. Amiranoff², S.D. Baton², J. Fuchs^{2,4}, J.L. Miquel¹, G. Malka¹, J.C. Adam³, G. Bonnaud¹, M. Busquet¹, S. Guérin³, G. Laval³, E. Lefebvre¹, P. Mora³, and D. Pesme²

⁽¹⁾ CEA-Limeil/Valenton, 94195 Villeneuve-Saint-Georges Cedex, France

⁽²⁾ LULI, CNRS, Ecole Polytechnique, 91128 Palaiseau Cedex, France

⁽³⁾ CPhT, CNRS, Ecole Polytechnique 91128 Palaiseau Cedex, France

⁽⁴⁾ INRS-Energie, Montréal, Québec

Preliminary results of high-intensity interaction between a sub-picosecond laser pulse and a preformed critical plasma are presented. The experiment has been performed at 1.06 μm laser wavelength, in the 10^{18} to 10^{19} W/cm^2 intensity range by using the P102 laser facility (CEA/Limeil-Valenton). The preformed plasma is created by irradiating the rear side of a thin plastic foil with an auxiliary nanosecond beam. Transmission, transmitted and reflected light spectra of the picosecond interaction beam are presented. Picosecond, transverse shadowgraphy of the plasma at 0.53 μm wavelength is shown. These results are discussed in relation both with the hydrodynamic of the overdense plasma and the incident short pulse intensity.

Expansion Velocity Measurements of Solid Density Plasmas Produced By Intense Ultrashort Laser Pulses

G. Guethlein, M. Foord, W. Lawson, S. Wilks, D. Price, J. Bonlie, B. Young, R. Shepherd and R. Stewart

Lawrence Livermore National Laboratory, P.O. 808, M/S #L-43, Livermore, CA 94551

We report spatially and temporally localized measurements of 500 eV electron temperatures in solid density Al plasmas generated by a 3×10^{17} W/cm², 170 fs laser. The plasmas studied here were produced at the Ultra Short Pulse (USP) laser facility at LLNL. Expansion velocities of marker layers from various depths are sampled with mass resolved ion time-of-flight spectroscopy^[1] along the central axis of the expansion. These ions are subject only to the spatial peak of the laser intensity profile, thus providing spatial localization. Hydrodynamic simulations relate the measured velocities to the peak sound speed, determining the peak temperature along the central axis of the plasma. Results are consistent with conductive heating of the first 1000 Å. We believe these to be the first spatially and temporally localized measurements of electron temperature in solid density plasmas. In other experiments @ 10^{19} W/cm² incident upon 500 Å Al foils, we observe protons with energy up to 2 MeV. These observations will be compared with PIC simulations.

1. G. Guethlein, RSI **66** (1), 333 (1995).

* Work performed under the auspices of the U.S. Department of Energy by Livermore National Laboratory under contract number W-7405-ENG-48.

Interaction of an Ultra-Intense Electromagnetic Wave with an Overdense Plasma

S. Guérin, P. Mora, J.C. Adam, A. Heron and G. Laval

We present a theoretical and numerical study of the propagation of an ultra-intense electromagnetic wave in a flighty overdense plasma. We analyze the transparency induced by the relativistic effects due to the electrons oscillating in the electric field of the large amplitude wave. This effect allows the wave to propagate in a classically opaque plasma. Our work establishes that parametric instabilities arise in this relativistic regime. We determine analytically the dispersion relation of these instabilities in a one dimensional model. We then study their growth in one and two dimensional numerical simulations. They cause a strong electron heating; a large fraction of the incident wave is then absorbed in the plasma. We also study how the transmitted energy depends on the thickness, on the density of the plasma and on the pulse duration. Transverse effects such as filamentation and self-focusing occur in the two dimensional particle simulations after the parametric instabilities saturation. This emphasizes the role played by these instabilities in the laser-dense plasma interaction.

Space- and Time-Resolved Measurements of Ultra Short Pulse Laser-Produced Plasma Density Gradients

J.-C. Gauthier, J.-P. Geindre, P. Audebert

*Laboratoire pour l'Utilisation des Lasers Intenses, Ecole Polytechnique, 91128
Palaiseau, France*

C. Quoix, G. Hamoniaux, A. Mysyrowicz

*Laboratoire d'Optique Appliquee, Ecole Nationale Supérieure des Techniques Avancées,
91120 Palaiseau, France*

We have studied the variations of the electron density gradient scale length of plasmas produced by sub-picosecond and picosecond laser pulses at irradiances below 10^{16} W/cm² by measuring the phase shift of a 100fs probe pulse by Fourier-transform spectral interferometry. Results for S- and P-polarized probe light are in very good agreement with hydrodynamic simulations. The analysis of the data is underway to extract the electron density gradient scale length from the difference between the phase shift measured with S- and P-polarized probe light⁽¹⁾.

1. P. Blanc et al., JOSA B 13, 118 {1996}.

Magnetic Fields in Short-Pulse Laser Matter Interactions

Rodney J. Mason

Los Alamos National Laboratory, Los Alamos, NM 87545

We have studied the development of intense magnetic fields in short pulse laser-matter interactions as arising in the Fast Ignitor^[1]. Calculations have been performed with the 2D implicit ANTHEM multi-fluid model^[2]. We have explored field generation near the surface of target foils and in a low density atmosphere outside them, with and without the influence of ponderomotive forces.

Short-pulse light deposition at intensities above 10^{18} W/cm² results in the emission of megavolt suprathermal electrons. These draw an intense return current from the background plasma, and produce multi-megagauss B-fields in reverse thermo-electric polarity in low density surrounding plasmas. Ponderomotive forces generate even larger fields just inside high density regions, with polarity controlled by the pulse spatial profile. The intense fields can help direct the flow of suprathermals aimed at fast ignition.

1. M. Tabak, J. Hammer, M. Glinsky, W. Kruer, M. Campbell, M. Perry, J. Woodworth, S. Wilks, and R. Mason, "Ignition and Gain with Ultrapowerful Lasers," *Phys. Plasmas*, 1, 1626 (1994).
2. R. J. Mason, "An Electromagnetic Field Algorithm for 2D Implicit Plasma Simulation, *J. Comp. Phys.* 71, 429 (9187), R. J. Mason and C. W. Cranfill, "Hybrid Two-dimensional Electron Transport in Self-Consistent Electromagnetic Fields, *IEEE Trans. Plasma Sci.* PS-14, 45 (1986), and R. J. Mason, "ANTHEM: Users Manual - Edition 1.1" Los Alamos Report LA-UR-93-888, (1993).

* Work supported by the USDOE.

UV Coherent Emissions and Parametric Instabilities in Laser Irradiated Semiconductors

C.S. Liu and V.K. Tripathi*

*Institute for Plasma Research, University of Maryland at College Park, College Park,
Maryland 20742*

A short pulse (1ps, 1TW/cm²) laser, incident on a wide band gap semiconductor, eg. ZnS (E_g = 3.58 eV), can create a high density electron-hole plasma via tunnel excitation of valence band electrons into the conduction band. After the passage of this laser pulse, the electrons and holes recombine to give stimulated coherent radiation at an ultraviolet wavelength.

At longer pulse lengths, stimulated Raman and Brillouin scattering are important. The power density threshold for these processes in heavily doped semiconductors and semi-metals is on the order of a few GW/cm².

* Permanent address Physics Department, Indian Institute of Technology, New Delhi 110016, India.

Friday

ORAL PRESENTATIONS

8:30 AM – 12:30 PM

Long Pulse Laser

Denise Hinkel, Session Chair

Whole Beam Flow Exclusion¹

Harvey A. Rose and Sandip Ghosal

Los Alamos National Laboratory

Laser beam deflection by transverse plasma flow has been experimentally observed with un-smoothed laser beams in hohlraums² and exploding foil plasmas³, and with diffraction limited beams in exploding foils⁴. The results are in qualitative agreement with theory^{5,6} which also predicts⁵ that BSBS has a corresponding deflection outside the optical cone, as has been observed⁷.

Momentum conservation implies that the momentum transfer to the laser beam, which is proportional to its deflection, is compensated by a retardation of the plasma flow. This retardation is predicted⁵ to develop over a time scale of order one ns, and over a penetration depth of order 500 μm for parameters relevant to current gas filled hohlraum experiments at NOVA.

As the average laser intensity increases, these time and space scales decrease, and once smaller than the beam duration and diameter, plasma flow is effectively excluded from the beam, and beam deflection decreases. This is consistent with the experimentally observed⁷ dependence of BSBS light back into the optical cone which decreases over an intermediate range of intensities, as beam deflection turns on and the light is scattered outside of the optical cone, and then increases with further increase in intensity as beam deflection turns off.

Beam deflection and flow exclusion are dominated by small scale self focusing, as opposed to whole beam self focusing, because they are density gradient driven.

1. Research supported by USDOE.
2. N. Delameter et al., Phys. Plasmas, 3, 2022 (1996).
3. J. Moody, et al., submitted to Phys. Rev. Lett.
4. B. Bauer, Pvt. comm., 1995.
5. Harvey A. Rose, Phys. Plasmas, May, 1709 (1996).
6. D. E. Hinkel, E. A. Williams and C. H. Still, submitted to Phys. Rev. Lett.
7. J. Fernandez et al., Phys. Rev. E53, 2747 (1996).

Thomson Scattering from Two Species Laser-Produced Plasmas

S.H. Glenzer, C.A. Back, K.G. Estabrook, R. Wallace, K. Baker, B.J. MacGowan,
and B.A. Hammel

*L-399, Lawrence Livermore National Laboratory, University of California,
P.O. Box 808, CA 94551, USA*

R.E. Cid and J.S. DeGroot

*Department of Applied Science and Plasma Research Group, University of California,
Davis, CA 95616, USA*

We report on observations of two separate ion acoustic waves in a plasma composed of a heavy (Au) and of a light (Be) species with Thomson scattering. The experimental results show that the measurement of the phase velocities of both ion acoustic waves with Thomson scattering is a sensitive diagnostics to measure relative ion concentrations in mixture plasmas. Furthermore, besides the determination of the electron temperature from the Thomson scattering spectra, the measurement of the relative damping of the ion acoustic features offers an accurate method to derive the ion temperature of the plasma. The experiments are performed with the Nova laser facility at the Lawrence Livermore National Laboratory. The plasma is produced by illuminating a flat disk (2 mm diameter, 51 μm thick), which is coated with Au and Be multilayers of varying thickness (typically 0.5 nm Au and 5 nm Be with a total thickness of 2.5 μm), with one of the Nova beams. We used a 1 ns square pulse with 2.7 kJ energy at 3ω ($\lambda = 351.1$ nm) and a probe laser operating at 2ω ($\lambda = 526.6$ nm) with varying energies in a 4 ns square pulse. Ion acoustic waves belonging to both species, Au and Be, were detected spectroscopically by Thomson scattering at a distance of 250 μm and 500 μm from the disk. For very small Au concentrations of 1% of total ion density, the narrow ion feature of the Thomson scattering signal shows a central peak from scattering on electrons bunched in the Debye sphere of Au ions in addition to the ion acoustic waves belonging to the species of the main plasma ions (Be). Increasing the amount of the heavy species (Au) of the mixture plasma by increasing the relative Au concentration of the target, results in a larger ion acoustic velocity of the heavy species. For a mixture of 4% Au, 96% Be two separate ion acoustic waves, one belonging to Au, one belonging to Be ions, are clearly observed. By further increasing the amount of Au to 9% total density the ion acoustic waves almost mix together on wavelength scale. These results verify theoretical predictions for the phase velocities of ion acoustic waves in mixture plasmas.

*This work was performed under the auspices of the U.S. Department of Energy by the Lawrence Livermore National Laboratory under contract No. W-7405-ENG-48.

Filamentation of Laser Light in Inhomogeneous Plasmas: Effects of Refraction and Plasma Flow

R.W. Short

*Laboratory for Laser Energetics, University of Rochester, 250 East River Road,
Rochester, NY 14623-1299*

It has been known for some time that plasma flow transverse to a self-focused filament can cause the filament to bend in the downstream direction, as well as modify the filamentation growth rate.^[1] Recently this phenomenon has received increased attention because of its consequences for laser spot positioning on the walls of hohlraum targets.^[2,3] It may also have significance for direct drive targets, particularly since refraction in the plasma corona of such targets tends to increase the angle between the filament axis and the density gradient, thereby increasing the effective transverse flow velocity. Previous studies of filamentation have been based on plane wave models or the paraxial wave approximation and hence have been unable to deal with strong refraction.

Here, the full wave equation is used to determine the effects of refraction and plasma flow on filament growth and propagation in inhomogeneous plasmas. Using Green's functions to represent the solutions to the wave equation with the appropriate boundary conditions, the linear behavior of the filamentation instability is found to be described by a set of coupled integral equations, which can be solved numerically. This determines the growth of a perturbation with a given transverse wavelength; an individual filament can then be studied by resolving the incident hot spot into transverse components and following the growth of each.

1. R. W. Short, R. Bingham, and E. A. Williams, *Phys. Fluids* 25, 2302 (1982).
2. D. E. Hinkel, E. A. Williams, R. L. Berger, and L. V. Powers, presented at the 25th Annual Anomalous Absorption Conference, Aspen, CO, 27 May-1 June 1995.
3. H. A. Rose and D. F. DuBois, presented at the 25th Annual Anomalous Absorption Conference, Aspen, CO, 27 May-1 June 1995.

* This work was supported by the U.S. Department of Energy Office of Inertial Confinement Fusion under Cooperative Agreement No. DE-FC03-92SF19460, the University of Rochester, and the New York State Energy Research and Development Authority. The support of DOE does not constitute an endorsement by DOE of the views expressed in this article.

The Influence of Smoothing by Spectral Dispersion on Laser Scattering and Beam Propagation in Large-Scale-Length Plasmas Relevant to National Ignition Facility Hohlräume*

B.J. MacGowan, B.B. Afeyan, C.A. Back, R.L. Berger, B. Canaud, S.H. Glenzer, D.E. Hinkel, R.K. Kirkwood, H.N. Kornblum, A.B. Langdon, B.F. Lasinski, D.S. Montgomery, J.D. Moody, D.H. Munro, L.V. Powers, C.H. Still, R.J. Wallace, and E.A. Williams
Lawrence Livermore National Laboratory, University of California, Livermore, CA, U.S.A.

M.A. Blain and C. Rousseaux
Centre D'Etudes de Limeil-Valenton, France

We have used homogeneous plasmas of high density (up to 1.5×10^{21} electrons per cm^3) and temperature (~ 3 keV) with large density scalelengths (~ 2 mm) in order to approximate conditions within National Ignition Facility (NIF) scale hohlraums. Low-Z gasbag plasmas were used to emulate the uniform low-Z plasma filling most of the ignition-scale hohlraum. In addition smaller, Nova-scale hohlraums were used to replicate the shelf of gold that is ablated from the wall of the NIF hohlraum, in which the highest growth of SBS is expected to occur. Using these plasmas we have studied the dependence of stimulated Raman (SRS) and Brillouin (SBS) scattering on beam smoothing and plasma conditions at the NIF relevant laser intensity (3W at $2 \times 10^{15} \text{Wcm}^{-2}$). The plasmas were formed with nine of the Nova beams while a tenth beam was used as an interaction beam, with the same intensity and f/number as the beams in current NIF designs. The interaction beam was modified to have the $f/8$ geometry of the NIF in order to test the effect of beam smoothing in stabilizing filamentation. The beam was smoothed with a random phase plate and additional smoothing by spectral dispersion. Both SBS and SRS are affected by use of smoothing by spectral dispersion (SSD). We have also investigated the effect of smoothing on the characteristics of the beam transmitted through the plasma. The significance of the results of these different measurements will be discussed.

* This work was performed under the auspices of the U.S. Department of Energy by the Lawrence Livermore National Laboratory under contract No. W-7405-ENG-48.

Transmitted Light Characteristics in Nova Gasbag Plasmas

J.D. Moody, B.J. MacGowan, R.K. Kirkwood, C.A. Back, S.H. Glenzer, D.E. Munro,
and R.L. Berger

Lawrence Livermore National Laboratory, Livermore, CA, 94550

Propagation of laser energy through a long scalelength plasma is important to ICF because it determines the laser intensity and spot characteristics on the wall of an indirect drive hohlraum. This, in turn, can affect the temperature and symmetry of radiation on the capsule. Effects such as inverse bremsstrahlung absorption, stimulated scattering, filamentation, and beam deflection in the hohlraum plasma can both attenuate the amount of transmitted light as well as spread and shift the laser spot location on the hohlraum wall. Nova gasbag targets, due to their easy viewing accessibility, are used for transmission measurements. In these targets, back, side, and forward scattered (transmitted) light can be readily measured making possible a detailed analysis of laser propagation and interaction in this target. This paper presents an overview of the measurements of time resolved power, angular spreading, and spectral character of a 351 nm probe laser transmitted through Nova gasbag targets. These plasmas have $T_e = 3$ to 4 keV, $n_e/n_{cr} = 0.07$ to 0.15, incident laser intensity ranging from 0.8×10^{15} W/cm² to 6×10^{15} W/cm², and probe f/number either 4.3 or 8. We study the effects of plasma density, laser intensity, plasma composition, and laser smoothing on the nature of the transmitted light. Transmitted light angular spreading increases with both probe intensity and plasma density. Narrowband spectral measurements near 351 nm show that the plasma always increases the bandwidth of the probe laser. Time dependent transmission measurements allow us to infer the plasma temperature evolution and, combined with scattering measurements, carry out a detailed power balance analysis. We will discuss the measurements and compare with calculations using the hydrodynamic code Lasnex and the three dimensional filamentation code F3D.

* Work performed under the auspices of the U. S. Department of Energy by the Lawrence Livermore National Laboratory under contract number W-7405-ENG-48.

Plasma Diagnostics on OMEGA

W. Seka and A.V. Chirikikh

Laboratory for Laser Energetics, University of Rochester, Rochester, NY 14623-1299

The new OMEGA 60-beam UV laser facility has been used to set up and diagnose plasma spectroscopic signals in view of studying long-scale-length laser-plasma interaction processes, such as SBS, SRS, etc., in the future. The initial setup experiments were carried out on implosion experiments with 20 to 30 kJ driving plastic or glass capsules. At this time these experiments have yielded survey data on various spectral signatures that can serve to identify scattering levels and accidental—though very useful—Thomson scattering configurations. The 60-beam configuration is very well suited for such applications, and the results will be compared to similar ones observed on the old 24-beam system. We will present plasma diagnostic features on OMEGA and discuss planned long-scale-length experiments.

* This work was supported by the U.S. Department of Energy Office of Inertial Confinement Fusion under Cooperative Agreement No. DE-FC03-92SF19460, the University of Rochester, and the New York State Energy Research and Development Authority. The support of DOE does not constitute an endorsement by DOE of the views expressed in this article.

Large-Scale Three-Dimensional Particle-In-Cell Simulations of Laser Beam Deflection and Stimulated Brillouin Scattering

H.X. Vu

Los Alamos National Laboratory, Los Alamos, New Mexico 87545

In Inertial Confinement Fusion (ICF) applications, an external high-frequency monochromatic electromagnetic wave such as a laser is employed to irradiate the plasma. The wave, due to its interaction with the plasma, can undergo either electron-driven or ion-driven parametric instabilities, and decay into various combinations of daughter waves^[1]. Recent experiments^[2-3] and fluid simulations^[4-7] indicate that ion-driven parametric instabilities, which affect the propagation of external driving electromagnetic fields, are prevalent in current ICF plasmas of interest. Due to a multitude of spatial and temporal scales that exist in such plasmas and the fact that the external driving electromagnetic field is of high frequency, general-purpose explicit, implicit, and hybrid PIC algorithms are either incapable of simulating the actual physics, or computationally inefficient. In a recent work^[8], HERCULES, a special-purpose massively parallel hybrid particle-in-cell (PIC) code appropriate for simulating ion-driven parametric instabilities, was developed and implemented on the CRAY-T3D platform. In this paper, large-scale three-dimensional PIC simulations (16 million computational cells, 256 million particles) of laser beam deflection and stimulated Brillouin scattering (SBS), using HERCULES, are presented. The physical processes to be examined are the angular dependence of SBS in three dimensions, and the dependence of laser beam deflection on transverse plasma flows.

1. W.L. Kruer, *The Physics of Laser Plasma Interactions* (Addison-Wesley, New York, 1988).
2. B.J. MacGowan, *Bull. Am. Phys.* 40, 1645 (1995).
3. J.D. Moody, B.J. MacGowan, D.E. Hinkle, W.L. Kruer, E.A. Williams, K. Estabrook, T.D. Shepard, R.K. Kirkwood, D.S. Montgomery, and R.L. Berger, *Phys. Rev. Lett.*, submitted.
4. H.A. Rose, *Phys. Plasmas*, to be published.
5. W.L. Kruer, *Bull. Am. Phys.* 40, 1824 (1995).
6. D.F. Dubois and H.A. Rose, *Bull. Am. Phys.* 40, 1824 (1995).
7. E.A. Williams and D.E. Hinkle, *Bull. Am. Phys.* 40, 1824 (1995).
8. H.X. Vu, "A Massively Parallel Three-Dimensional Hybrid Code for Simulating Ion-Driven Parametric Instabilities," *J. Comput. Phys.*, submitted.

Modeling of a Stimulated Brillouin Scattering Experiment with Statistical Distribution of Speckles

C. Labaune, H.A. Baldis

LULI, Ecole Polytechnique, Palaiseau, France

V.T. Tikhonchuk

P. N. Lebedev Physics Institute, Moscow, Russia

The results of experimental studies of stimulated Brillouin scattering (SBS) from a laser beam smoothed with a random phase plate (RPP) in a preformed expanding plasma are compared with the statistical theory of SBS from an inhomogeneous plasma. The theory assumes that SBS occurs in randomly distributed independent speckles. This hypothesis naturally combines observed pump depletion effects within a speckle, with relatively minor SBS reflectivity of the whole interaction beam. Our comparison shows, for the first time, agreement between the theory and experiment on the temporal evolution, the reflectivity levels and the time-resolved spectra of stimulated Brillouin scattering, as well as the temporal evolution, the spatial location of the peak of the density fluctuations and the levels of the ion acoustic waves, measured with Thomson scattering technique.

Ion Wave Parametric Instabilities

E.A. Williams, B.I. Cohen, R.L. Berger, B.F. Lasinski and A.B. Langdon
Lawrence Livermore National Laboratory, Livermore, CA 94550

Simulations of ion acoustic waves driven by a prescribed ponderomotive potential with our 2-D Boltzmann electron, PIC ion code BZOHAR, have shown some interesting saturation behaviour⁽¹⁾. After initial 1-D growth, the ion acoustic waves develop two dimensional, long wavelength structure and crash in amplitude. Ion waves with k-vector one half that of the driving wave, together with a transverse k-component, are found to grow up at this time. We have obtained the dispersion relation for the parametric coupling of the driven ion wave to other ion waves. The fastest growing branch of this instability^(2,3) (with growth rate $\sim(1/4) \delta N/N k_0 c_s$) is a decay into the modes observed in our BZOHAR simulations. We present an analysis of this dispersion relation. Important features affecting the parametric instability of a driven ion wave are the driving frequency relative to the normal mode frequency and the ratio of the electron Debye length to the wavelength.

1. Resonantly Excited Nonlinear Ion Waves (submitted to Physics of Plasmas).
2. S. J. Kartunnen, J. N. McMullin and A. A. Offenberger. Phys. Fluids 24, 447 (1981).
3. W. L. Kruer in *From Fusion to Light Surfing*, edited by T. Katsouleas (Addison Wesley, 1991).

* Work performed under the auspices of the U.S. Department of Energy by Lawrence Livermore National Laboratory under Contract No. W-7405-ENG-48.

Laser Hot-Spot Interaction Taking Into Account the Effects of Plasma Dynamics

S. Hüller, Ph. Mounaix, D. Pesme, V.T. Tikhonchuk¹
CPHT and LULI, Ecole Polytechnique, Palaiseau, France

D. Mourenas, M. Casanova
CEA Limeil-Valenton, Villeneuve-St.Georges, France

We present results of our code⁺⁾ KOLIBRI which models the interaction of intense laser light with the low-frequency dynamics of the plasma fluid in two or three spatial dimensions. In this code the light propagation is treated without the restriction of the paraxial optics approximation. We study the interaction dynamics between neighboring laser hot spots in hot underdense plasmas.

In a first step, we discuss the case of two focussed beams interacting with each other. This can be considered as a reduced model for multiple hot spot interaction in optically smoothed laser beams. This study allows us to understand in detail the dynamics of coalescence of hot spots and the mutual influence between SBS and the merging process.

In a further step we consider the more complex problem of multiple-beam interaction by simulating a smoothed laser beam, taking into account the effects of common smoothing techniques. The parameters of these simulations are those envisaged for the future projects of the French Megajoule Laser (LMJ) and the US-National Ignition Facility (NIF). In particular we pay attention to the peak and mean levels of SBS reflectivity and analyse the angular distribution of both transmitted and reflected light.

^{+) S. Hüller, Ph. Mounaix, D. Pesme, Physica Scripta (1996).}

^{1) on leave from Lebedev Physics Institute, Moscow, Russia.}

Power Exchange Between Crossed Laser Beams and the Associated Frequency Cascade

V.A. Smalyuk and C.J. McKinstrie

*Laboratory for Laser Energetics, University of Rochester, 250 East River Road,
Rochester, NY 14623-1299*

R.E. Giacone and H.X. Vu

Los Alamos National Laboratory, Los Alamos, NM 87545

The indirect-drive approach to ICF involves multichromatic laser beams that overlap as they enter the hohlraum.^[1] SBS allows the frequency components of one beam to interact with the frequency components of another beam. Because a power exchange between the beams affects the implosion symmetry adversely, it is important to understand this process.

Previous studies of the power transfer between crossed laser beams^[2-4] were based on the standard model in which the beams are monochromatic initially. We have analyzed a two-dimensional model that allows each beam to have many frequency components. The beam evolution depends sensitively on whether the beams are monochromatic or multichromatic initially, and whether their intersection region lies partially or wholly within the plasma.

1. J. D. Lindl, *Phys. Plasmas* 2, 3933 (1995).
2. W. L. Kruer, S. C. Wilks, B. B. Afeyan and R. K. Kirkwood, *Phys. Plasmas* 3, 382 (1996).
3. V. V. Eliseev, W. Rozmus, V. T. Tikhonchuk, and C. E. Capjack, *Phys. Plasmas* (in press).
4. C. J. McKinstrie, J. S. Li, R. E. Giacone, and H. X. Vu. *Phys. Plasmas* (in press).

* This work was supported by the U.S. Department of Energy Office of Inertial Confinement Fusion under Cooperative Agreement No. DE-FC03-92SF19460, the University of Rochester, and the New York State Energy Research and Development Authority. The support of DOE does not constitute an endorsement by DOE of the views expressed in this article.

Observation of Relativistic Electrons Produced in the Interaction of a 400-fs Laser Pulse With a Solid Target

G. Malka, C. Rousseaux, E. Lefebvre and J.L. Miquel

CEA-Limeil/Valenton, 94195 Villeneuve Saint-Georges Cedex, France

Relativistic electrons (0.5-20 MeV) produced by the interaction of a short 400-fs, 1.06- μm laser pulse on solid target, in the 3×10^{17} to 2×10^{19} W/cm² intensity range, have been measured. The results demonstrate the role of the ponderomotive force via the $\mathbf{J} \times \mathbf{B}$ effect: the hot temperature T_h of electrons accelerated along the laser axis is equal to the electron oscillation energy in the laser field, $T_h \sim (\gamma_{\text{osc}} - 1)mc^2$. For electrons emitted at 22° and 135°, T_h scales as $I^{1/3}$. X-ray spectroscopic measurements and numerical simulation show that the plasma is characterized by a step (a few microns) density gradient near the critical density. These data are compared with 1D PIC simulations.

In recent experiments, at a laser wavelength of 0.53 μm , the number of hot electrons sharply decreases as compared with the 1.06 μm experiments, and a cut-off appears in the hot electron distribution tail, due to interaction with dense plasma characterized by a very short gradient scale length ($L < \lambda$).

(Ref: "Experimental Confirmation of Ponderomotive-Force Electrons Produced by an Ultra Relativistic Laser Pulse on a Solid Target," G. Malka and J.L. Miquel, accepted for publication to Phys. Rev. Lett. May 96).

Spreading of Intense Laser Beams in Underdense Plasmas

V. Eliseev*, I. Ourdev, W. Rozmus and V.T. Tikhonchuk*

Department of Physics, University of Alberta, Edmonton, Canada

C.E. Capjack

Department of Electrical Engineering, University of Alberta, Edmonton, Canada

P.E. Young

Lawrence Livermore National Laboratory, Livermore, CA, USA

We present results of multidimensional numerical studies employing our nonparaxial wave interaction code^[1]. For parameters of the experiment^[2], we have confirmed the important role of filamentation and self-focusing as explained in the previous interpretation of the measurements^[3]. However, we also found that the stimulated Brillouin scattering affects in an essential way most of the processes occurring during the beam propagation in a plasma. The initial dynamical evolution of backscattered light reflectivity is affected by self-focusing and displays characteristic time oscillations. The forward and side Brillouin scattering instabilities are the main contributors to transmitted light spreading. Initially the filamentation instability provides enhancement of ion acoustic fluctuations which scatter the light and provide the seed for the forward SBS. At later times, the scattering instability is a dominant factor. The angular spread of the laser beam is defined by the side SBS gain and the width of the pump in the front of the target. After accounting for the additional increase in the pump width due to nonlinear evolution of self-focusing we have obtained good agreement between linear side SBS growth estimates and results of full simulations. Experimentally observed spectra of transmitted light is red-shifted in agreement with a SBS scenario.

1. V. Eliseev, W. Rozmus, V. T. Tikhonchuk, and C. E. Capjack, *Phys. Plasmas*, 2, 1712 (1995); 3, 2215 (1996).
2. P. E. Young, et al., *Phys. Plasmas* 2, 7 (1995); *Phys. Rev. Lett.* 75, 1082 (1996).
3. S. Wilks, P. E. Young, J. Hammer, M. Tabak, and W. L. Kruer, *Phys. Rev. Lett.* 73, 2994 (1994).

* On leave from Russian Academy of Sciences, Moscow, Russia.

Index

A

Abdallah, Joseph, Jr. 165
Adam, J.C. 168, 170
Afeyan, B. 39, 83
Afeyan, B.B. 86, 87, 120, 178
Afeyan, Bedros 155
Afeyan, Bedros B.
32, 123, 158
Aglitskiy, Y. 55
Alon, Uri 136, 137
Amendt, P. 82, 126
Amiranoff, F. 46, 115, 164,
168
Antonetti, A. 67, 115
Archuleta, Tom 31
Arnett, W.D. 26
Armiranoff, F. 105
Audebert, P. 67, 115, 171
Azehi, H. 56

B

Babine, A. 113
Back, C. 39
Back, C.A.
42, 79, 87, 120, 167, 176,
178, 179
Badger, A.D. 67
Baker, K. 176
Baldis, H.A. 182
Bar-Shalom, Avraham 15
Barbee, T.W. 44
Barbee, T.W., Jr. 79
Barnes, Cris W. 126, 140
Batani, D. 21, 74
Baton, S.D. 168
Beck, J. Bradley 140
Benuzzi, A. 21, 74
Beretta, D. 21, 74
Berger, R. 39
Berger, R.L.
35, 42, 83, 84, 87, 90, 120, 132,
154, 157, 178, 179, 183
Berkey, T. 152
Bernhardt, P.A. 4
Berning, M. 60
Betti, R. 63, 147
Bezzarides, B. 36, 89, 138
Bingham, R. 52
Blain, M. 39
Blain, M.A. 83, 120, 132, 178

Bodner, S.E. 55, 78
Bodner, Stephen E. 77
Boehly, T.R. 58
Bonadio, R. 46, 164
Bonlie, J. 169
Bonnaud, G. 168
Bonnaud, Guy 102, 153
Bossi, S. 21, 74
Boudenne, J.M. 21
Boyd, R. 161
Bradley, D. 126
Bradley, D.K. 54, 58, 61
Brandon, S.T. 81
Britten, J.A. 161
Brown, C. 55, 99
Brown, C.G. 161
Budil, K.S. 26, 60
Busquet, M. 168
Bychenkov, V. Yu. 41, 159

C

Cable, M.D. 126
Canaud, B. 178
Capjack, C.E. 40, 93, 187
Casanova, M. 37, 38, 91, 184
Cauble, R. 14, 79
Celliers, P. 14, 79
Celliers, Peter 145
Chan, L-Y. 78
Chan, Y. 55
Chan, Yung 97
Chaturvedi, K.P. 34
Chessa, P. 105
Cheung, Peter 6
Chiou, T.C. 51, 112
Chirokikh, A.V. 180
Choi, Chan K. 140
Chou, Al 32
Chou, Albert E. 123, 158
Chrien, R. 75
Chrien, R.E. 62
Cid, R.E. 176
Clayton, C.E. 17, 50, 106
Clover, M.R. 130
Cobble, J.A. 116, 118
Cohen, B.I. 163, 183
Collins, J.L. 130, 146
Collins, Richard L. 11
Colombant, D.G. 55, 78, 166
Colombant, Denis 25, 73, 77
Colvin, J. 26

Coulaud, C. 164
Cowley, Steve 151
Cranfill, C.W. 130
Craxton, R.S. 126, 134
Cremer, S. 69

D

Dahlburg, J. 166
Dahlburg, J.P. 55, 78
Dahlburg, Jill P. 77
Daido, H. 44
Dalhed, S. 52
Dangor, A.E. 50, 106
Danson, C.N. 50, 106
DaSilva, L.B. 14, 44, 59, 79
Davis, J.F. 13
Dawson, J.M. 52
Decker, C. 14, 126
Decker, Chris D. 45
DeGroot, J.S. 176
Delamater, N.D.
126, 129, 130, 131
Delettrez, J.A. 47, 54, 58, 61
Demir, A. 59
Deniz, A.V. 55, 78
Desenne, D. 87
Desenne, D.E. 120
DeWispelaere, E. 46, 105, 164
Dezulian, R. 74
Divol, L. 38
Dorchies, F. 105, 115
Downer, M.C. 113
DuBois, D.F. 85, 121, 122
DuBois, Don 6
DuBois, Donald F. 118
Dunn, J. 144

E

Eimerl, David 22
Eliseev, V. 40, 187
Epstein, R. 63, 68
Estabrook, K. 39, 159
Estabrook, K.G. 120, 167, 176
Estabrook, Kent 145
Evans, R. 67

F

Failor, B.A. 129
Failor, B.H. 131
Failor, Bruce H. 118

Index (Contd.)

Fallies, F. 67
Fedosejevs, R. 104
Feldman, U. 55
Fernandez, Juan C. 118, 119
Fisher, D. 113
Fisher, Y. 47
Fontes, Christopher J. 165
Foord, M. 169
Freeman, R. 109
Frycz, P. 12
Fuchs, J. 168

G

Gaeris, A.C. 47
Galmiche, D. 26
Gardner, J. 166
Gardner, J.H. 55, 78
Gardner, John H. 25, 77
Gauthier, J.-C. 67, 115, 171
Geindre, J.-P. 67, 115, 171
Gerber, K. 55
Gerber, K.A. 78
Ghosal, Sandip 175
Giacone, R.E. 162, 185
Gifford, K. 129
Glendinning, G. 129
Glendinning, S.G.
26, 59, 82, 132
Glenzer, S. 39, 79
Glenzer, S.H. 42, 87, 120, 167,
176, 178, 179

Gobby, P. 75, 126
Gold, D.M. 144
Goldman, M.V. 86
Goldman, S.R. 29, 146
Goncharov, V.N. 63, 147
Grandjouan, N. 74
Grillon, G. 46, 67, 105, 115
Griswold, D. 26
Guérin, S. 168, 170
Guethlein, G. 169
Guethlein, Gary 98
Guzdar, N. 33, 34

H

Haan, S.W. 80, 133
Hall, T.A. 21, 67, 74
Hammel, B. 99
Hammel, B.A. 82, 126, 176
Hammer, J.H. 103

Hamoniaux, G. 105, 171
Hanssen, Alfred 85
Hargrove, J. 55
Harris, D.B. 149
Harris, David B. 30
Hartmann, F. 109
Hashimoto, H. 44
Hatchett, S.P. 103
Hauer, A.A. 126, 129, 130
Helmersen, E. 5
Herman, S. 161
Heron, A. 170
Hinkel, D.E. 35, 90, 132, 157,
178
Ho, D.D.M. 81
Ho, Darwin 150
Hoffman, N.M. 23, 62
Hoffman, Nelson M. 140
Holland, G. 55
Hollis, R. 75
Honda, M. 56
Honrubia, J.J. 74
Hsing, W.W. 26
Hsing, Warren W. 140
Hughes, Michael KY. 117
Hüller, S. 37, 91, 164, 184
Hunt, John 145

I

Isizaki, R. 56

J

Jaanimagi, P.A. 54
Johnson, R.P. 116
Johnston, T.W. 159
Joshi, C. 50, 99, 106

K

Kalantar, D. 75
Kalantar, D.H. 26, 59
Kane, J. 26
Kato, Takato 98
Kato, Y. 44
Katsouleas, T. 51, 112
Kauffman, R.L. 13, 129, 132
Keane, Chris 96
Keck, R. 126
Keck, R.L. 58
Kelly, J. 126
Kerman, A. 109

Keskinen, M.J. 8
Key, M. 26
Key, M.H. 24, 59
Kim, N.S. 59
Kirkwood, R. 39
Kirkwood, R.K. 42, 83, 84, 87,
87, 120, 157, 167, 178, 179
Kishony, Roy 139
Klapisch, M. 15, 55, 73, 77,
78, 166
Knauer, J. 75, 126
Knauer, J.P. 24, 26, 58, 59
Kodama, R. 44, 56
Koenig, M. 21, 74
Kopp, R. 75
Kopp, R.A. 138, 146
Kopp, Roger A. 64
Kornblum, H.N. 178
Kotelnikov, Alexei D. 20
Kremens, R. 126
Krishnan, J. 21, 74
Kruer, W. 39
Kruer, W.L. 83, 84, 86, 87,
93, 95, 120, 123
Kruer, William L. 32, 101

L

Labaune, C. 182
Laming, M. 55
Landen, O. 82
Landen, O.L. 126, 132, 135
Langdon, A.B. 35, 84, 90, 92,
109, 154, 157, 163, 178, 183
Langer, Steven H. 96
Larroche, O. 19
Lasinski, B.F.
87, 120, 163, 178, 183
Laval, G. 168, 170
Lawson, W. 169
LeBlanc, S.P. 113
Lee, R.W. 43
Lee, Y.T. 81
Lefebvre, E. 100, 168, 186
Lefebvre, Erik 102
Lehecka, T. 55, 78
Lehmberg, H. 33
Lehmberg, R.H. 55, 78
Lerche, R. 75
Lewis, C.L.S. 59
Lin, J. 59
Lindl, J.D. 135

Index (Contd.)

Lindman, E.L. 129, 130, 131
Liu, C.S. 173
London, R.A. 14
London, Richard A. 45
Löwer, Th. 21, 74
Lummerzheim, Dirk 11
Lynn, A. 9

M

MacGowan, B. 39, 75
MacGowan, B.J. 42, 83, 84, 87,
120, 157, 167, 176, 178, 179
MacGowan, Brian 145
Maekawa, O. 56
Magelssen, G.R. 62, 129, 126,
130, 131
Mahdieh, M. 21, 67, 74
Malka, G. 100, 168, 186
Malka, V.
46, 50, 105, 106, 164
Manes, Ken 145
Marinak, M.M. 26, 80
Marquès, J.R. 46, 105, 115
Marsh, K.A. 50, 106
Marshall, F.J. 126
Marshall, Frederic J. 31
Mason, R. 75
Mason, R.J. 116, 146
Mason, Rodney J. 64, 172
Matte, J.P. 159
Maximov, A.V. 93
Maxon, M.S. 13
McCrary, R.L. 63, 147
McKenty, P. 75
McKinstry, C.J.
88, 110, 111, 185
McLean, E.A. 55, 78
McPhee, A. 59
Metzler, N. 78
Meyer, Jochen 117
Meyerhofer, D.D. 47, 58
Mikaelian, K.O. 60
Miller, J.L. 161
Miller, P.L. 60
Mima, K. 44, 56
Miquel, J.L. 100, 168, 186
Miyayana, N. 56
Mjølhøus, E. 5
Modena, A. 50, 106, 164
Montgomery, D.S.
87, 120, 157, 167, 178

Montgomery, David C. 20
Montgomery, David S. 71, 118
Moody, J. 39, 99
Moody, J.D. 42, 83, 87, 103,
120, 157, 167, 178, 179
Moore, J.B. 126, 129
Mora, P. 105, 168, 170
More, R.M. 43
More, Richard 98
Moreno, J.C. 14, 79
Mori, W.B. 48, 49, 51, 107,
112
Mostovych, A.N. 78
Mostovych, Andrew N. 97
Mounaix, Ph. 37, 46, 91, 105,
160, 164, 184
Mourenas, D.
37, 91, 156, 184
Muggli, P. 50
Munro, D.E. 42, 179
Munro, D.H. 87, 178
Murphy, T.J. 126, 129
Murray, Jim 145
Myatt, J.F. 41
Mysyrowicz, A. 67, 171

N

Najmudin, Z. 50, 106
Nakai, M. 56
Neely, D. 50, 59, 106
Nelson, M. 75
Newman, D.L. 86
Nguyen, H. 161
Nibbering, E. 46
Nichols, E. 9
Nishihara, K. 56

O

Obenschain, S.P. 55, 78
Oertel, J.A. 126
Oertel, John A. 31
Ofer, Dror 136, 137
Offenberger, A. 99
Olsen, W. 161
Oron, Dan 136, 137
Orzechowski, T.J. 83, 84
Ossakow, L. 34
Osterheld, A.L. 43, 98
Ourdev, I. 40, 187

P

Papadopoulos, K. 34
Pau, J. 10, 152
Pawley, C.J. 55, 78
Pennington, D.M. 161
Perry, M. 99
Perry, M.D. 161
Perry, T.S. 60
Pesme, D. 37, 91, 160, 168,
184
Peysner, T.A. 60
Phillips, Lee S. 77
Pollaine, S.M. 28, 131, 133
Pollaine, Steve 22
Pollak, Greg D. 30
Powers, L.V. 83, 84, 129,
132, 148, 154, 178
Powers, W.J. 130
Price, D. 169
Price, Dwight 98
Pronko, M.S. 55, 78
Puissant, D. 164

Q

Quoix, C. 171

R

Rambo, P.W. 79, 95
Rankin, R. 12
Rekanati, Avi 136
Remington, B.A. 26, 59, 60
Ress, D. 132
Riazuelo, Gilles 153
Richard, A.L. 129, 132
Rodriguez, P. 4
Rose, H.A. 129
Rose, Harvey 122
Rose, Harvey A.
85, 94, 118, 121, 175
Rosen, M.D. 83, 84, 135
Rothenberg, Joshua E. 66
Rousseaux, C. 87, 100, 168,
178, 186
Rowland, H.L. 8
Rozmus, W.
40, 41, 93, 159, 187
Rubenchik, A. 26
Rubenchik, A.M. 60
Russell, David 6, 85, 121, 122

Index (Contd.)

S

Salazar, M.A. 129
Samson, J.C. 12
Schmitt, A.J. 55, 78
Schmitt, Andrew J. 25, 77, 155
Schnittman, J.D. 28, 134
Scott, Howard A. 96
Seely, J. 55
Seka, W. 126, 180
Sentman, D. 10
Sergeev, A. 113
Serlin, V. 55, 78
Sethian, J.D. 55, 78
Shepard, T.D.
 131, 132, 135, 148
Shepherd, R. 144, 169
Shepherd, R.L. 43
Shepherd, Ronnie 98
Shigemori, K. 56
Shiraga, H. 56
Shore, B. 161
Short, R.W. 65, 177
Shvarts, Dov 136, 137, 139
Siders, C.W. 113
Siefiring, C.L. 4
Simon, Albert 124
Skupsky, S. 69
Smalyuk, V.A. 58, 185
Smith, R. 59
Smith, Roger W. 11
Smitherman, D.P. 62
Soures, J.M. 58, 126
Springer, P.S. 83
Springer, P.T. 84
Stamper, J.A. 55, 78
Startsev, E.A. 110, 111
Stenz, C. 164
Stepanov, A. 113
Stewart, R. 144, 169
Stewart, R.E. 43
Stewart, Richard 98
Still, C.H.
 84, 90, 154, 157, 178
Stone, G.F. 79, 87, 167
Stone, Gary 145
Stuart, B.C. 161
Sullivan, A. 144
Sullivan, C.A. 55, 78
Sulzer, Michael P. 142

Suter, L.J. 13, 82, 83, 84,
 126, 129, 132, 135
Swenson, F.J. 23

T

Tabak, M. 103
Tabak, Max 150
Tajima, T. 113
Takabe, H. 56
Takahashi, K. 44
Takenaka, H. 44
Tallents, G.J. 59
Tanaka, K.A. 44
Thompson, C.A. 36
Tietbohl, G. 161
10 Tikhonchuk, V.T. 12, 40, 41, 91,
 93, 159, 160, 182, 184, 187
Tipton, R.E. 80
Toupin, Catherine 102
Town, R.P.J. 65
Trebess, J.E. 14, 79
Tripathi, V.K. 173
Tsai, L.C. 152
Tsakiris, G.D. 104
Turano, E.J. 88
Turner, R.E. 126
Tzeng, K.-C. 49, 107

V

Valeo, E. 151
Van Wouterghem, Bruno 145
Varnum, W.S. 149
Verdon, C.P.
 24, 58, 61, 63, 65, 75, 126, 147
Villasenor, J. 9, 152
Villasenor, J.S. 8
Vu, H.X.
 36, 138, 162, 181, 185
Vu, Hoanh X. 64, 118

W

Wallace, I.D. 29
Wallace, J. 126
Wallace, J.M.
 36, 128, 129, 131
Wallace, R. 120, 176
Wallace, R.J. 126, 178
Wallace, Russel 145
Walling, R.S. 43

Walling, Rosemary 98
Walsh, F.N. 50, 106
Wan, A. 44
Wan, A.S. 14, 79
Wang, X.F. 104
Wark, J.S. 59
Warwick, J. 59
Watt, R. 126
Watt, R.G. 75
Waxman, Eli 139
Weber, F. 14, 59, 79
Weber, S.V. 26, 59
Weber, Stephen V. 66
Wharton, K. 39, 99
Wilde, Bernhard H. 118
Wilke, M.D. 131
Wilks, S. 99, 169
Wilks, S.C. 93, 95
Wilks, Scott C. 32, 101, 109
Willi, O. 75
Williams, E.A.
12 35, 84, 87, 90, 92, 120,
 132, 154, 157, 163, 178, 183
Wilson, D.C. 29, 62, 75
Wolfram, E. 24
Wolfrum, E. 59
Wong, A.Y. 3, 7, 8, 9, 10, 152
Wood, Wm. Monty 119
Wood-Vasey, W.M. 26, 60
Woodworth, J. 109
Wuerker, R. F. 7

Y

Yanovsky, V. 99, 161
Yedov, Yanai 136, 137
Young, B. 169
Young, Bruce 98
Young, P.E. 40, 154, 187

Z

Zakharenkov, Y. 99
Zerlauth, Pierre 153
Zhang, J. 59
Zimmerman, G.B. 80
Zwi, H. 7
Zwi, H.R. 9, 10